

1970

# Phase Reactions In The System Nepheline - Diopside - Sanidine And Their Significance To Alkaline Rock Genesis

Richard Garth Platt

Follow this and additional works at: <https://ir.lib.uwo.ca/digitizedtheses>

---

## Recommended Citation

Platt, Richard Garth, "Phase Reactions In The System Nepheline - Diopside - Sanidine And Their Significance To Alkaline Rock Genesis" (1970). *Digitized Theses*. 441.  
<https://ir.lib.uwo.ca/digitizedtheses/441>

This Dissertation is brought to you for free and open access by the Digitized Special Collections at Scholarship@Western. It has been accepted for inclusion in Digitized Theses by an authorized administrator of Scholarship@Western. For more information, please contact [tadam@uwo.ca](mailto:tadam@uwo.ca), [wlsadmin@uwo.ca](mailto:wlsadmin@uwo.ca).

The author of this thesis has granted The University of Western Ontario a non-exclusive license to reproduce and distribute copies of this thesis to users of Western Libraries. Copyright remains with the author.

Electronic theses and dissertations available in The University of Western Ontario's institutional repository (Scholarship@Western) are solely for the purpose of private study and research. They may not be copied or reproduced, except as permitted by copyright laws, without written authority of the copyright owner. Any commercial use or publication is strictly prohibited.

The original copyright license attesting to these terms and signed by the author of this thesis may be found in the original print version of the thesis, held by Western Libraries.

The thesis approval page signed by the examining committee may also be found in the original print version of the thesis held in Western Libraries.

Please contact Western Libraries for further information:

E-mail: [libadmin@uwo.ca](mailto:libadmin@uwo.ca)

Telephone: (519) 661-2111 Ext. 84796

Web site: <http://www.lib.uwo.ca/>



**NATIONAL LIBRARY  
OF CANADA**

**CANADIAN THESES  
ON MICROFILM**

**BIBLIOTHÈQUE  
NATIONALE  
DU CANADA**

**THÈSES CANADIENNES  
SUR MICROFILM**

**No 5049**

PHASE RELATIONS IN THE SYSTEM  
NEPHELINE ( $\text{NaAlSi}_3\text{O}_8$ )-DIOPSIDE ( $\text{CaMgSi}_2\text{O}_6$ )-  
SANIDINE ( $\text{KAlSi}_3\text{O}_8$ ) AND THEIR  
SIGNIFICANCE TO ALKALINE ROCK GENESIS

by

Richard Garth Platt

Department of Geology

Submitted in partial fulfillment  
of the requirements for the degree of  
Doctor of Philosophy

Faculty of Graduate Studies  
The University of Western Ontario  
London, Canada.  
September 1969

## ABSTRACT

Phase relations have been determined for the system Nepheline-Diopside-Sanidine at atmospheric pressure. Leucite, nepheline, diopside and olivine occur at the liquidus; melilite and a Ca-poor ternary feldspar are subliquidus phases. This system is a plane within the tetrahedron Nepheline-Kalsilite-Silica-Diopside, but because of the extensive solid solution of each crystallizing phase, it must be considered as a plane in the 6 component system  $\text{CaO-MgO-Al}_2\text{O}_3\text{-Na}_2\text{O-K}_2\text{O-SiO}_2$ .

The system has two piercing points at  $1158^\circ \pm 10^\circ\text{C}$  and  $\text{Ne}_{51}\text{Di}_{21}\text{San}_{28}$  where nepheline, olivine, diopside and liquid coexist; and at  $1120^\circ \pm 5^\circ\text{C}$  and  $\text{Ne}_{44.5}\text{Di}_{12}\text{San}_{43.5}$  where nepheline, leucite, diopside and liquid coexist. These piercing points represent intersections of univariant lines in the system Nepheline-Diopside-Sanidine. Two invariant points occur at subliquidus temperatures, consisting of nepheline, leucite, Ca-poor ternary feldspar, diopside and liquid; and melilite, olivine, diopside, nepheline and liquid. The former lies within the volume of the tetrahedron and the latter outside its volume. The first invariant point shows a leucite-liquid reaction, the second an olivine-liquid reaction.

Olivine and melilite react out completely and leucite

partially reacts out at subliquidus temperatures. Olivine reacts with liquid to form pyroxene. The melilite stability is governed by the feldspar content of the liquids with which it reacts to form diopside, nepheline and potential wollastonite. Leucite reacts with liquid to form feldspar and nepheline.

With crystallization in the system Nepheline-Diopside-Sanidine, residual liquids migrate from the plane of the system as a consequence of the crystallization of melilite, olivine and other complex solid solutions. Under conditions of equilibrium crystallization, residual liquids trend towards an invariant point within the tetrahedron Nepheline-Kalsilite-Silica-Diopside, at which nepheline, leucite, Ca-poor ternary feldspar, diopside and liquid coexist, and/or a temperature minimum where diopside, nepheline and Ca-poor ternary feldspar coexist.

With fractionation of leucite, residual liquid trends are controlled by the phase relations within the tetrahedron. The assemblages formed by such fractionation fall into three main rock series: leucitite (or nephelinite, if nepheline fractionates first) -leucitophyre-leucite phonolite-phonolite; leucitite-leucite trachyte-trachyte-phonolite; and leucitite-leucite trachyte-trachyte-rhyolite. With fractionation of melilite and olivine or olivine alone, residual liquid trends are controlled by phase relations lying outside the volume of the tetrahedron. With fractionation of

melilite and olivine, the two rock series which can form are: olivine melilitite-melilitite-melilite nephelinite-phonolite or wollastonite nephelinite?-wollastonite phonolite?; and olivine melilite nephelinite-nephelinite-phonolite or wollastonite nephelinite?-wollastonite phonolite?. With fractionation of olivine, the rock series olivine nephelinite-nephelinite-phonolite-wollastonite phonolite? is possibly obtained.

The results obtained indicate that, pseudoleucites can form by a leucite-liquid reaction; melilites originate from the desilication of pyroxene molecules by nepheline; olivine reactions may occur in rocks akin to alkali olivine basalts; residual liquids produced by fractionation of complex magmas become enriched in alkali aluminosilicate minerals and impoverished in more basic minerals, and the close association of nephelinitic lavas, often containing melilite and olivine, with phonolites may result from fractional crystallization in magmas rich in nepheline and pyroxene molecules and containing small amounts of sanidine or alkali feldspar molecules.

## ACKNOWLEDGEMENTS

The problem studied was suggested by Dr. H.S. Yoder and Dr. J.F. Schairer of the Geophysical Laboratory, Carnegie Institution of Washington, Washington, D.C., to whom, the author wishes to express his sincere thanks. The author wishes to thank Dr. A.D. Edgar for his constant support and guidance during the course of this study. Especial thanks are due Dr. J.F. Schairer for making available his facilities at the Geophysical Laboratory, for instructing the author in glass making techniques and for the unselfish way he gave of his time.

During the course of this study, helpful discussions were had with Dr. A.D. Edgar, Dr. J.F. Schairer, Mr. M.K. Sood and Dr. H.S. Yoder. The author is grateful to his wife, Jerrilyn, for typing the rough drafts of this thesis and for drafting certain of the figures.

Financial support, in the form of an Ontario Graduate Fellowship (1966-1967), a National Research Council Post-graduate Scholarship (1967-1969), The Society of the Sigma XI Grant-in-Aid of Research (1967), and a Penrose Bequest Research Grant (1142-67), Geological Society of America (1967), is gratefully acknowledged.



## TABLE OF CONTENTS

	Page
ABSTRACT . . . . .	.iii
ACKNOWLEDGEMENTS . . . . .	vi
LIST OF TABLES . . . . .	x
LIST OF FIGURES. . . . .	xi
CHAPTER	
1 Introduction. . . . .	1
2 Experimental Methods. . . . .	10
2.1 Preparation of the Starting Materials. . . . .	10
2.11 Preparation of the Glass Components. . . . .	10
2.12 Preparation of the Glasses . . . . .	13
2.13 Homogeneity of the Glasses . . . . .	15
2.14 Crystallization of the Glasses . . . . .	15
2.2 Apparatus. . . . .	18
2.21 'Dry' Furnaces . . . . .	18
2.211 The Crystallization Furnace. . . . .	18
2.212 The Making Furnace . . . . .	19
2.213 The Quenching Furnace. . . . .	20
2.22 Hydrothermal Apparatus . . . . .	21
2.3 Temperature Control and Measurement. . . . .	21
2.4 Quenching Experiments. . . . .	22
2.5 Identification and Compositions of the Phases . . . . .	23
2.6 Determination of Equilibrium . . . . .	24
3 Previous Studies and Experimental Results in the System Nepheline-Diopside-Sanidine. . . . .	27
3.1 Introduction . . . . .	27
3.2 Bounding Systems of the System Nepheline-Diopside-Sanidine. . . . .	27

## TABLE OF CONTENTS continued

CHAPTER		Page
3	3.21 The System Sanidine-Diopside . . . . .	27
	3.22 The System Nepheline-Sanidine. . . . .	29
	3.23 The System Nepheline-Diopside. . . . .	29
	3.3 Liquidus Phase Relations in the System Nepheline-Diopside-Sanidine. . . . .	34
	3.4 Subliquidus and Solidus Relations in the System Nepheline-Diopside- Sanidine . . . . .	45
	3.5 Instability of Melilites . . . . .	47
	3.6 Mineralogy of the Crystallizing Phases in the System Nepheline-Diopside- Sanidine . . . . .	49
	3.61 Nepheline. . . . .	50
	3.62 Olivine. . . . .	51
	3.63 Diopside . . . . .	51
	3.64 Leucite. . . . .	52
	3.65 Melilite . . . . .	52
	3.66 Feldspars. . . . .	53
	3.7 The Pseudoternary Nature of the System Nepheline-Diopside-Sanidine. . . . .	54
4	Residual Liquid Flow Diagrams for the System Nepheline-Kalsilite-Silica-Diopside . . . . .	56
	4.1 Introduction . . . . .	56
	4.2 Derivation of Flow Diagrams for the System Nepheline-Kalsilite-Silica- Diopside . . . . .	59
5	Crystallization and Residual Liquid Trends in the System Nepheline-Diopside-Sanidine . . . . .	85
	5.1 Introduction . . . . .	85
	5.2 Equilibrium Crystallization. . . . .	87
	5.3 Fractional Crystallization . . . . .	89
	5.31 Fractionation of Residual Liquids on the Line di + ne + lc + liq. . . . .	89

## TABLE OF CONTENTS continued

CHAPTER		Page
5	5.32 Fractionation of Residual Liquids on the Line di + fp + lc + liq. . . . .	92
	5.33 Fractionation of Residual Liquids on the Line ne + ol + di + liq. . . . .	93
	5.34 Fractionation of Residual Liquids on the Line di + ol + mel + liq. . . . .	95
	5.35 Fractionation of Residual Liquids on the Line ne + ol + mel + liq. . . . .	97
	5.35 Fractionation of Residual Liquids After the Disappearance of Melilite and Olivine. . . . .	97
6	Petrological Implications . . . . .	102
7	Conclusions and Proposals For Future Work . .	112
	7.1 Conclusions. . . . .	112
	7.2 Proposals for Future Work. . . . .	115
APPENDIX . . . . .		118
REFERENCES . . . . .		119
VITA . . . . .		124

## LIST OF TABLES

TABLE		Page
1	Mineral Molecule Formulae and Abbreviations . .	2
2	Glass Compositions and Refractive Indices . . .	16
3	Reversibility of the Quenching Experiments. . .	26
4	Experimental Results. . . . .	35
5	Piercing Points of Univariant Lines in Systems of the Tetrahedron Nepheline-Kalsilite-Silica- Diopside. . . . .	66
6 a.	Univariant Lines in the Volume of the Tetrahedron Nepheline-Kalsilite-Silica- Diopside. . . . .	67
b.	Univariant Lines Outside the Volume of the Tetrahedron Nepheline-Kalsilite-Silica- Diopside. . . . .	67
c.	Invariant Points Within the Volume of the Tetrahedron Nepheline-Kalsilite-Silica- Diopside. . . . .	67
d.	Invariant Points Lying Outside the Volume of the Tetrahedron Nepheline-Kalsilite-Silica- Diopside. . . . .	68
e.	Temperature Minima Within the Volume of the Tetrahedron Nepheline-Kalsilite-Silica- Diopside. . . . .	68
7	Rock Types Corresponding to Assemblages of Univariant Lines, Invariant Points and Temper- ature Minima of Figures 13 and 15 . . . . .	84
8	Equilibrium Crystallization History of Mixture Ne <sub>30</sub> Di <sub>10</sub> San <sub>60</sub> . . . . .	88

## LIST OF FIGURES

FIGURE	Page
1. The relationship of the system Nepheline-Diopside-Sanidine to the tetrahedron Nepheline-Kalsilite-Silica-Diopside . . . . .	5
2. Liquidus phase relations in the system Nepheline-Kalsilite-Silica (after Schairer, 1957) . . . . .	7
3. Liquidus phase relations in the system Potash Feldspar-Diopside (after Schairer and Bowen, (1938)). . . . .	28
4. Liquidus phase relations in the system Nepheline-Sanidine extrapolated from the system Nepheline-Kalsilite-Silica (after Schairer, 1957) . . . . .	30
5. Partial isothermal, isobaric phase relations in the system Nepheline-Kalsilite-Silica (after Fudali, 1963). . . . .	31
6. Phase relations in the system Nepheline-Diopside (after Schairer, Yagi and Yoder, 1962) . . . . .	33
7. Liquidus phase relations in the system Nepheline-Diopside-Sanidine . . . . .	43
8. Liquidus phase relations in the system Leucite-Diopside-Silica (after Schairer and Bowen, 1938). . . . .	61
9. Liquidus phase relations in the system Nepheline-Diopside-Silica (after Schairer and Yoder, 1960). . . . .	62
10. Partial liquidus phase relations in the system Diopside-Albite-Orthoclase (after Morse, 1968). . . . .	63
11. Liquidus phase relations in the system Diopside-Albite-Leucite (after Sood, 1969). . .	64

FIGURE		Page
12.	The system Nepheline-Kalsilite-Silica-Diopside. . . . .	65
13.	Flow diagram showing the univariant and invariant equilibria involving liquid lying within the system Nepheline-Kalsilite-Silica-Diopside . . . . .	70
14.	Schematic arrangement of univariant lines around the invariant point $ne + lc + fp + di + liq. (R')$ . . . . .	71
15.	Flow diagram showing the univariant and invariant equilibria involving liquid lying outside the system Nepheline-Kalsilite-Silica-Diopside . . . . .	79
16.	Simplified rock types produced by fractionation of residual liquids reaching the univariant line $di + ne + lc + liq.$ (Line 2, Figure 13). . . . .	91
17.	Simplified rock types produced by fractionation of residual liquids reaching the univariant line $di + fp + lc + liq.$ (Line 3, Figure 13). . . . .	94
18.	Simplified rock types produced by fractionation of residual liquids on the univariant line $ne + ol + di + liq.$ (Line 1, Figure 15). . . . .	96
19.	Simplified rock types produced by fractionation of residual liquids on the univariant line $di + ol + mel + liq.$ (Line 11, Figure 15) . . . . .	98
20.	Simplified rock types produced by fractionation of residual liquids on the univariant line $ne + ol + mel + liq.$ (Line 10, Figure 15) . . . . .	99
21.	Relationship between all possible rock types formed by the fractional crystallization of synthetic compositions crystallizing melilite and/or olivine. . . . .	100
22.	Differentiation trends of the mildly and strongly alkaline rocks of the northern Tanganyika alkaline district as indicated by a plot of $SiO_2$ against the Solidification Index (after Saggerson and Williams, 1964). . . . .	105

## CHAPTER I

### INTRODUCTION

This thesis is a study of the phase relations and residual liquid trends in the condensed system<sup>1</sup> Nepheline ( $\text{NaAlSi}_3\text{O}_8$ ) - Diopside ( $\text{CaMgSi}_2\text{O}_6$ ) - Sanidine ( $\text{KAlSi}_3\text{O}_8$ )<sup>2</sup> at atmospheric pressure. As such, it forms part of a more comprehensive study on the effects of adding a simplified pyroxene molecule ( $\text{CaMgSi}_2\text{O}_6$ ) to the system Nepheline-Kalsilite-Silica (Petrogeny's Residua System, Bowen, 1937). Other work in this study includes the system Diopside-Albite-Leucite (Sood, 1969) and the system Diopside-Albite-Orthoclase (Morse, 1968).

The system Nepheline-Diopside-Sanidine may be considered as a slice or join through the system Nepheline-Kalsilite-Silica-Diopside; and more specifically as a join through the

---

1. A condensed system is one in which the vapour pressures of the solid and liquid phases are negligible, or small, in comparison to atmospheric pressure. As pressure may be considered constant, one degree of freedom is lost and Gibb's phase rule may be modified to  $P + F = C + 1$ . In this thesis the term condensed system will be shortened to 'system' unless otherwise stated.

2. A list of mineral molecule formulae and abbreviations used in this thesis are given in Table 1.

TABLE 1  
Mineral Molecule Formulae and Abbreviations

<u>Mineral</u>	<u>Formula</u>	<u>Abbreviation</u> (if used)
Acmite	$\text{NaFeSi}_2\text{O}_6$	
Aegirine	"	
Aegirine-augite	$(\text{Na}, \text{Ca})(\text{Fe}^{+3}, \text{Fe}^{+2}, \text{Mg}, \text{Al})(\text{Si}_2\text{O}_6)$	
Akermanite	$\text{Ca}_2\text{MgSi}_2\text{O}_7$	Ak
Albite	$\text{NaAlSi}_3\text{O}_8$	Ab
Alkali feldspar	$\text{NaAlSi}_3\text{O}_8 - \text{KAlSi}_3\text{O}_8$	
Anhydrous Analcite	$\text{NaAlSi}_2\text{O}_6$	
Anorthite	$\text{CaAl}_2\text{Si}_2\text{O}_8$	
Ca Tschermak's molecule	$\text{CaAl}_2\text{SiO}_6$	
Cristobalite	$\text{SiO}_2$	
Diopside	$\text{CaMgSi}_2\text{O}_6$	Di
Forsterite	$\text{Mg}_2\text{SiO}_4$	
Gehlenite	$\text{Ca}_2\text{Al}_2\text{SiO}_7$	Geh
Jadeite	$\text{NaAlSi}_2\text{O}_6$	
Kalsilite	$\text{KAlSiO}_4$	Ks
Larnite	$\text{Ca}_2(\text{SiO}_4)$	
Leucite	$\text{KAlSi}_2\text{O}_6$	Lc
Mg Tschermak's molecule	$\text{MgAl}_2\text{SiO}_6$	
Nepheline	$\text{NaAlSiO}_4$	Ne
Olivine	mainly $\text{Mg}_2\text{SiO}_4$ in iron free systems. Natural olivine contains $\text{Fe}_2\text{SiO}_4$	Ol
Orthoclase	$\text{KAlSi}_3\text{O}_8$	Or
Plagioclase	$\text{NaAlSi}_3\text{O}_8 - \text{CaAl}_2\text{Si}_2\text{O}_8$	Plag.
Potash Feldspar	$\text{KAlSi}_3\text{O}_8$	Or or San
Quartz	$\text{SiO}_2$	
Sanidine	$\text{KAlSi}_3\text{O}_8$	San
Silica minerals	$\text{SiO}_2$	Sil



TABLE 1 continued.

<u>Mineral</u>	<u>Formula</u>	<u>Abbreviation</u> (if used)
Soda Melilite	$\text{NaCaAlSi}_2\text{O}_7$	SM
Sphene	$\text{CaTiSiO}_4(\text{O}, \text{OH}, \text{F})$	
Ternary feldspar	$\text{NaAlSi}_3\text{O}_8$ - $\text{KAlSi}_3\text{O}_8$ - $\text{CaAl}_2\text{Si}_2\text{O}_8$	Fp
Wollastonite	$\text{CaSiO}_3$	

silica-undersaturated portion of this system represented by the polyhedron Nepheline-Kalsilite-Albite-Sanidine-Diopside (Figure 1). This expanded system provides a better basis for the understanding of the genesis of undersaturated alkaline rocks than can be provided by the system Nepheline-Kalsilite-Silica alone.

The undersaturated alkaline rocks constitute a group of silica-deficient, alkali-enriched igneous rocks which is reflected in their mineralogy by the development of feldspathoids, sodic pyroxenes and sodic amphiboles. Chemically, the plutonic rocks of this type are characterized by their high volatile and rare element contents. Petrographically, undersaturated alkaline rocks are found in association with silica-saturated and oversaturated rocks although their volume, in comparison to those of basalts and granites, is relatively small.

'Petrogeny's Residua System'<sup>1</sup> (Bowen, 1937) represents the system towards which residual liquids produced on fractionation of complex magmas trend. These liquids are enriched in the alkali aluminosilicate and silica minerals with respect to more basic minerals (e.g. forsterite, fayalite, diopside and anorthite) representing early crystallizing phases. This concept of the 'residua system' developed from the study of systems such as Diopside-Albite-

---

1. 'Petrogeny's Residua System' will, unless otherwise stated, be abbreviated to 'residua system'.

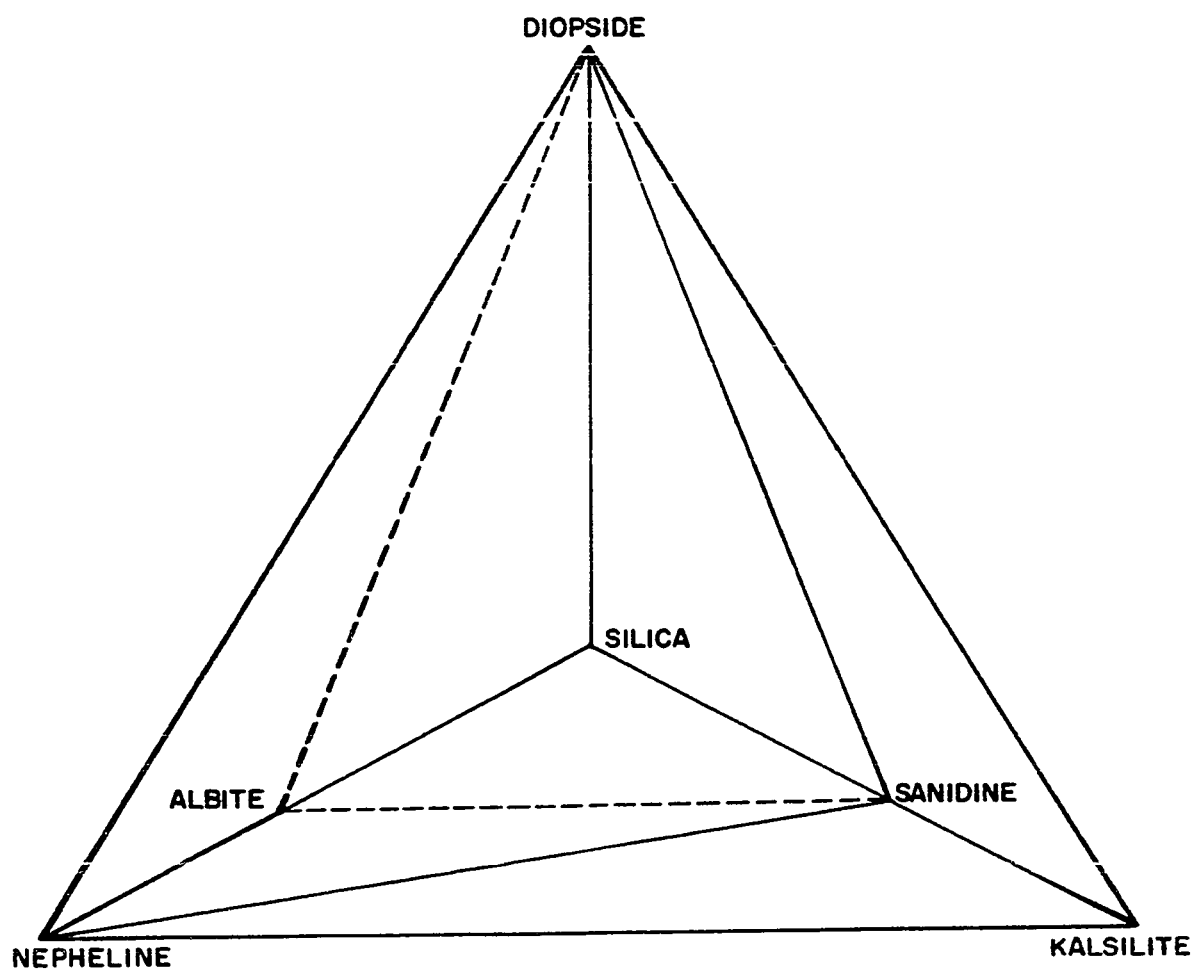


FIGURE 1. The relationship of the system Nepheline-Diopside-Sanidine to the tetrahedron Nepheline-Kalsilite-Silica-Diopside.

Anorthite (Bowen, 1915), Leucite-Diopside-Silica (Schairer and Bowen, 1938), Nepheline-FeO-Silica (Bowen and Schairer, 1938) and Anorthite-Leucite-Silica (Schairer and Bowen, 1947), all of which show an enrichment of the alkali-aluminosilicate and silica minerals in the residual liquids with fractional crystallization.

The 'residua system' is characterized by two low temperature troughs of minimum melting liquids separated by a high temperature 'saddle' on the Albite-Sanidine join (Figure 2). If crystal-liquid equilibria has been operative in the formation of rocks whose mineralogy can be represented by the 'residua system' (i.e. granites/rhyolites and nepheline syenites/phonolites), these rocks should be related to these belts of minimum melting liquids. This relationship has been proven by various workers (Tuttle and Bowen, 1958; Hamilton and MacKenzie, 1965).

Petrologically important as the 'residua system' is, it has certain deficiencies. Most alkaline rocks, even of the phonolitic type, contain appreciable amounts of basic molecules, principally pyroxenes, olivines, micas and/or amphiboles. The addition of a basic constituent to the 'residua system' increases the number of rock types which can be represented by such a system, and consequently, relationships between the more basic undersaturated alkaline rocks and the felsic undersaturated alkaline rocks can be studied.

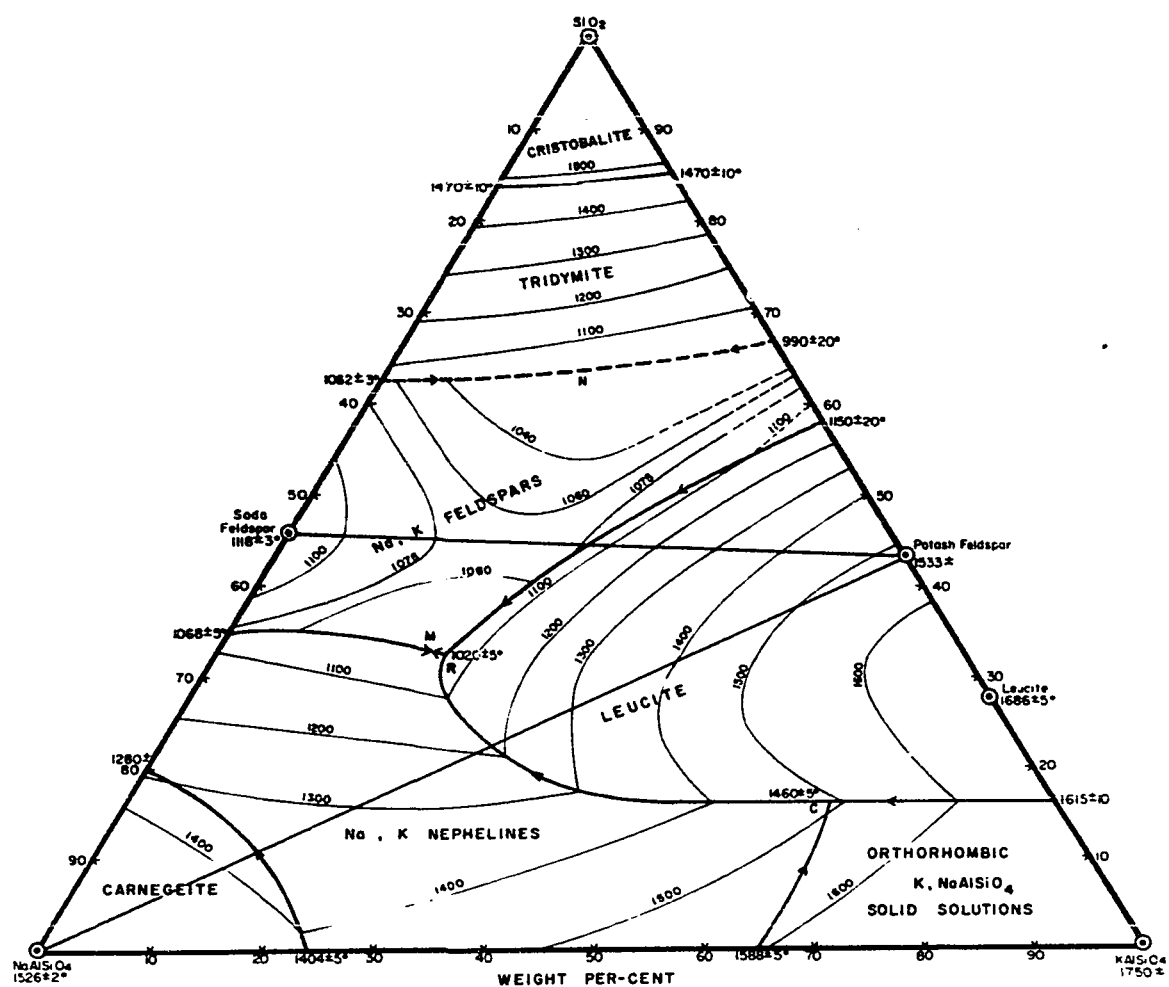


FIGURE 2. Liquidus phase relations in the system Nepheline-Kalsilite-Silica (after Schairer, 1957).

Although diopside is perhaps not the most important basic mineral molecule, it does constitute an important pyroxene molecule of many alkaline undersaturated rocks. Diopside is an important pyroxene molecule in many nephelinites (nepheline-pyroxene rocks). Tyler and King (1967) have shown that such rocks from Uganda contain nearly colourless or pale-green, diopside. Many leucitites (leucite-pyroxene rocks) also contain diopsidic pyroxenes, although the compositions may range from diopside to aegirine-augite to aegirine (Johannsen, 1938, V. IV., p. 354). Pyroxenes of leucitophyres (leucite-nepheline-pyroxene rocks) are augitic in composition (Johannsen, 1938, V. IV., p. 360); these pyroxenes probably being solid solutions of  $\text{CaMgSi}_2\text{O}_6$  -  $\text{CaFeSi}_2\text{O}_6$  -  $\text{MgSiO}_3$  -  $\text{FeSiO}_3$  -  $\text{NaFeSi}_2\text{O}_6$ .

In the more felsic alkaline rocks (e.g. phonolites), the pyroxenes are usually rich in acmitic molecules ( $\text{NaFeSi}_2\text{O}_6$ ), as is the case in the Ugandan rocks (Tyler and King, 1967). For a study of these rocks, the pyroxene molecules added to the synthetic systems should really be composed of a mixture of acmite and diopside instead of diopside alone, as in the present study.

This study is one of the first to combine sodium and potassium aluminosilicate mineral molecules with an early-forming basic molecule. As subsequently discussed (Chapters 3 and 4), there is good evidence that the oxide constituents of the system Nepheline-Diopside-Sanidine (i.e.  $\text{CaO}$ ,  $\text{MgO}$ ,

$\text{Al}_2\text{O}_3$ ,  $\text{Na}_2\text{O}$ ,  $\text{K}_2\text{O}$  and  $\text{SiO}_2$ ) act independently, resulting in a six component system. Consequently, mixtures in this system are analagous to complex undersaturated alkaline magmas, although simplified due to the lack of iron oxides and volatiles. Its study augments the understanding of equilibrium and fractional crystallization trends in such magmas. However, the results obtained are limited to the interpretation of volcanic rocks in that the work was undertaken at atmospheric pressure.

## CHAPTER 2

### EXPERIMENTAL METHODS

#### 2.1 Preparation of the Starting Materials

The starting materials used in this study consisted of chemically homogeneous glasses, crystallized, in whole or in part, to prevent supercooling during the quenching experiments. The glasses were prepared by the repeated fusions of the required proportions of 'pure'  $\text{SiO}_2$ ,  $\text{Al}_2\text{O}_3$ ,  $\text{MgO}$ ,  $\text{CaCO}_3$ , crystalline sodium disilicate ( $\text{Na}_2\text{Si}_2\text{O}_5$ ) and crystalline potassium disilicate ( $\text{K}_2\text{Si}_2\text{O}_5$ ) at temperatures in excess of  $1300^\circ\text{C}$ . These fusions were carried out in a platinum crucible using a platinum wound furnace.

##### 2.11 Preparation of the Glass Components.

$\text{SiO}_2$ : High purity quartz from Lisbon, Maryland, kindly supplied by Dr. J.F. Schairer of the Geophysical Laboratory, Carnegie Institution of Washington, was used as the source of  $\text{SiO}_2$ . Three determinations of the  $\text{SiO}_2$  content of the quartz by HF evaporation gave an average yield of 99.97%. The quartz was crushed in a steel mortar to pass through a 60 mesh sieve and stray steel fragments were removed with a strong magnet and by hand picking. After treating with a hot solution of dilute  $\text{H}_2\text{SO}_4$  and  $\text{HCl}$  to remove traces of iron oxides, the crushed quartz was washed with distilled water,



dried and roasted for two hours at  $1500^{\circ}\text{C}$ . to remove liquid inclusions and to convert it to  $\beta$ -cristobalite. Cristobalite was preferred to quartz as a source of  $\text{SiO}_2$  because of its higher chemical potential and hence its greater reactivity.

$\text{Al}_2\text{O}_3$ : Aluminum dust, stated to be 99.99% pure and kindly supplied by the British Aluminium Company Ltd., was used as the source of  $\text{Al}_2\text{O}_3$ . The aluminum was dissolved in hot concentrated  $\text{HNO}_3$  and from the resulting solution  $\text{Al}(\text{NO}_3)_3$  was decomposed to the oxide by gentle heating over a 'Meker burner'. The  $\text{Al}_2\text{O}_3$  was roasted for four hours in an electric furnace at  $1400^{\circ}\text{C}$ . producing corundum.

$\text{MgO}$ : Analar Grade  $\text{MgO}$  (British Drug Houses Company Ltd.) was dried for five hours at  $500^{\circ}\text{C}$ . and used as the source of  $\text{MgO}$ .

$\text{CaO}$ : Spec. pure  $\text{CaCO}_3$  (Johnson Matthey and Mallory Ltd., Laboratory Number S6569) was dried for five hours at  $500^{\circ}\text{C}$ . and used as the source of  $\text{CaO}$ .

$\text{Na}_2\text{O}$ : Crystalline  $\text{Na}_2\text{Si}_2\text{O}_5$  was used as the source of  $\text{Na}_2\text{O}$ . The  $\text{Na}_2\text{Si}_2\text{O}_5$  was prepared by the method of Schairer and Bowen (1956). The required proportions of  $\text{Na}_2\text{CO}_3$  (Fisher Certified Reagent Lot 744706) and  $\text{SiO}_2$  were heated for two days at a temperature a little below the minimum melting temperature of  $789 \pm 1^{\circ}\text{C}$ . in the system  $\text{Na}_2\text{O} - \text{SiO}_2$  (Kracek, 1930, 1939). At this temperature most of the  $\text{CO}_2$  can be expelled without melting of the mixture and serious loss of alkalies and other material. This was followed by fusions

at progressively higher temperatures up to  $1200^{\circ}\text{C}$ . to allow for the maximum combination of  $\text{Na}_2\text{O}$  and  $\text{SiO}_2$ . The molten material was quenched in a desiccator to prevent addition of moisture. Any loss of  $\text{Na}_2\text{O}$ , as determined from the weight loss of the crucible after fusion, was corrected by the addition of further  $\text{Na}_2\text{CO}_3$ . The glass-carbonate mixture was then heated at  $750^{\circ}\text{C}$ . for 12 hours to allow for complete decomposition of the  $\text{Na}_2\text{CO}_3$ . This was followed by three, one hour fusions; the glass being crushed after each fusion. This gave a homogeneous glass of  $\text{Na}_2\text{Si}_2\text{O}_5$ . As this glass is hygroscopic, it was crystallized at  $800^{\circ}\text{C}$ .

$\text{K}_2\text{O}$ : Crystalline  $\text{K}_2\text{Si}_2\text{O}_5$ , used as the source of  $\text{K}_2\text{O}$ , was prepared by the method of Schairer and Bowen (1955). The required proportions of Analar Grade  $\text{KHCO}_3$  (British Drug Houses Company Ltd., Lot 26229) and  $\text{SiO}_2$  were heated for approximately 5 days at a temperature slightly below the minimum melting temperature of  $742 \pm 2^{\circ}\text{C}$ . in the system  $\text{K}_2\text{O} \cdot \text{SiO}_2 - \text{SiO}_2$ , (Kracek, Bowen and Morey, 1929). At  $700^{\circ}\text{C}$ .,  $\text{KHCO}_3$  and  $\text{SiO}_2$  combine with the loss of  $\text{CO}_2$  and  $\text{H}_2\text{O}$  but with little or no loss of alkalies or other material by volatilization, frothing or spattering. The mixture was then fused slowly to  $1200^{\circ}\text{C}$ . After fusion, the molten material was quenched in a desiccator to prevent addition of moisture. Any loss of alkalies was determined by the weight loss of the crucible after quenching. This loss was corrected with the further addition of  $\text{KHCO}_3$ . This was followed by decompo-

sition of the bicarbonate at  $750^{\circ}\text{C}$ . for twelve hours and by three, one hour fusions at  $1200^{\circ}\text{C}$ . with intermediate crushings. According to Kracek (1932) and Schairer and Bowen (1955), this procedure produces a homogeneous glass of  $\text{K}_2\text{Si}_2\text{O}_5$ . As the resulting glass was extremely hygroscopic, it was crystallized at  $750^{\circ}\text{C}$ .

The prepared glass components were kept free from  $\text{CO}_2$  and moisture by storing them in a desiccator containing KOH.

#### 2.12 Preparation of the Glasses.

Five grams of glass for each of the required compositions were made by the fusion of the glass components in a 25 cc. platinum crucible using a platinum-wound vertical furnace. The crucible was placed in the 'hot spot' of the furnace, using a length of platinum wire, and heated for one hour periods at  $1000^{\circ}\text{C}$ . and  $1250^{\circ}\text{C}$ . to decompose the  $\text{CaCO}_3$ . This was followed by fusion of the mixture at a temperature in excess of  $1300^{\circ}\text{C}$ ., the actual temperature depending on the liquidus temperature of the glass and the amount of  $\text{Al}_2\text{O}_3$  to be dissolved. Glasses with high liquidus temperatures required correspondingly higher fusion temperatures than glasses with lower liquidus temperatures. Likewise, glasses rich in  $\text{Al}_2\text{O}_3$  required higher fusion temperatures than glasses with smaller amounts of  $\text{Al}_2\text{O}_3$ . As a general rule a temperature approximately  $200^{\circ}\text{C}$ . higher than the liquidus temperature of the glass, with six to eight fusions and intermediate crushings, was usually sufficient to ensure the

complete solution of the  $\text{Al}_2\text{O}_3$  and rapid attainment of homogeneity in the glass.

A major problem in fusing the glasses at high temperatures is the loss of alkalies by volatilization. Various workers (see Schairer and Bowen, 1956, pp. 159-160) have shown that the addition of  $\text{CaO}$  and  $\text{MgO}$  to an alkali silicate melt tends to increase the loss of alkalies, while the addition of  $\text{Al}_2\text{O}_3$  has the opposite effect, tending to stabilize the alkalies. The solution of the  $\text{Al}_2\text{O}_3$  in the melt is, however, one of the major difficulties encountered during preparation but this can be overcome with the use of finely powdered  $\text{Al}_2\text{O}_3$ , carefully mixed with the other glass components, and by crushing the glass after every fusion.

After each fusion the molten glass was quenched by placing the crucible in a shallow tray of cold water; the crucible being covered with a platinum lid to prevent loss of material by decrepitation. Following this, two methods of crushing the quenched glass were employed. Rough crushing and fine crushing, were used depending on the degree of homogeneity attained. Until the majority of the  $\text{Al}_2\text{O}_3$  had dissolved, loss of material was prevented by rough crushing which involved breaking the glass from the crucible by tapping with a small hammer. At the stage where only microscopic  $\text{Al}_2\text{O}_3$  remained undissolved, the glass was crushed to a fine powder using a steel mortar and pestle, steel fragments being removed with a strong magnet. After each

crushing and before refusion, the glass was reheated at 1000°C. for 10 minutes to prevent loss of material by decrepitation.

A list of the glass compositions is given in Table 2.

### 2.13 Homogeneity of the Glasses.

The degree of homogeneity attained by the glass was determined with refractive index liquids following the method outlined by Schairer (1959). A small portion of powdered glass is placed under a cover slip on a microscope slide and immersed in a refractive index liquid approximately 0.005 higher than that of the glass. The slide is heated on a hot plate to lower the refractive index of the liquid below that of the glass, and then placed on the stage of a petrographic microscope. On cooling, a temperature is reached at which glass and liquid have exactly the same refractive index and at this time, if homogeneous, every fragment of glass visible in the microscopic field of view disappears simultaneously. Any inhomogeneity is readily apparent because of the varying refractive indices of the individual fragments.

The refractive index of the glasses is given in Table 2.

### 2.14 Crystallization of the Glasses.

Silicate glasses, especially those rich in alkali aluminosilicates, show a marked tendency to undercool (Schairer, 1959) and unless crystallized before use they may give erroneous results from the quenching experiments. For this reason, each glass was crystallized at approximately

TABLE 2

Glass Compositions and Refractive Indices

<u>Composition (weight percent)</u>			<u>Refractive Index</u> (white light, 25°C)
<u>Nepheline</u>	<u>Diopside</u>	<u>Sanidine</u>	
45	50	5	1.553
40	50	10	1.552
43	40	17	1.539
8	32	60	1.521
8	30	62	1.518
55	30	15	1.531
50	26	24	1.527
23	26	51	1.519
52.5	25.5	22	1.528
68	25	7	1.527
32	23	45	1.518
25	20	55	1.513
30	20	50	1.515
40	20	40	1.518
50	20	30	1.518
48	15	37	1.514
43	13	44	1.511
44	12	44	1.510
43.5	10.5	46	1.508
30	10	60	1.504
45	10	45	1.510
42	8.5	49.5	1.506
42	6	52	1.503
45	5	50	1.504

1000°C. for a period ranging from a few days to several months, the crystallization being aided by frequent crushings. A close check on the degree of crystallization of the glass was made by periodic identification of the phases using x-ray and microscopic techniques.

Of the phases encountered in this study (leucite solid solution,<sup>1</sup> diopside, nepheline, olivine, melilite and feldspar),<sup>2</sup> all but the feldspar crystallized readily, although temperatures considerably higher than 1000°C. were required for the crystallization of melilite and olivine. The crystallization of the feldspar is prevented by the high viscosity of the alkali aluminosilicate-rich residual liquids (cf. Schairer and Bowen, 1935, 1947).

This problem was overcome by hydrothermal crystallization of the glasses at 675°C. and 15,000 p.s.i.  $P_{H_2O}$  for approximately 7 days in cold-seal pressure vessels (Tuttle, 1949), using the sealed capsule technique of Goranson (1931). Approximately 7 to 8 percent by weight of water in each charge allowed crystallization to take place under vapour deficient conditions and eliminated the possible loss of material to a vapour phase.

---

1. As all the solid phases discussed in this thesis are solid solutions, the term solid solution is omitted during the remainder of the thesis.

2. The feldspar is believed to be a Ca-poor ternary feldspar. This is abbreviated to feldspar or fp. for the remainder of the thesis.

## 2.2 Apparatus.

### 2.21 'Dry' Furnaces.

Three types of dry furnace were used in this study, these were;

1. A furnace used primarily for the crystallization of the glasses, (Crystallization Furnace).
2. A furnace used for glass making, (Making Furnace).
3. A furnace used for the quenching experiments, (Quenching Furnace).

The furnace shells were made of 1/8" sheet steel, rolled to the required diameter and enclosed at the top and bottom by 1/4" sheet asbestos. Electrical binding posts set either in the side or base of each furnace served as connections between the furnace windings and the voltage supply. Light calcined MgO was used as an insulating medium which required periodic repacking because of its shrinking tendencies at high temperatures.

#### 2.211 The Crystallization Furnace

The basic component of this furnace was a spiralled 'alundum' muffle tube (Norton International Inc.) with the following specifications:

core 4" bore

length 4 7/16"

wall thickness 3/8"

grove 3/16" deep, width 5/16", 2 1/2 turns per inch.

The windings consisted of #14 B and S gauge 'Nichrome V'



wire (0.064" in diameter) supplied by Driver Harris Co. and coiled into a 10 foot length (exclusive of the leads). This coil had an inside diameter of 9/64" and 9 turns per inch and was inserted into the spiral groove of the muffle tube and held in place with 'alundum' cement.

#### 2.212 The Making Furnace.

This furnace consisted of two RA 98 'alundum' tubes (Norton International Inc.) inserted one inside the other. The inner tube had specifications of:

1 3/4" bore

1/16" wall thickness

12" length.

The bore was sufficiently large to permit insertion of a 25 cc. platinum crucible. The furnace windings of 8 turns per inch, wound around the inner tube, required 95 grams of #20B and S gauge platinum wire (0.8 mm. in diameter) supplied by Johnson Matthey and Mallory Ltd.

The outer tube had specifications of:

2 3/4" bore

1/8" wall thickness

12" length

The space between the tubes was packed with 60 mesh granular 'alundum' (Blue Label Alundum Grain, Norton International Inc.) which, because of its good heat conductivity, provided a more even heat distribution along the windings. This is particularly important as shrinkage of the MgO insulation may

lead to a local increase in temperature along the windings with subsequent melting and failure.

### 2.213 The Quenching Furnace.

This type of furnace was similar in design to the Making Furnace but consisted of three coaxial tubes instead of two. The innermost tube, composed of Mullite MV 30 (McDanel Refractory Porcelain Company Ltd.) had the following specifications:

9/16" bore

1/4" wall thickness

12" length

Small portions of this tube protruded from the top and bottom of the furnace to facilitate placement and removal of the charge.

The middle tube was composed of RA 98 'alundum' and had specifications of:

7/8" bore

1/8" wall thickness

10 1/2" length

The furnace windings, consisting of 95 grams of #20 B and S gauge platinum wire (0.8 mm. in diameter Johnson Matthey and Mallory Ltd.), were wound at 11 turns per inch around this tube.

The outer tube of RA 98 'alundum' had specifications of:

1 1/2" bore

1/8" wall thickness

10 1/4" length

The space between the middle and outer tubes was packed with grain 'alundum' for the same reasons mentioned previously (pp. 19-20). The inner sample tube provides a safety device to protect the platinum wound middle tube from liquid leaking from the platinum capsules during the experiments.

## 2.22 Hydrothermal Apparatus

The hydrothermal apparatus consisted of a Tem-Pres Research Inc. high pressure - high temperature hydrothermal research unit, Model HR - 1B fitted with cold-seal pressure vessels (Tuttle, 1949). Water was pumped into the pressure vessel by an air-operated pressure generator and the pressure measured with a Bourdon tube gauge. The recorded pressure is believed to be accurate to within  $\pm 4\%$  of the stated value.

## 2.3 Temperature Control and Measurement

Temperature control of the dry furnaces was obtained by regulating the voltage to the furnace windings with a variable voltage regulator ('Variac' Model W 20, General Radio Company) placed in circuit between the windings and the main line voltage. This type of controller does not automatically compensate for variations in the line voltage and fluctuations of  $\pm 10^{\circ}\text{C}$ . were common.

The temperature of the quenching furnace was measured with a Pt - Pt 10% Rh. thermocouple (0.01" in diameter, Johnson Matthey and Mallory Ltd.) previously calibrated at the melting points of sodium chloride ( $800.4^{\circ}\text{C}$ .) and diopside

(1,391.5°C.). Recalibrations of the thermocouple were made every three months. A 0°C. reference junction was used to standardize the temperature measurements. The difference in potential between the reference junction and the furnace thermocouple was recorded on a Leeds and Northrup of Canada Ltd. millivolt potentiometer (Catalogue Number 8690) and converted to temperature using the National Bureau of Standards Circular #561 (1955). All temperatures measured are accurate to within  $\pm 5^{\circ}\text{C}$ .

Temperature control of the hydrothermal furnaces was obtained by using pyrometric controllers (Gardsmen Indicating Pyrometric Controller, Model JP, West Instrument Corporation) and chromel - alumel controlling thermocouples (0.0201" in diameter) supplied by Driver Harris Company Ltd.) The temperatures of the hydrothermal experiments were measured on a Honeywell, continuously recording, multipoint potentiometer using chromel - alumel thermocouples (0.0076" in diameter, supplied by Driver Harris Company Ltd.) calibrated at the melting point of sodium chloride (800.4°C.). The recording thermocouples were replaced after each experiment and the temperatures obtained are believed to be accurate to within  $\pm 10^{\circ}\text{C}$ .

#### 2.4 Quenching Experiments

Quenching experiments on the crystallized glasses were conducted using the method of Shepherd, Rankin and Wright (1909). A small charge of powdered glass was wrapped in an

envelope of 0.005" platinum foil having an area of 0.35 square inches. This envelope was suspended in the 'hot spot' of the furnace at a 'fixed temperature' for a desired length of time. At the end of the experiment the sample was quenched rapidly in air and the products examined. Where it was suspected that products might form on cooling, the charge was quenched by passing a current through the thin platinum wire holding it. This allowed the charge to drop into a dish of mercury placed directly under the inner tube of the furnace, thus permitting extremely rapid quenching.

## 2.5 Identification and Compositions of the Phases.

After quenching, the charge was crushed in an agate mortar and the products identified using microscopic, x-ray and electron microprobe techniques. Microscopic identification was based on the optical and morphological properties of the phases. To aid examination, the crushed powder was mounted in an appropriate refractive index liquid. Routine x-ray examinations of the products were made using Cu  $K_{\alpha}$  radiation with a Philips high angle diffractometer with an auto focusing monochrometer. The diffractometer was set to scan at  $1^{\circ} 2\theta$  per minute with a chart speed of 600 mm. per hour. Electron microprobe identification of the phases was made using an MAC 400 electron microprobe utilizing a specimen current of .075  $\mu$ amps and an acceleration voltage of 15 Kv.

In the majority of cases exact phase compositions could

not be determined, for the following reasons:

- a. the size of crystals; which limited the use of optical and electron microprobe techniques and,
- b. the lack of x-ray methods for determining the compositions of the complex solid solutions encountered in this study (see Chapter 3).

In certain instances, semiquantitative determinations of compositions were made with the electron microprobe to determine the types of solid solutions occurring.

## 2.6 Determination of Equilibrium.

Fyfe (1960, p. 564) stated that; "Conditions of experimental synthesis need not necessarily reflect conditions of stability. Unless reversibility of reactions is rigorously established, synthetic results should not be considered as equilibrium results". Reversibility in the above sense was defined by Turner and Verhoogen (1960, p. 7) as follows: "A reaction is said to proceed reversibly when the system is balanced in such a manner that an infinitesimal change in conditions will cause the reaction to proceed in the opposite direction". If, therefore, the crystallization and reaction processes operative in the present system are reversible, equilibrium is presumed to be established.

Whether this equilibrium is stable or metastable can not be proved with certainty. Fyfe (1960) states that crystallization of metastable phases from a glass is much less common than from other starting materials (e.g. coprecipitated gels). Other tests of equilibrium in dry systems have

been outlined by Schairer (1959) and Roedder (1959).

Reversibility in the present study was tested by approaching the crystallization or reaction temperature from the high temperature assemblage (powdered glass) and from the low temperature assemblage (powdered crystalline material). The temperatures of reversibility obtained agreed within  $\pm 10^{\circ}\text{C}$  (see Table 3) and equilibrium was therefore assumed to have been established. One exception in reversibility was encountered in the case of feldspar crystallization, where the feldspar could only be crystallized hydrothermally and not directly from the glass by 'dry' crystallization. Consequently the reactions involving feldspars could only be approached from one direction and therefore should not be considered as equilibrium reactions ("sensu stricto").

TABLE 3

Reversibility of the Quenching ExperimentsCOMPOSITION  $\text{Ne}_{45}\text{Di}_{50}\text{San}_5$ 

<u>T°C</u>	<u>Time</u> (hours)	<u>Phases</u>	
		<u>Crystalline Material</u>	<u>Powdered Glass</u>
1249	24	gl.	gl.
1238	24	ol + gl.	ol + gl.
1198	28	di + ol + gl.	di + ol + gl.
1186	41	mel + di + ol + gl.	mel + di + ol + gl.
1153	53	mel + di + ol + gl.	mel + di + ol + gl.
1141	48	ne + mel + di + ol? + gl.	ne + mel + di + ol? + gl.

COMPOSITION  $\text{Ne}_{42}\text{Di}_{8.5}\text{San}_{49.5}$ 

1186	37	gl.	gl.
1172	45	lc + gl.	lc + gl.
1130	43	lc + gl.	lc + gl.
1118	49	ne + lc + gl.	ne + lc + gl.
1108	53	ne + lc + gl.	ne + lc + gl.
1091	67	di + ne + lc + gl.	di + ne + lc + gl.

For an explanation of the symbols, see Table 4, page 35.



## CHAPTER 3

PREVIOUS STUDIES AND EXPERIMENTAL RESULTS IN THE  
SYSTEM NEPHELINE-DIOPSIDE-SANIDINE3.1 Introduction.

This chapter deals primarily with the liquidus, sub-liquidus and solidus phase relations in the system Nepheline-Diopside-Sanidine at atmospheric pressure. These relations were obtained from more than 400 quenching experiments of 24 homogeneous glasses, the results of which are given in Table 4. The liquidus phase relations are represented in Figure 7. The application of these data in defining the trends of residual liquids with equilibrium and fractional crystallization, and the petrological significance of these trends, will be discussed in the proceeding chapters.

3.2 Bounding Systems of the System Nepheline-Diopside-Sanidine.3.21 The System Sanidine-Diopside.

This system forms part of the larger system Leucite-Diopside-Silica (Schairer and Bowen, 1938). The liquidus is characterized by a temperature minimum at  $\text{San}_{65}\text{Di}_{35}$  and  $1300 \pm 3^\circ\text{C}$ . where leucite and diopside coexist (Figure 3). Although not shown in Figure 3, the crystallization of leucite results from the incongruent melting of sanidine at  $1150 \pm 20^\circ\text{C}$ . to produce a liquid of composition  $\text{Lc}_{57.8}\text{Si}_{42.2}$

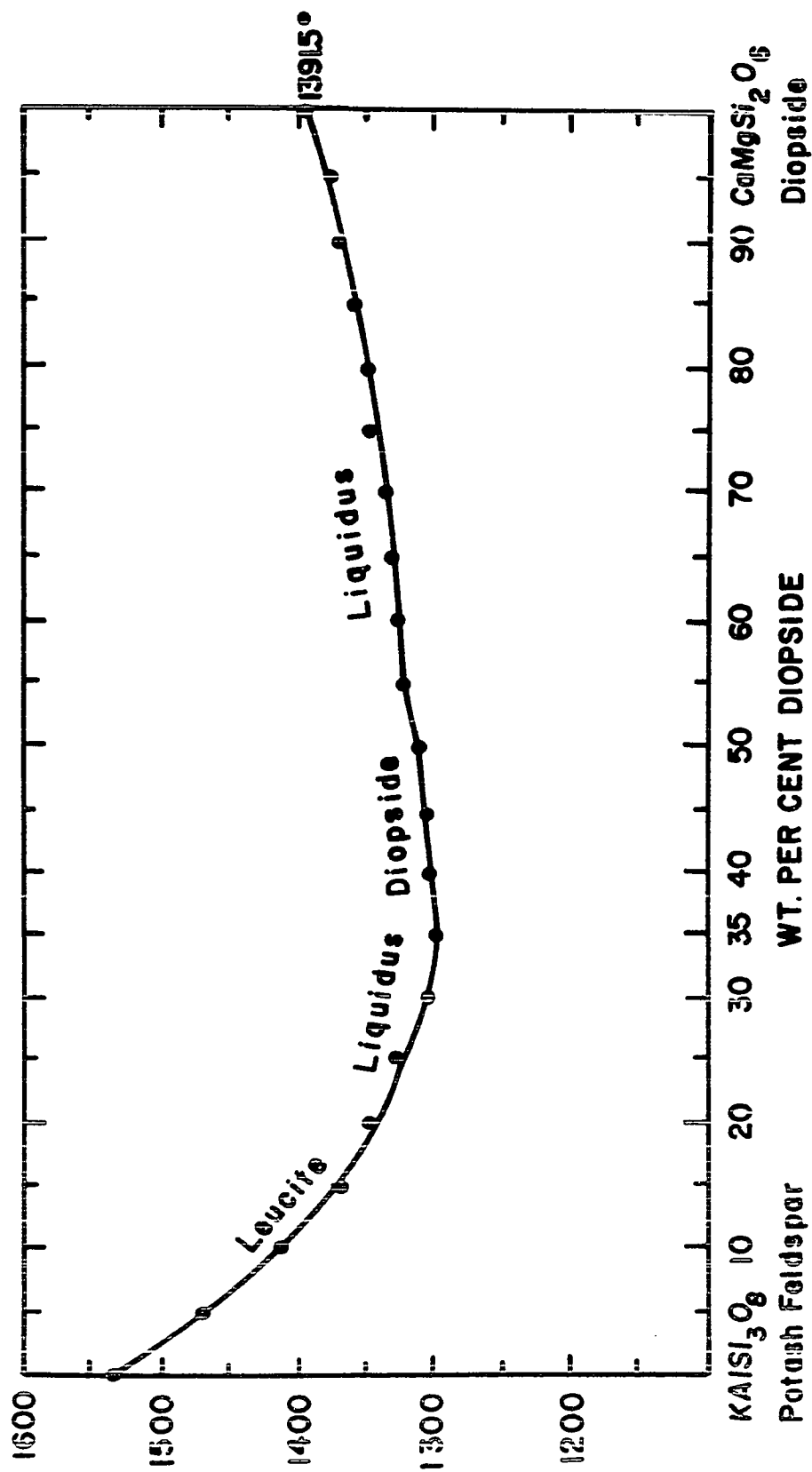


FIGURE 3. Liquidus phase relations in the system Potash Feldspar-Diopside  
(after Schairer and Bowen, 1938).

(Schairer and Bowen, 1955). Completely crystalline products in this system consist of potash feldspar (sanidine) and diopside.

### 3.22 The System Nepheline-Sanidine.

Liquidus phase relations were extrapolated from the system Nepheline-Kalsilite-Silica (Schairer, 1957) and from data kindly supplied by Dr. J. F. Schairer. The system is pseudobinary with a minimum melting temperature of slightly less than 1200°C. at a composition of  $\text{Ne}_{47}\text{San}_{53}$ . Leucite occurs at the liquidus due to the incongruent melting of sanidine and to a region of primary leucite crystallization. The point at which leucite begins crystallizing independently of the sanidine component is not known. Some indication as to the nature of the liquidus surface for this system can be obtained from Figure 4.

Although complete subliquidus and solidus data are lacking for the 'dry' system, some estimate of these relationships can be obtained from the partial, isothermal, isobaric diagram of the 'residua system' published by Fudali (1963) and reproduced here as Figure 5. Wholly crystalline assemblages comprise alkali feldspar + leucite, nepheline + alkali feldspar + leucite and nepheline + alkali feldspar.

### 3.23 The System Nepheline-Diopside.

This system was first studied by Bowen (1922) in an attempt to explain the genesis of the alnöitic rocks at Isle Cadieux, Quebec. A revised phase diagram, after Schairer,

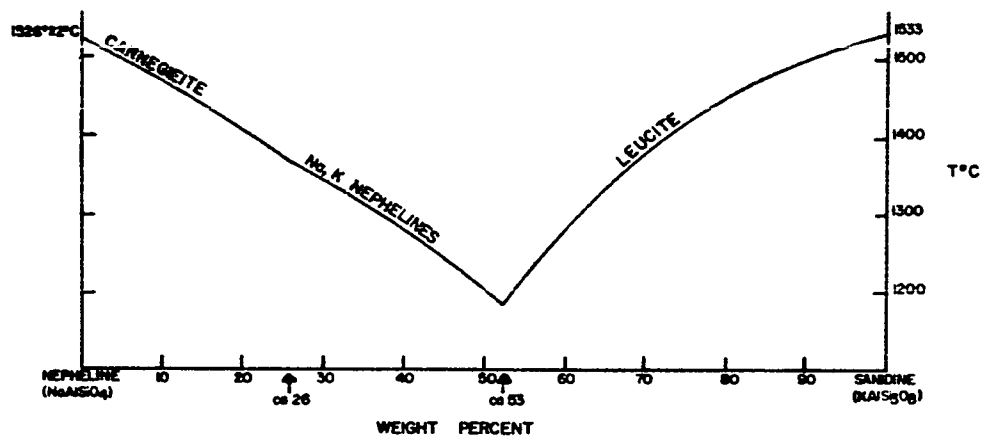


FIGURE 4. Liquidus phase relations in the system Nepheline-Sanidine extrapolated from the system Nepheline-Kalsilite-Silica (after Schairer, 1957).

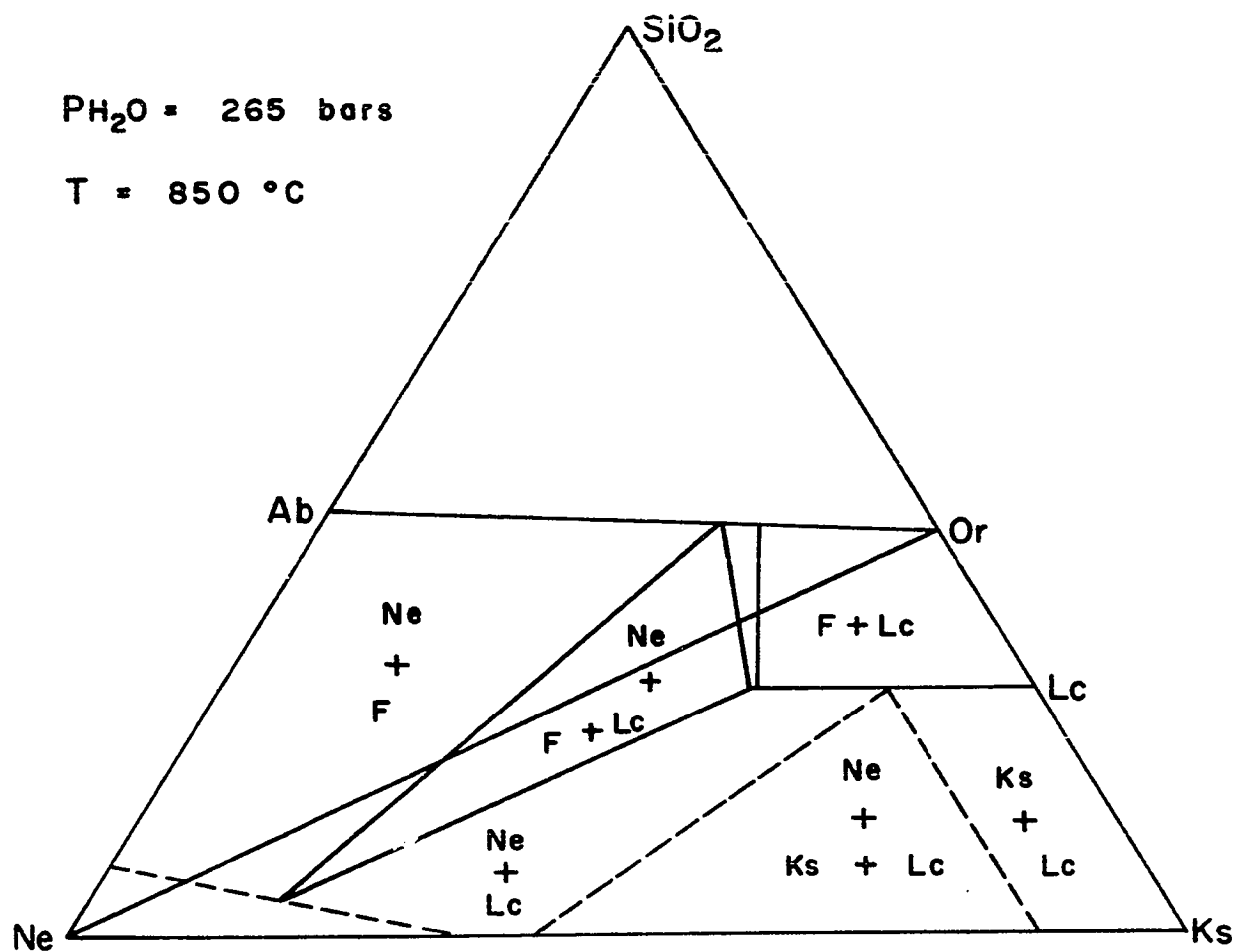
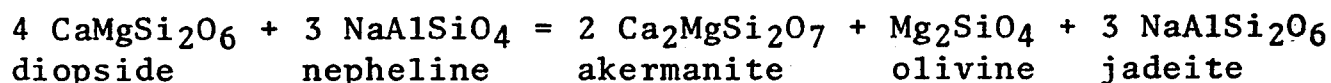


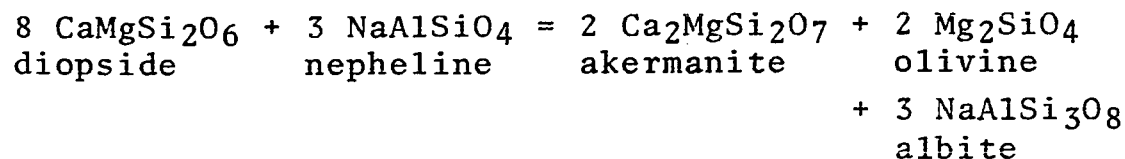
FIGURE 5. Partial isothermal, isobaric phase relations in the system Nepheline-Kalsilite-Silica (after Fudali, 1963).

Yagi and Yoder (1962), is shown as Figure 6. It is characterized by primary crystallization of olivine, nepheline and diopside and the subliquidus crystallization of melilite. The liquidus field of olivine extends from  $\text{Ne}_{38}\text{Di}_{62}$  at  $1193 \pm 2^\circ\text{C}$ . to  $\text{Ne}_{68}\text{Di}_{32}$  at  $1258 \pm 3^\circ\text{C}$ . This system is pseudobinary and represents a join in the quinary system  $\text{Na}_2\text{O}-\text{CaO}-\text{MgO}-\text{Al}_2\text{O}_3-\text{SiO}_2$ .

Reaction of nepheline and diopside at high temperature results in the formation of olivine and melilite, for which Bowen (1922) proposed the reaction:



the jadeite molecule entering into solid solution with the diopside. Yoder and Tilley (1962) reject this mechanism, on the grounds that clinopyroxenes of melilite-bearing lavas contain insufficient jadeite molecules, and proposed the alternative reaction:



the albite molecules entering into solid solution with nepheline. It is more probable that melilites crystallizing in this system are solid solutions of akermanite and soda melilite rather than pure akermanite. To account for the formation of soda melilite, Yoder and Tilley (1962) proposed a further reaction:

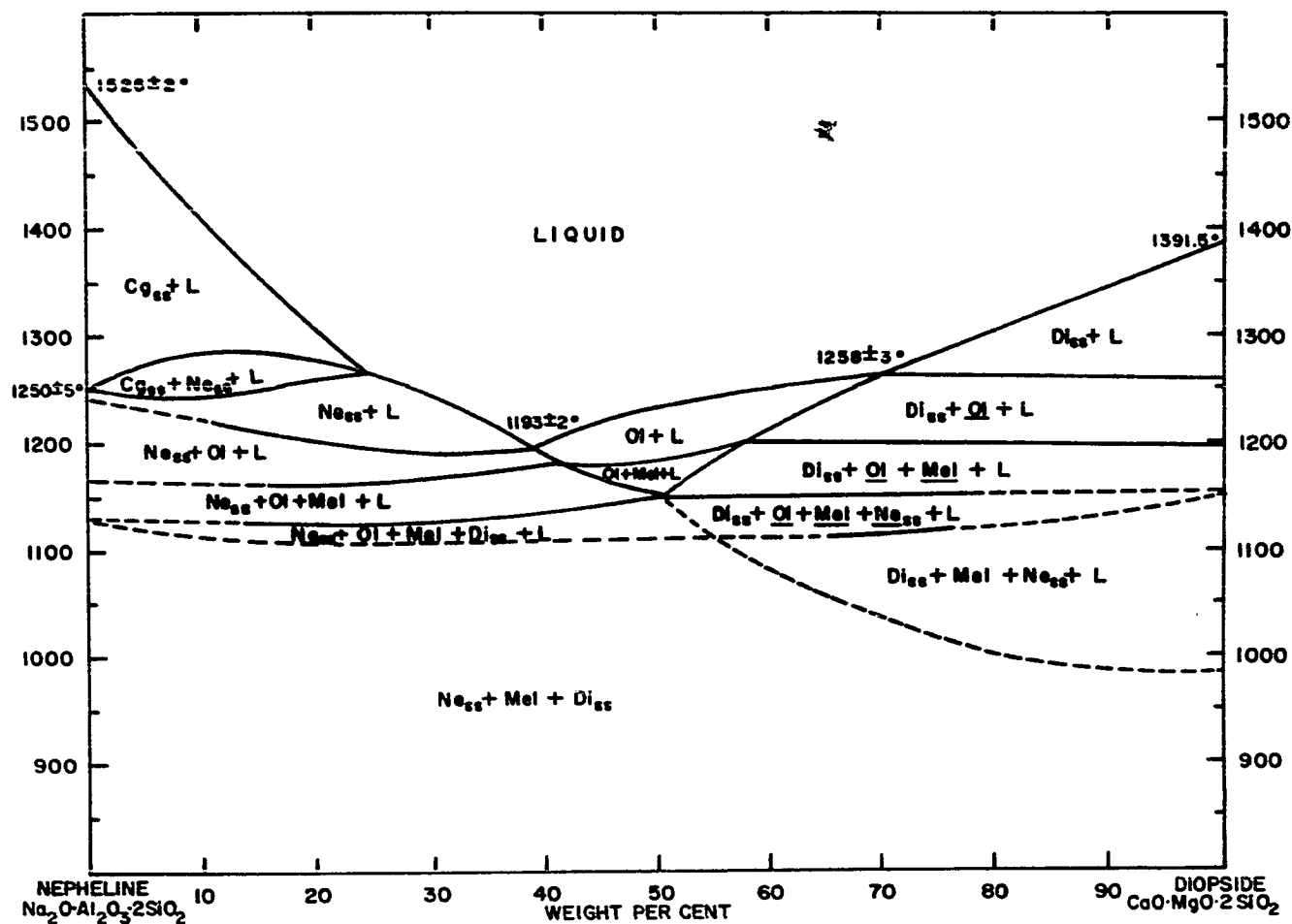
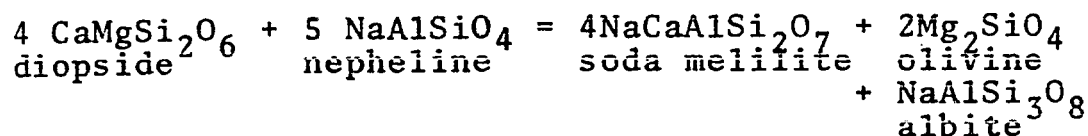
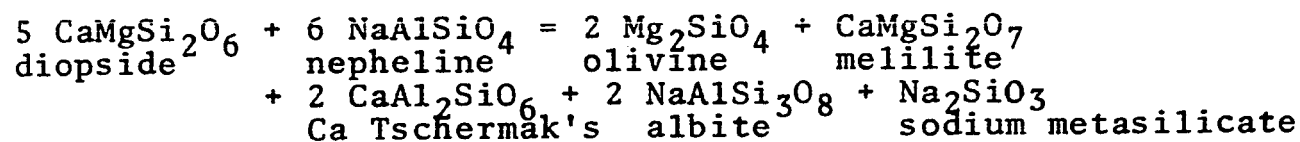


FIGURE 6. Phase relations in the system Nepheline-Diopside  
(after Schairer, Yagi and Yoder, 1962).

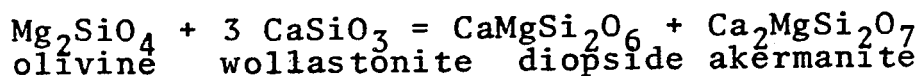


Yet another reaction has been suggested by Onuma and Yagi (1967):



in which the Ca Tschermak's molecules are in solid solution with diopside, and the albite and sodium metasilicate molecules are in solid solution with nephelines.

At temperatures approaching the solidus, olivine disappears by a crystal-liquid reaction similar to that suggested by Onuma and Yagi (1967):



Subsolidus assemblages in this system consist of nepheline + diopside + melilite.

### 3.3 Liquidus Phase Relations in the System Nepheline-Diopside-Sanidine.

Data for liquidus phase relations in this system are given in Table 4 and shown in Figure 7 where liquidus isotherms are drawn as thin black lines and the compositions studied are represented as solid black dots. Points A and B represent the compositions of liquids in equilibrium with three solid phases, the importance of these points will be discussed in detail later.

The primary crystallization of leucite and olivine on



TABLE 4  
Experimental Results

<u>Composition</u> (weight percent)			<u>Results of Microscopic and/or x-ray examination</u>		
<u>NE</u>	<u>DI</u>	<u>SAN</u>	<u>T°C.</u>	<u>Time</u> ( <u>hours</u> )	<u>Phases</u>
45	50	5	1245	24	gl.
			1240	48	ol + gl.
			1200	72	di? + ol + gl.
			1195	24	di + ol + gl.
			1190	24	tr. mel + di + ol + gl.
			1155	24	mel + di + ol + gl.
			1150	24	ne? + mel + di + ol? + gl.
			1145	24	ne + mel + di + ol? + gl.
			1140	120	ne + mel? + di + gl.
			1130	120	ne + di + gl.
40	50	10	1235	24	gl.
			1230	48	ol + gl.
			1200	72	tr. di + ol + gl.
			1180	24	di + ol + gl.
			1175	48	mel + di + ol + gl.
			1145	24	mel + di + ol? + gl.
			1135	120	ne + di + gl.
					B.M. 1010° ± 20°C.
43	40	17	1215	24	gl.
			1210	24	di + gl.
			1145	24	di + gl.
			1135	168	ne + di + gl.
					B.M. 1030° ± 20°C.

TABLE 4 continued.

<u>NE</u>	<u>DI</u>	<u>SAN</u>	<u>T°C.</u>	<u>Time</u> (hours)	<u>Phases</u>
8	32	60	1275	23	gl.
			1270	23	lc + gl.
			1265	72	di + lc + gl.
			1125*	94	di + lc + gl.
			1106*	113	tr. iso. lc + di + lc + gl.
			1085	96	iso. lc + di + lc + gl.
hydrothermally crystallized starting material					
			1070*	168	di + lc + gl.
			1060*	120	fp + di + lc + gl.
					B.M. 1050° ± 20°C.
8	30	62	1300	23	gl.
			1295	24	tr. lc + gl.
			1275	168	lc + gl.
			1270	24	di + lc + gl.
			1125*	94	di + lc + gl.
			1106*	113	tr. iso lc + di + lc + gl.
			1085	96	iso. lc + di + lc + gl.
55	30	15	1180	24	gl.
			1175	72	ol + gl.
			1170	48	tr. ne + ol + gl.
			1162*	51	tr. ne + ol + gl.
			1150	24	di + ne + ol + gl.
			1144*	40	di + ne + ol + gl.
			1130	120	di + ne + gl.
					B.M. 1015° ± 20°C.
50	26	24	1170	24	rare ol + gl.
			1145	72	ol + gl.
			1140	120	tr. ne + ol + gl.
			1135	120	di + ne + ol? + gl.
			1125	96	di + ne + gl.

TABLE 4 continued.

<u>NE</u>	<u>DI</u>	<u>SAN</u>	<u>T°C.</u>	<u>Time</u> (hours)	<u>Phases</u>
50	26	24	1043*	96	lc? + di + ne + gl.
(continued)			1034*	144	tr. lc + di + ne + gl. B.M. 1010° ± 20°C.
23	26	51	1245	24	gl.
			1240	48	lc + gl.
			1225	24	lc + gl.
			1220	24	di + lc + gl.
			1052*	121	ne? + di + lc + gl.
			1034*	144	ne + di + lc + gl.
52.5	25.5	22	1175	72	gl.
			1170	48	ol + gl.
			1155	120	ol + gl.
			1150	24	ne + ol + gl.
			1140*	21	di + ne + ol? + gl.
			1130	120	di + ne + gl.
68	25	7	1245*	24	gl.
			1236*	20	ne + gl.
			1170*	24	ne + gl.
			1159*	69	ol + ne + gl.
			1144*	40	tr. mel + ol + ne + gl.
			1136*	38	di? + mel + ol + ne + gl.
			1125*	40	tr. di + mel + ol + ne + gl.
			1115*	68	di + ne + gl. B.M. 1030° ± 20°C.
32	23	45	1190	24	gl.
			1185	24	di + gl.
			1180	24	tr. lc + di + gl.
			1105	120	lc + di + gl.
			1100	72	ne + lc + di + gl.

TABLE 4 continued.

NE	DI	SAN	T°C.	Time (hours)	Phases
25	20	55	1255	120	gl.
			1250	24	lc + gl.
			1205	24	lc + gl.
			1200	24	di + lc + gl.
hydrothermally crystallized starting material					
			1070*	168	ne? + di + lc + gl.
			1051*	168	ne + di + lc + gl.
			1034*	144	ne + di + lc + gl.
			1017*	156	fp? + ne + di + lc + gl.
					B.M. 1005° ± 20°C.
30	20	50	1215	24	gl.
			1210	24	lc + gl.
			1180	48	lc + gl.
			1175	48	di + lc + gl.
			1050*	156	di + lc + gl.
			1034*	144	ne + di + lc + gl.
40	20	40	1160	24	gl.
			1155	376	tr. di + gl.
			1110	168	di + gl.
			1105	168	tr. lc + di + gl.
			1100	36	ne + lc + di + gl.
			hydrothermally crystallized starting material		
			1030*	144	ne + lc + di + gl.
			1025*	156	fp + ne + lc + di + gl.
					B.M. 1000° ± 20°C.
50	20	50	1155	336	gl.
			1150	24	tr. di + tr. ne + gl.
			1075	672	di + ne + gl.
			1070	504	tr. lc + di + ne + gl.

TABLE 4 continued.

<u>NE</u>	<u>DI</u>	<u>SAN</u>	<u>T°C.</u>	<u>Time</u> (hours)	<u>Phases</u>
48	15	37	1140	120	gl.
			1135	72	ne + di + gl.
			hydrothermally crystallized starting material.		
			1070*	168	ne + di + gl.
			1060*	120	lc + ne + di + gl.
			1020*	156	lc + ne + di + gl.
			1007*	156	fp + lc + ne + di + gl.!
					B.M. 990° ± 20°C.
43	13	44	1130	120	v. rare di + tr. lc + gl.
			1125	168	tr. di + lc + gl.
			1110	120	di + lc + gl.
			1105	120	tr. ne + di + lc + gl.
			hydrothermally crystallized starting material		
			1027*	184	ne + di + lc + gl.
			1007*	156	fp + ne + di + lc + gl.
					B.M. 990° ± 20°C.
44	12	44	1130	120	gl.
			1125	168	lc + gl.
			1120	72	tr. ne + lc + gl.
			1115	168	di + ne + lc + gl.
			hydrothermally crystallized starting material		
			1015*	288	di + ne + lc + gl.
			1000*	156	fp + di + ne + lc + gl.!
					B.M. 990° ± 20°C.
43.5	10.5	46	1150	24	gl.
			1145	72	lc + gl.
			1125	168	lc + gl.
			1120	72	ne + lc + gl.
			1100	72	ne + lc + gl.

TABLE 4 continued.

<u>NE</u>	<u>DI</u>	<u>SAN</u>	<u>T°C.</u>	<u>Time</u> (hour)	<u>Phases</u>
43.5	10.5	46	1095	144	di + ne + lc + gl.
(continued) hydrothermally crystallized starting material.					
			1052*	121	di + ne + lc + gl.
			1027*	156	fp + di + ne + lc + gl.
					B.M. 1000° ± 20°C.
30	10	60	1275	18.	gl.
			1270	6	tr. lc + gl.
			1135	17	v. rare di + lc + gl.
			1065	504	di + lc + gl.
			1060	672	fp + di + lc + gl.
			1035	336	fp + di + lc + gl.
			1030	504	ne + fp + di + lc + gl.
					B.M. 980° ± 20°C.!
45	10	45	1130	48	gl.
			1125	96	ne + gl.
			1110	72	v. rare di + ne + gl.
			1100	336	di + ne + gl.
			1095	192	lc + di + ne + gl.
			1070	504	lc + di + ne + gl.
			1065	504	fp + lc + di + ne + gl
					B.M. 980° ± 20°C.!
42	8.5	49.5	1180	24	gl.
			1175	48	lc + gl.
			1125	96	lc + gl.
			1120	72	ne + lc + gl.
			1100	72	ne + lc + gl.
			1095	144	di + ne + lc + gl.
			1052*	121	di + ne + lc + gl.

TABLE 4 continued.

<u>NE</u>	<u>DI</u>	<u>SAN</u>	<u>T°C.</u>	<u>Time</u> (hour)	<u>Phases</u>
42 (continued)	8.5	49.5	1025	184	fp + di + ne + lc + gl. B.M. 985° ± 20°C.
42	6	52	1210	24	gl.
			1205	24	lc + gl.
			1130	168	lc + gl.
			1125	96	ne + lc + gl.
			1080	168	ne + lc + gl.
			1075	168	di + ne + lc + gl.
45	5	50	1175	72	gl.
			1170	48	lc + gl.
			1150	24	lc + gl.
			1145	24	ne + lc + gl.
			1105	120	ne + lc + gl.
			1095	144	v. rare di + ne + lc + gl.

Temperatures marked with asterisks\* are believed accurate to ± 10°C. All other temperatures were measured at the Geophysical Laboratory, Washington, D.C. and are believed accurate to ± 1°C.

Symbols: gl = glass, ol = olivine, di = diopside solid solution, mel = melilite, ne = nepheline solid solution, lc = leucite, iso. lc = isometric leucite, fp = Ca-poor ternary feldspar, B.M. Beginning of melting (solidus), v. rare = very rare, tr. = trace, ! = apparent decrease in leucite over that recorded at higher temperatures.

the liquidus surface and the crystallization of solid solution phases indicate the pseudoternary nature of this system. Any discussion of residual liquid trends with crystallization must, therefore, be referred to some system of higher complexity. The nature of this more complex system and the residual liquid trends will be discussed in Chapters 4 and 5.

The primary phase areas of leucite, nepheline, diopside and olivine are defined by the compositions of liquids in equilibrium with one of these solid phases. No attempt was made to delineate the primary phase area of carnegieite occurring at nepheline-rich compositions, as it is petrologically unimportant. The primary crystallization of olivine can be attributed to a high temperature nepheline-diopside reaction, as discussed previously. However, in the majority of mixtures, crystallization of olivine was not proceeded by that of melilite as would be expected if the reactions proposed by previous workers for the system Nepheline-Diopside were applicable in this system. Therefore, the addition of sanidine must somehow suppress the crystallization of melilite as discussed later in this chapter. Similar characteristics were found by Schairer and Yoder (1960) in the Nepheline-Albite-Diopside portion of the system Nepheline-Diopside-Silica.

The primary crystallization of leucite, in compositions close to the bounding system Sanidine-Diopside, is due to the incongruent melting of sanidine whereas for compositions



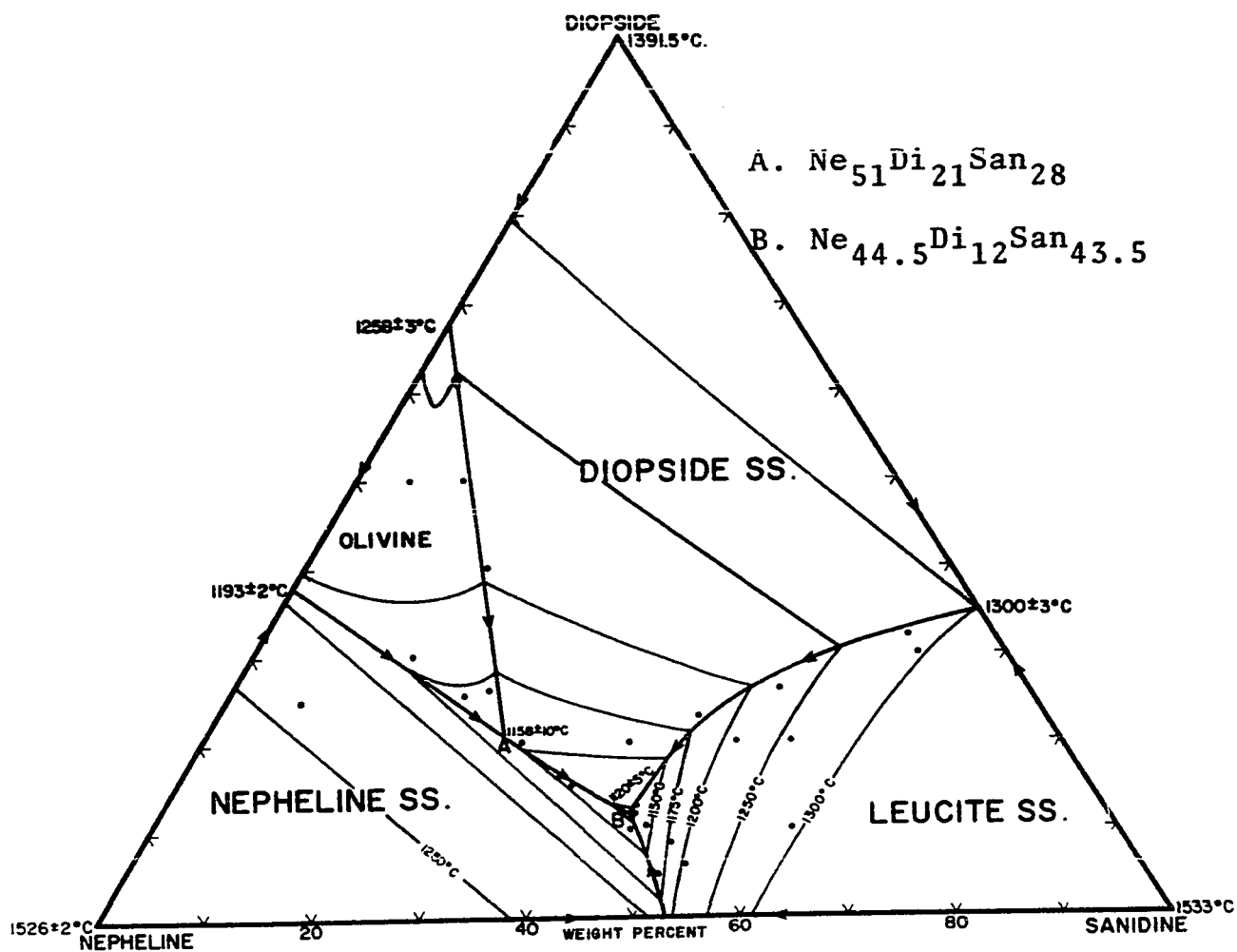


FIGURE 7. Liquidus phase relations in the system Nepheline-Diopside-Sanidine.

in the nepheline molecule, leucite crystallizes independently analagous to its crystallization in the Nepheline-Sanidine bounding system.

Boundary curves, representing the compositions of all liquids in equilibrium with two solid phases, are represented as thick dark lines in Figure 7. With one exception, these curves represent liquid compositions from which two solid phases crystallize, i.e. diopside + nepheline, diopside + leucite, leucite + nepheline and olivine + nepheline. The odd curve is that of olivine + diopside, along which olivine reacts with liquid to form pyroxene (cf. Schairer and Yoder, 1960). The calculated  $\text{SiO}_2$  contents of liquids defining this curve are almost constant, varying between 51.3% at  $\text{Ne}_{38}\text{Di}_{62}$  to 51.4% at  $\text{Ne}_{51}\text{Di}_{21}\text{San}_{28}$  (Point A, Figure 7), suggesting that the olivine-liquid reaction is in some way controlled by the  $\text{SiO}_2$  content of the liquids.

The boundary curves intersect at a four phase point which represents the composition of a liquid phase in equilibrium with three solid phases. Two such points, A and B (Figure 7), are located on the liquidus surface. Point A of composition  $\text{Ne}_{51}\text{Di}_{21}\text{San}_{28}$  at  $1158 \pm 10^\circ\text{C}$ . locates the assemblage nepheline + diopside + olivine + liquid. At this point, olivine undergoes a crystal-liquid reaction forming pyroxene. Point B of composition  $\text{Ne}_{44.5}\text{Di}_{12}\text{San}_{43.5}$  at  $1120 \pm 5^\circ\text{C}$ . locates the assemblage nepheline + leucite + diopside + liquid.

### 3.4 Subliquidus and Solidus Relations in the System Nepheline-Diopside-Sanidine.

Results of subliquidus determinations in this system are presented in Table 4 and indicate crystallization of melilite in certain compositions rich in nepheline and diopside molecules caused by the high temperature reactions between nepheline and diopside mentioned previously. In the similar system Nepheline-Diopside-Silica (Nepheline-Diopside-Albite) Schairer and Yoder (1960, pp. 280-281) state:

"No melilite was encountered at any temperature in mixtures in the system nepheline-diopside-silica, although it appears in the system nepheline-diopside. In compositions in nepheline-diopside-silica near the side line nepheline-diopside where melilite and/or plagioclase might be expected, only nepheline and diopside were detected in the x-ray powder patterns of the completely crystalline material. The lack of plagioclase or melilite may be due to the inability of x-rays methods to detect small amounts of these products."

The lack of melilite in the completely crystalline products of the system Nepheline-Diopside-Silica can be explained by its disappearance by reaction at subliquidus temperatures, as is the case in the present study. The absence of melilite at subliquidus temperatures in the system Nepheline-Diopside-Silica is probably a consequence of the bulk compositions studied. The lowest albite content of any mixture studied by Schairer and Yoder was 10.9 weight percent, whereas in the present study melilite appeared only in compositions with 10 weight percent or less of the sanidine molecule, but at 15 weight percent sanidine, olivine alone

crystallized.

Olivine disappears by crystal-liquid reaction at temperatures ranging approximately from  $1120^{\circ}$  to  $1145^{\circ}\text{C}$ . Problems in identifying small amounts of olivine in large amounts of diopside make determination of the exact temperature of disappearance extremely difficult.

In mixtures crystallizing feldspar, it was usually the last phase to form, occurring at temperatures close to the solidus. In compositions containing greater than 55 weight percent of the sanidine molecule, feldspar crystallization precedes that of nepheline. With the crystallization of feldspar, there is an apparent decrease in the amount of leucite; a relationship similar to that found by Schairer and Bowen (1935) in the system Nepheline-Kalsilite-Silica due to the reaction:

leucite + liquid  $\rightarrow$  nepheline + alkali feldspar.

However, for the quenching experiments in which feldspar crystallized, hydrothermally crystallized glasses consisting entirely of feldspar, diopside and nepheline, with no leucite were used. The apparent decrease in leucite, although believed to be real, could be due to kinetic factors, especially in experiments close to the solidus, where solid-liquid reaction rates are retarded due to the small amount of liquid present.

In compositions close to the Diopside-Sanidine sideline, two forms of leucite crystallize together below  $1115^{\circ}\text{C}$ .,

isometric leucite, the high temperature form; and tetragonal leucite, the low temperature form. In runs above  $1115^{\circ}\text{C}$ . only the tetragonal form is found after quenching, suggesting that the high temperature isometric leucite forms metastably below  $1115^{\circ}\text{C}$ . Additional information for this assumption is provided by the failure of isometric leucite to crystallize below  $1115^{\circ}\text{C}$ . when using hydrothermally crystallized starting materials, where the only leucite phase to crystallize is the low temperature tetragonal form.

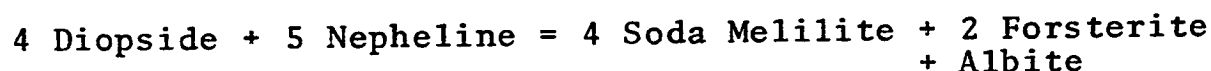
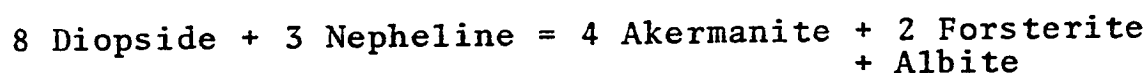
Solidus temperatures vary according to the bulk compositions studied, the lowest melting temperature recorded being  $980 \pm 20^{\circ}\text{C}$ . Fully crystalline assemblages consist of nepheline + diopside + leucite, nepheline + diopside + leucite + feldspar, leucite + diopside + feldspar and nepheline + diopside. Other possible assemblages are leucite + diopside and nepheline + diopside + feldspar, but these were not found. It is possible that feldspar occurs in some of the assemblages marked nepheline + diopside but in amounts too small to be detected by either optical or x-ray methods.

### 3.5 Instability of Melilites.

In certain compositions olivine crystallizes but melilite does not (see Table 4). If the origin of olivine is caused by reaction between nepheline and diopside at high temperatures, melilite should also crystallize from those mixtures in which olivine crystallizes (see pp. 32-34 ) unless some other molecule prevents its formation. In the present system,

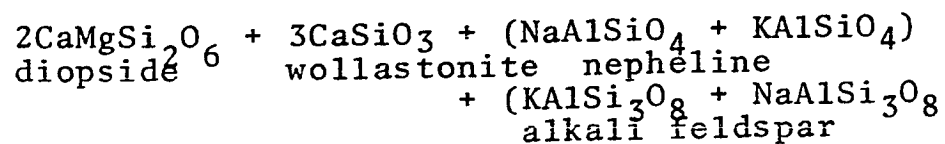
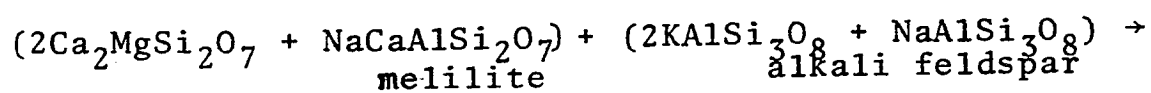
the presence of sanidine must cause the melilite instability, as melilite is stable at the solidus of the system Nepheline-Diopside (Schairer, Yagi and Yoder, 1962), (see Figure 6).

To discuss the effects of sanidine on the stability of melilites, the high temperature reactions of nepheline and diopside with the addition of sanidine must be considered. In the Nepheline-Diopside system (Schairer, Yagi and Yoder, 1962), the reactions between nepheline and diopside are given by Yoder and Tilley (1962) as:



the akermanite and soda melilite combining to form melilite molecules.

In the present study, a possible reaction between melilite and alkali feldspar molecules is



For bulk compositions with 10 weight percent or less of the sanidine molecule, melilite initially crystallizes but reacts at lower temperatures and ultimately disappears. This is due to an increase of potential feldspars in the residual liquids, which reaches an optimum value allowing the above reaction to take place.

Although the effects of sanidine on melilite stability are not known, that of albite has been documented in the system Nepheline-Albite-Akermanite (Schairer and Yoder, 1964). Compositions with greater than 50 weight percent albite crystallize a mixture of diopside, plagioclase and nepheline, whereas compositions with approximately 40 to 50 weight percent albite initially crystallize melilite which later disappears by reaction, producing a final assemblage of nepheline, plagioclase, diopside and occasional wollastonite. These products are comparable to those formed by the proposed melilite-feldspar reaction. For compositions with less than 40 weight percent albite, melilite is stable at solidus temperatures. Schairer and Yoder (1964) report similar results from studies in the system Albite-Akermanite-Diopside.

In the present study, the reaction of melilite with alkali feldspar may account for:

1. The initial crystallization of melilite and its subsequent disappearance at subliquidus temperatures; and
2. The failure of melilite to coexist with olivine with an increase in the potential sanidine content of the liquid.

### 3.6 Mineralogy of the Crystallizing Phases in the System Nepheline-Diopside-Sanidine.

The crystallizing mineral phases exhibit complex solid solutions, although quantitative determinations of their compositions could not be made due to the size of crystals, and inclusions within the crystals, limiting the use of

optical and electron microprobe techniques. No known x-ray methods were of use in determining the compositions. Semi-quantitative electron microprobe studies gave some indication as to the possible solid solutions occurring.

### 3.61. Nepheline.

Nepheline crystallized with a typical hexagonal or rectangular outline. Exact compositions of these nephelines are not known but certain assumptions as to the nature of their solid solutions can be made. Nephelines in the system Nepheline-Kalsilite-Silica (Schairer and Bowen, 1935), and consequently in the system Nepheline-Sanidine (see Figure 2), exhibit solid solution in which K replaces Na. This is termed Substitution Solid Solution by Donnay, Schairer and Donnay (1959), (i.e.  $K_XNa_{8-X}Al_8Si_8O_{32}$ ). Nephelines in the system Nepheline-Kalsilite-Silica also show the solid solution of albite molecules (Hamilton and MacKenzie, 1960), or, as it is termed by Donnay, Schairer and Donnay (1959), Omission and Substitution solid solution (i.e.  $Na_{8-Y} \square_Y Al_{8-Y} Si_{8+Y} O_{32}$  in which vacant sites  $\square$  replace Na and Si replaces Al).

As the system Nepheline-Diopside-Sanidine contains Ca atoms, other possible types of nepheline solid solutions occurring are:

- i. Double Substitution: (Donnay, Schairer and Donnay, 1959): Ca replacing Na and Al replacing Si, i.e.  $Na_{8-Z}Ca_ZAl_{8+Z}Si_{8-Z}O_{32}$ . This is represented by nephelines in the system Nepheline- $CaAl_2O_4$  (Goldsmith, 1949).



ii. Substitution plus Omission; (Donnay, Schairer and Donnay, 1959), Ca and vacant sites  $\square$  in equal proportions replacing Na, i.e.  $\text{Na}_{8-z}\text{Ca}_z \square_z \text{Al}_8\text{Si}_8\text{O}_{32}$ . This type is exhibited by nephelines in the system Nepheline-Anorthite (Bowen, 1912, Gummer, 1943).

### 3.62 Olivine

At temperatures close to the liquidus, the olivine forms small, well-faceted crystals of high relief and high birefringence. At lower temperatures, their outlines become rounded due to crystal-liquid reaction. Occasionally they form length-slow, prismatic crystals with straight extinction.

A semiquantitative electron microprobe study of olivine crystallizing from the mixture  $\text{Ne}_{45}\text{Di}_{50}\text{San}_5$  at  $1215^\circ\text{C}$ . gave a chemical formula, based on 4 oxygen atoms, of:

Si	0.99	0.99
Al	0.02	} 2.02
Mg	1.99	
Ca	0.01	

### 3.63 Diopside

This phase usually has a prismatic habit with inclined extinction. In experiments in which olivine or melilite and olivine were present, the diopside tended to form rounded grains.

Solid solution of  $\text{Al}_2\text{O}_3$  in the diopsides was confirmed from semi-quantitative electron microprobe data. No detec-

table  $\text{Na}_2\text{O}$  was found by this method. The presence of  $\text{Al}_2\text{O}_3$  can be explained by the formation of Ca Tschermak's molecules ( $\text{CaAl}_2\text{SiO}_6$ ) and Mg Tschermak's molecules ( $\text{MgAl}_2\text{SiO}_6$ ), the solid solution of which involves the substitution of  $\text{Al}^{3+}$  in the four and six-fold co-ordination positions of diopside. Segnit (1953), determined the limits of solid solution in the systems  $\text{CaMgSi}_2\text{O}_6 - \text{Al}_2\text{O}_3$ ,  $\text{CaMgSi}_2\text{O}_6 - \text{CaAl}_2\text{SiO}_6$  and  $\text{CaMgSi}_2\text{O}_6 - \text{MgAl}_2\text{SiO}_6$  as 13, 25 and 20 weight percent respectively.

### 3.64 Leucite

At high temperatures leucite crystallized with a characteristic eight-sided form but at low temperatures the crystals were small and rounded. Its refractive index was approximately 1.500, and its birefringence very weak. The glass surrounding the leucite showed anomalous birefringence as a result of straining caused by volume shrinkage in the leucites as they inverted from the high temperature isometric form during quenching.

No attempt was made to determine the composition of the leucites. However, as synthetic leucites in the system  $\text{NaAlSi}_2\text{O}_6 - \text{KAlSi}_2\text{O}_6$  contain approximately 40 weight percent  $\text{NaAlSi}_2\text{O}_6$  at atmospheric pressure and  $1000^\circ\text{C}$ . (Fudali, 1963), it is assumed that leucites in the present study also contain some  $\text{NaAlSi}_2\text{O}_6$  in solid solution.

### 3.65 Melilite

The melilites crystallized as squares and prisms exhibiting high relief and no birefringence. Occasionally they

give anomalous deep blue interference colours in thin section.

The isotropic nature of the melilite precludes the possibility of its having the composition of pure akermanite or gehlenite. Soda melilite, a third possible end-member of the melilite series, is unstable at 1 atmosphere (Yoder, 1964). Schairer, Yoder and Tilley (1965) found that isotropic melilites in the system Gehlenite-Soda Melilite-Akermanite range in composition from  $\text{Geh}_{45}\text{Ak}_{55}$  to approximately  $\text{Ak}_{68}\text{SM}_{32}$ .

The presence of  $\text{CaO}$ ,  $\text{MgO}$ ,  $\text{Al}_2\text{O}_3$ ,  $\text{Na}_2\text{O}$  and  $\text{SiO}_2$  in the melilites was confirmed by electron microprobe studies. Although exact compositions of the melilites were not determined, the optical and electron microprobe data suggest they consist of a complex solid solution of the three end-members, akermanite, gehlenite and soda melilite.

### 3.66 Feldspars

Due to the size of crystals, the presence of feldspars among the crystallizing phases could only be determined by x-ray methods. Feldspars in the system Nepheline-Kalsilite-Silica, and consequently in the system Nepheline-Sanidine (see Figure 2), are rich in alkalis, and it is presumed, therefore, that those crystallizing in the present study are also alkali-rich.

The presence of  $\text{CaO}$  in bulk compositions of the system Nepheline-Diopside-Sanidine probably results in the forma-

tion of ternary feldspars in a manner similar to the formation of plagioclase in systems containing albite and a calcium-bearing phase (the 'Plagioclase Effect', Bowen, 1945).

### 3.7 The Pseudoternary Nature of the System Nepheline-Diopside-Sanidine.

The phase rule for a condensed ternary system may be written as:

$$P + F = C + 1$$

where  $C = 3$ ; and where  $P$  is the number of phases,  $F$  the degrees of freedom<sup>1</sup> and  $C$  the number of components in the system. For a four phase assemblage, the degrees of freedom for the system must be zero and the assemblage will only exist at one point (invariant point) having a fixed temperature and composition.

Points A and B of Figure 7 represent four phase assemblages, and if the system is ternary, these will be invariant. Point A is characterized by the reaction of olivine with liquid and, if strictly invariant, all the olivine must disappear at this point. From the data in Table 4 it can be seen that olivine exists at temperatures well below that of

---

1. "The number of intensive variables which can be altered independently and arbitrarily without bringing about the disappearance of a phase or the formation of a new one is called the number of degrees of freedom of a system." (MacDougall, F.J., 1939, Thermodynamics and Chemistry. John Willey and Sons, New York).

Point A, which cannot, therefore, be invariant. Similarly, Point B should mark the disappearance of the last liquid phase in the system, but again the results in Table 4 show that a liquid phase exists well below the temperature of this point. Therefore, Point B is also not invariant.

For the system to be ternary, the compositions of all the phases must be represented by mixtures of the three components (i.e. nepheline, diopside and sanidine). It is not possible, however, to represent the compositions of any of the phases, solid or liquid, occurring in this system in terms of these three components.

## CHAPTER 4

### RESIDUAL LIQUID FLOW DIAGRAMS FOR THE SYSTEM NEPHELINE - KALSILITE - SILICA - DIOPSIDE

#### 4.1 Introduction

In the preceding chapter, evidence supporting the pseudoternary nature of the system Nepheline-Diopside-Sanidine was given. The question now arises as to the exact number of components<sup>1</sup> necessary to define this system completely. From considerations of the complex solid solutions (see Chapter 3), possible components of the system are the mineral molecules:

Ca Tschermak's molecule	Nepheline
Mg Tschermak's molecule	Kalsilite
$Al_2O_3$	$CaAl_2O_4$
Sanidine	Gehlenite
Anorthite	Akermanite
Albite	Soda Melilite
Leucite	Forsterite
Jadeite (anhydrous analcite)	

---

1. Components can be defined as: "The smallest number of independently variable chemical constituents necessary and sufficient to express the composition of each phase present in any state of equilibrium." (Phase Diagrams for Ceramists, American Ceramic Society, 1964, p.5).

However, the composition of each of the solid and liquid phases, may be considered in terms of their constituent oxides. If these oxide constituents are considered as components, the system Nepheline-Diopside-Sanidine may be described as a plane within the six component system:  $\text{CaO-MgO-Al}_2\text{O}_3\text{-Na}_2\text{O-K}_2\text{O-SiO}_2$ .

In Chapter 1, it was shown that the system Nepheline-Diopside-Sanidine constitutes a join through the tetrahedron Nepheline-Kalsilite-Silica-Diopside (Figure 1). Consequently, the volume of this tetrahedron represents a volume within the six component system  $\text{CaO-MgO-Al}_2\text{O}_3\text{-Na}_2\text{O-K}_2\text{O-SiO}_2$ .

In a condensed six component system, the relationship between all possible mixtures of the six components and temperature, can only be represented in hypothetical six dimensional space requiring mathematical concepts for its definition. Because of this, certain simplifications described below are used in this thesis as a basis for the representation of the results.

A true univariant line possesses one degree of freedom and is represented by the compositions of liquids in equilibrium with (P-1) solid phases, where P is the number of phases present in the univariant assemblage. It is assumed that the four phase assemblages in the system Nepheline-Diopside-Sanidine (e.g. Points A and B of Figure 7) are indicative of univariant assemblages, ie. the liquid phase of such an assemblage would lie on a univariant line and be in

equilibrium with three solid phases. This is not strictly correct as any four phase assemblage in a six component system, possesses three degrees of freedom and, therefore, the liquid composition must lie in a volume.

A true invariant point possesses no degree of freedom and represents the composition of a single liquid phase in equilibrium with  $(P-1)$  solid phases, where  $P$  is the number of phases present at the invariant point. In the present study, it has been assumed that the five phase assemblages are, in fact, invariant assemblages, i.e. only one liquid composition is in equilibrium with four solid phases. This, again, is not strictly correct from phase rule considerations, as a five phase assemblage in a six component system possesses two degrees of freedom and the liquid composition must lie on a divariant surface.

True univariant and invariant assemblages in a condensed six component system would have six and seven coexisting phases respectively. The actual number of discrete phases which coexist, could, however, be reduced by solid solution between the phases.

If four and five phase assemblages are considered as indicative of univariant lines and invariant points, it is possible to construct flow diagrams which show generalized residual liquid trends with crystallization. Consequently the problems of representing such trends in six dimensional space are overcome without seriously affecting the generalized



liquid trends in the system.

#### 4.2 Derivation of Flow Diagrams for the System Nepheline-Kalsilite-Silica-Diopside.

Flow diagrams may be derived from a knowledge of univariant lines<sup>1</sup> and invariant points within a complex system. This knowledge can be obtained from the study of a number of planes or joins through such a system. For instance, points A and B in the system Nepheline-Diopside-Sanidine (Figure 7) are four phase assemblages formed by the intersection of the plane of this system with lines within the tetrahedron Nepheline-Kalsilite-Silica-Diopside. Such points of intersection are known as piercing points<sup>2</sup> and from their location co-ordinates for the framework of lines within the tetrahedron can be obtained. For a detailed account of flow diagrams, the reader is referred to Schairer (1942).

From the liquidus phase diagrams of the known systems of the tetrahedron, i.e. Nepheline-Kalsilite-Silica (Schairer, 1957) (Figure 2), Leucite-Diopside-Silica (Schairer and Bowen, 1938) (Figure 8), Nepheline-Diopside-Silica (Schairer and Yoder, 1960) (Figure 9), Diopside-Albite-Orthoclase (Morse, 1968) (Figure 10), Diopside-Albite-Leucite (Sood,

---

1. Univariant lines will be referred to as lines for the remainder of this thesis.

2. Piercing points will be referred to as points for the remainder of this thesis.

1969) (Figure 11) and Nepheline-Diopside-Sanidine (this work) (Figure 7), eleven points are located. These are listed in Table 5 and are designated by letters corresponding to those in Figures 13 and 15. These points are formed from the intersections of seven lines lying within the volume of this tetrahedron. These lines are listed in Table 6 and are designated by numbers corresponding to those in Figures 13 and 15.

Data in Table 4 show that four phase assemblages corresponding to the lines  $ne + ol + mel + liq$ . (Line 10 Table 6. Figure 15) and  $di + ol + mel + liq$  (Line 11 Table 6. Figure 15) occur at subliquidus temperatures in the system Nepheline-Diopside-Sanidine. There are no points involving either of these lines in any known systems of the tetrahedron Nepheline-Kalsilite-Silica-Diopside (Figure 12) and it is therefore presumed that these lines lie outside its volume.

In the system Nepheline-Diopside-Sanidine two, five phase assemblages  $ne + lc + fp + di + liq$ . (Point R', Table 6, Figures 13 and 14) and  $mel + ol + di + ne + liq$ . (Point X, Table 6, Figure 15) are found (Table 4). These correspond to invariant points; the former (Point R') lying inside the tetrahedron Nepheline-Kalsilite-Silica-Diopside, the latter (Point X) lying outside this volume.

From a knowledge of these lines and invariant points (Table 6) flow diagrams showing residual liquid trends with crystallization can be constructed. During the following discussion, the reader is referred to Figures 12 to 15.

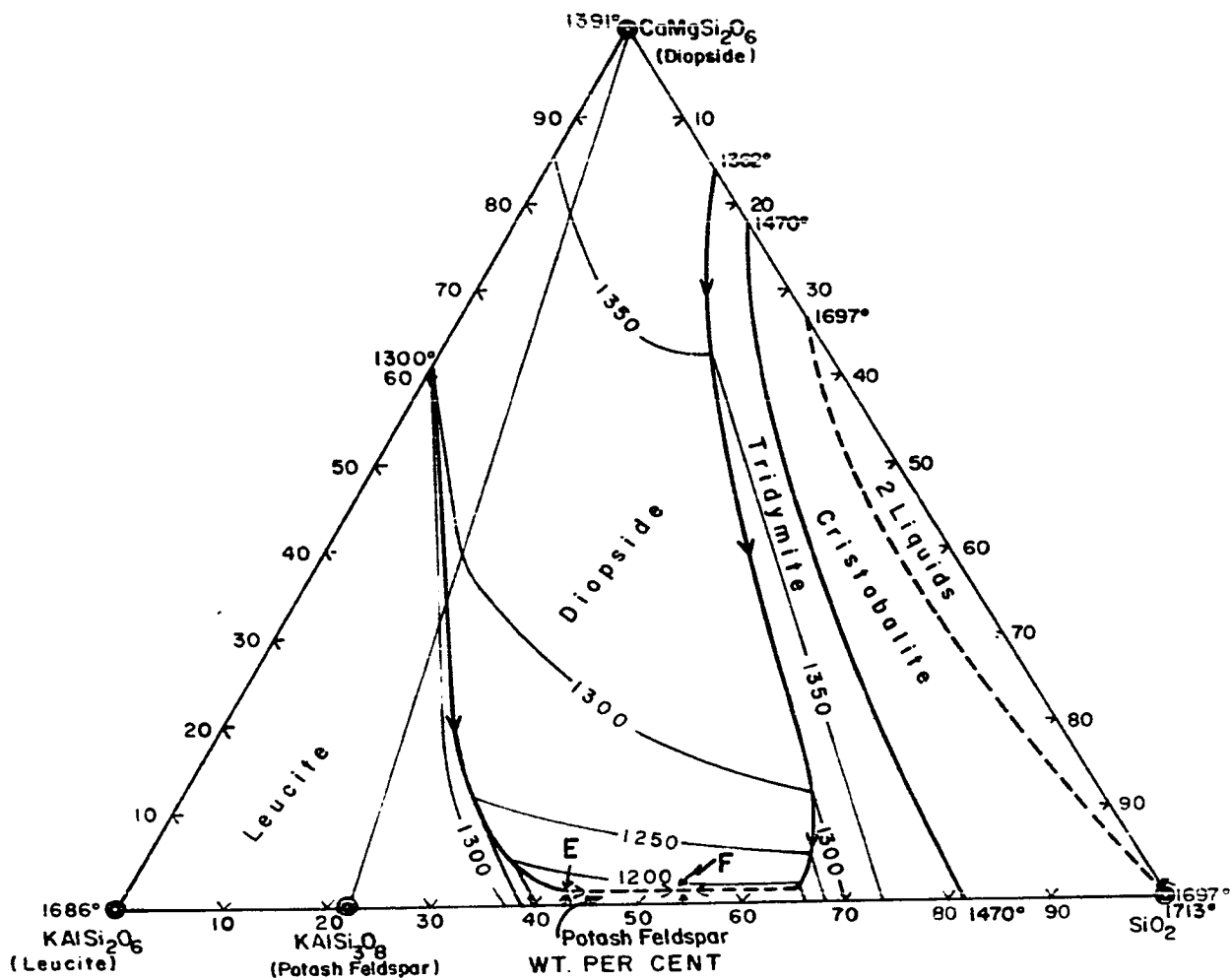


FIGURE 8. Liquidus phase relations in the system Leucite-Diopside-Silica (after Schairer and Bowen, 1938).

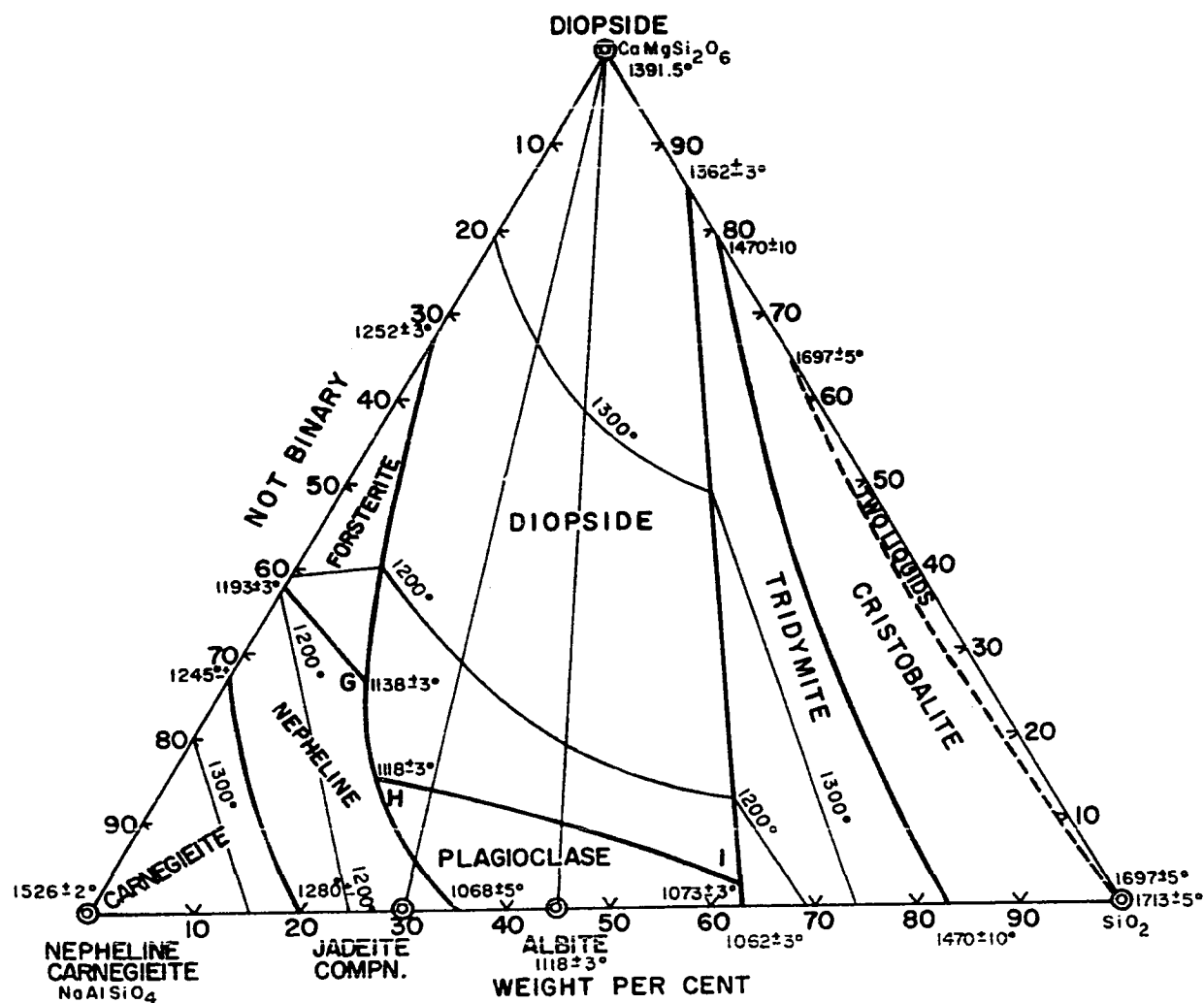


FIGURE 9. Liquidus phase relations in the system Nepheline-Diopside-Silica (after Schairer and Yoder, 1960).

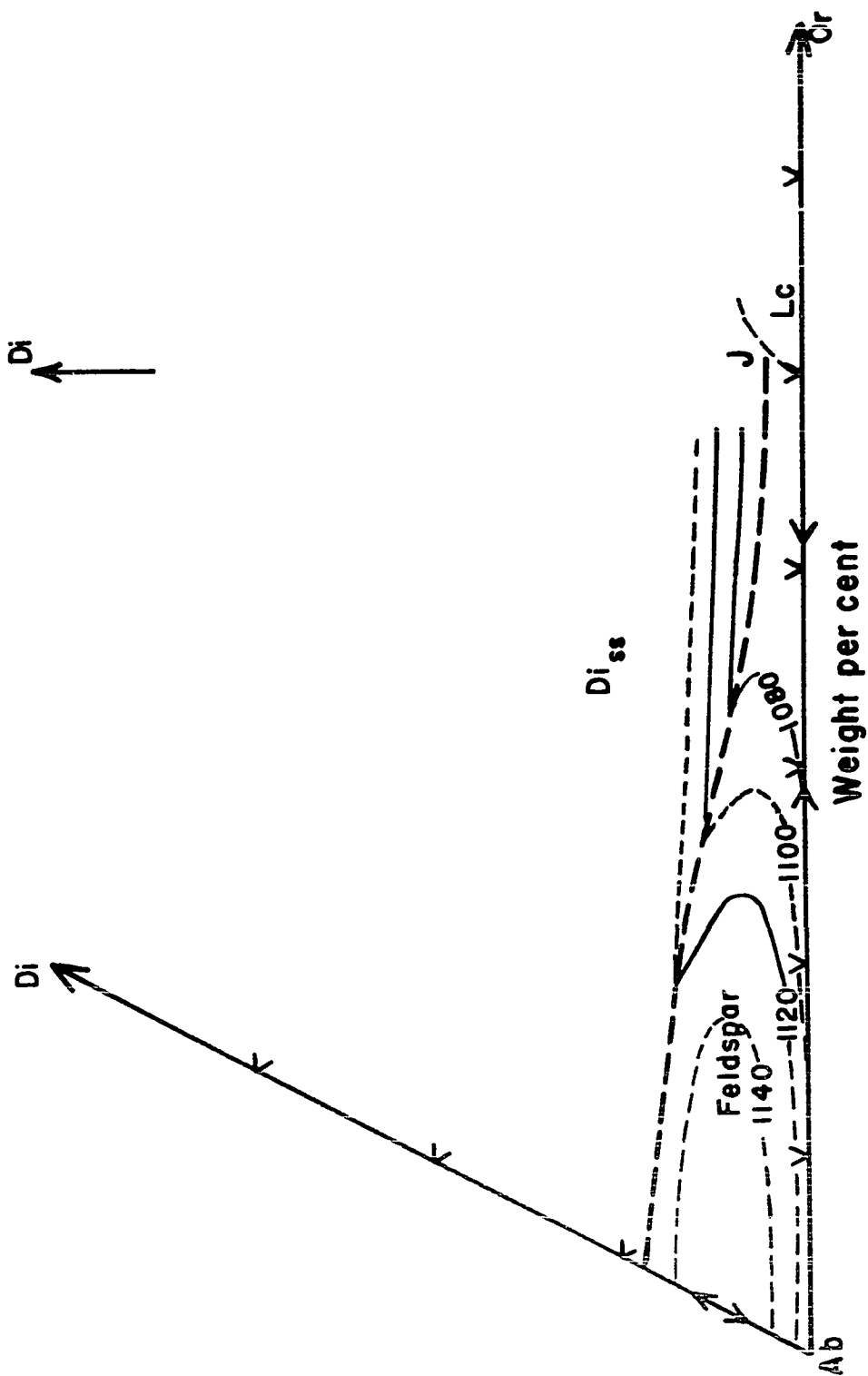


FIGURE 10. Partial liquidus phase relations in the system Diopside-Albite-Orthoclase (after Morse, 1968).

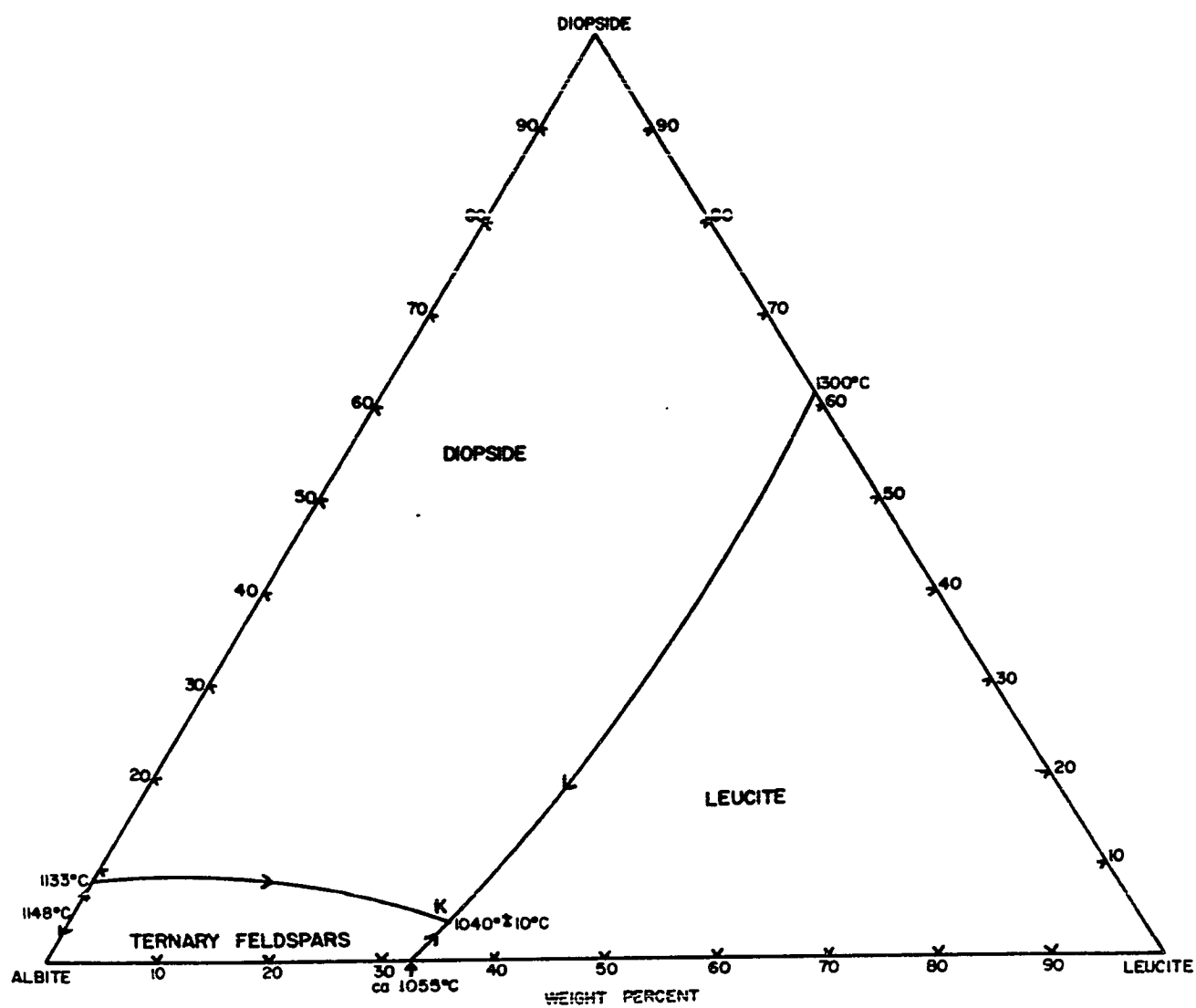


FIGURE 11. Liquidus phase relations in the system  
Diopside-Albite-Leucite (after Sood, 1969).

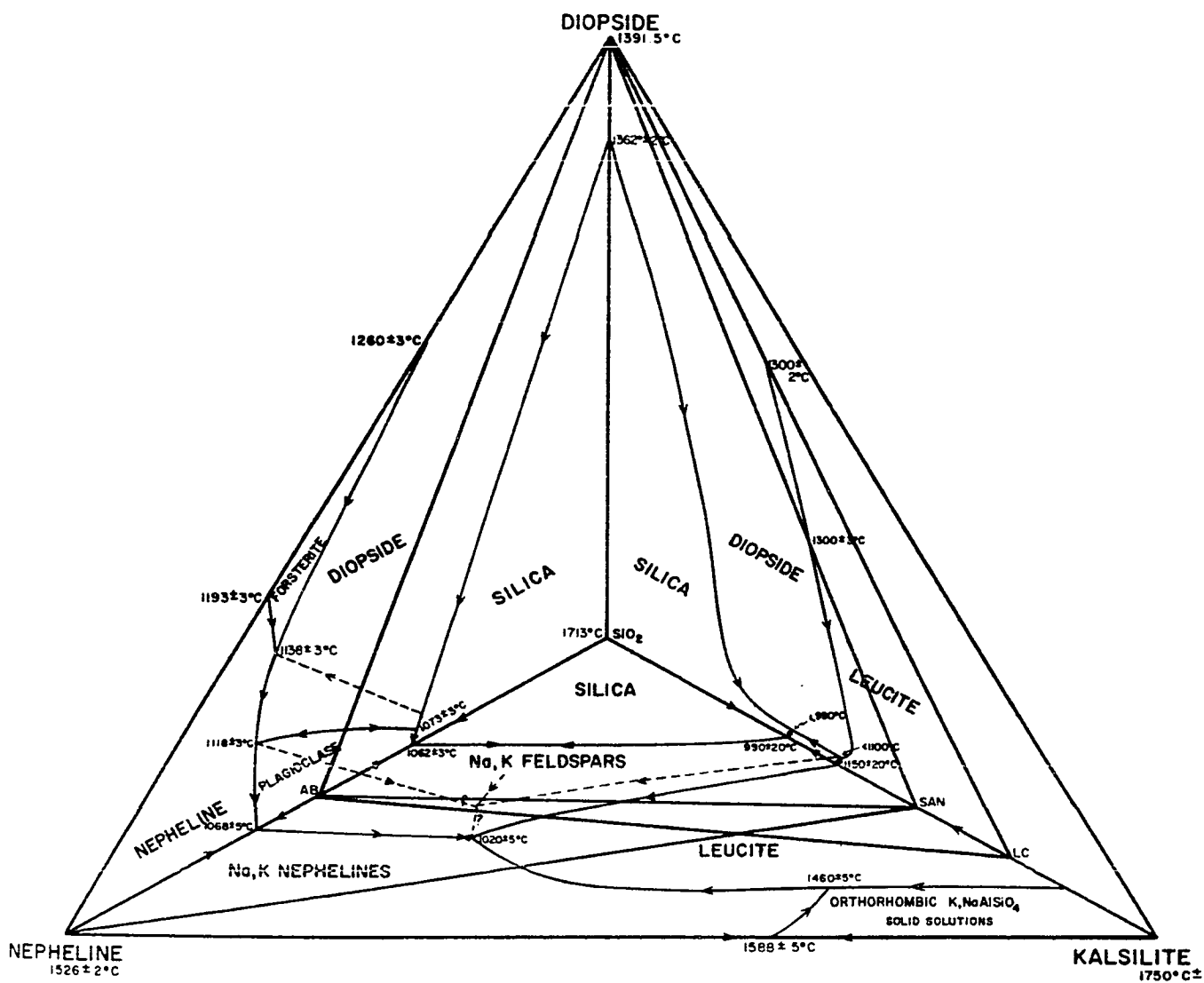


FIGURE 12. The system Nepheline-Kalsilite-Silica-Diopside.

TABLE 5

Piercing Points of Univariant Lines in Systems of the Tetrahedron  
Nepheline-Kalsilite-Silica-Diopside

<u>System</u>	<u>Point</u>	<u>Solid Phases</u>	<u>Composition</u>	<u>Temperature</u>
Ne-Di-San	A (Figure 7)	ne, ol, di.	Ne <sub>51</sub> Di <sub>21</sub> San <sub>28</sub>	1158° ± 10°C.
	B ( " )	di, ne, lc.	Ne <sub>44.5</sub> Di <sub>12</sub> San <sub>43.5</sub>	1120° ± 5°C.
Ne-Ks-SiO <sub>2</sub>	C (Figure 2)	ks, lc, ne.	ca. Ne <sub>20.5</sub> Ks <sub>63.5</sub> Si <sub>116</sub>	1460° ± 5°C.
	R ( " )	ne, lc, fp.	ca. Ne <sub>47</sub> Ks <sub>21</sub> Si <sub>132</sub>	1020° ± 5°C.
Lc-Di-SiO <sub>2</sub>	E (Figure 8)	di, fp, lc.	Ne <sub>56</sub> Di <sub>2</sub> Si <sub>42</sub>	below 1100°C.
	F ( " )	di, fp, sil.	Ne <sub>44</sub> Di <sub>2</sub> Si <sub>154</sub>	below 990°C.
Ne-Di-SiO <sub>2</sub>	G (Figure 9)	ne, ol, di.	Ne <sub>59</sub> Di <sub>28</sub> Si <sub>113</sub>	1138° ± 3°C.
	H ( " )	di, ne, plag.	Ne <sub>65</sub> Di <sub>15</sub> Si <sub>120</sub>	1118° ± 3°C.
	I ( " )	di, fp, sil.	Ne <sub>36</sub> Di <sub>3</sub> Si <sub>161</sub>	1073° ± 3°C.
Di-Ab-Or	J (Figure 10)	di, fp, lc.	ca. Di <sub>3</sub> Ab <sub>49</sub> Or <sub>48</sub>	ca. 1060°C.
Di-Ab-Lc	K (Figure 11)	di, fp, lc.	Di <sub>4</sub> Ab <sub>62</sub> Lc <sub>34</sub>	1040° ± 10°C.

A liquid phase coexists with the solid phases at each piercing point.



TABLE 6

a. Univariant Lines in the Volume of the Tetrahedron  
Nepheline-Kalsilite-Silica-Diopside

<u>Line Number</u>	<u>Solid Phases</u>	<u>Piercing Points (Table 5)</u>
1.	ne + ol + di.	A and G
2.	di + ne + lc.	B
3.	di + fp + lc.	E, J and K
4.	ne + lc + fp.	R
5.	di + ne + fp.	H
6.	di + fp + sil.	F and I
7.	ks + lc + ne.	C
8.	ne + ks + di.!	none
9.	ks + lc + di.!	none

b. Univariant Lines Outside the Volume of the Tetrahedron  
Nepheline-Kalsilite-Silica-Diopside

10.	ne + ol + mel.	none
11.	di + ol + mel.	none
12.	ne + mel + di.	none
13.	ne + di + fp.!	none
14.	ol + di + fp.!	none
15.	ne + ol + fp.!	none
16.	ne + di + wo.!	none
17.	fp + wo + di.!	none
18.	fp + wo + ne.!	none

c. Invariant Points Within the Volume of the Tetrahedron  
Nepheline-Kalsilite-Silica-Diopside

Invariant Point

R'. (Figure 13)	ne + lc + fp + di.
W. ( " )	lc + ne + ks + di.*

TABLE 6 continued

d. Invariant Points Lying Outside the Volume of the Tetrahedron  
Nepheline-Kalsilite-Silica-Diopside

---

X.	(Figure 15)	mel + ol + di + ne.
Y.	( " )	ne + ol + di + fp.*
Z.	( " )	ne + fp + di + wo.*

e. Temperature Minima Within the Volume of the Tetrahedron  
Nepheline-Kalsilite-Silica-Diopside

---

M'.	(Figure 13)	di + ne + fp.
N'.	( " )	di + fp + si.=

! Univariant Lines from theoretical considerations.

\* Invariant Points from theoretical considerations.

= Temperature Minimum from theoretical considerations.

A liquid phase coexists with the solid phases for each of the univariant lines and invariant points.

Any invariant point is surrounded by four lines derived from the combination of any three of the four solid phases together with a liquid occurring at the invariant point. For example, the invariant point  $ne + lc + fp + di + liq.$  (Point R', Table 6, Figure 13) must be formed at the intersection of the lines:

- i.  $di + ne + lc + liq.$  (Line 2, Table 6, Figures 13 and 14).
- ii.  $di + fp + lc + liq.$  (Line 3, Table 6, Figures 13 and 14).
- iii.  $ne + lc + fp + liq.$  (Line 4, Table 6, Figures 13 and 14).
- iv.  $di + ne + fp + liq.$  (Line 5, Table 6, Figures 13 and 14).

Schematic arrangements of these lines around this invariant point are given in Figures 13 and 14. From a knowledge of the systems of the tetrahedron Nepheline-Kalsilite-Silica-Diopside further details of these four lines can be deduced.

- i. The line  $di + ne + lc + liq.$  (Line 2, Table 6, Figures 13 and 14)

This line cuts the system Nepheline-Diopside-Sanidine at the Point B (Table 5, Figures 7 and 13). It is represented schematically in Figures 13 and 14. With crystallization of leucite, nepheline and diopside, the residual liquids change in composition towards the Invariant Point R' (Table 6, Figures 13 and 14). In the system Nepheline-Diopside-Sanidine, crystallization of leucite ( $KAlSi_2O_6$ ) rather than sanidine ( $KAlSi_3O_8$ ) increases the  $SiO_2$  content of the residual liquids. Thus with crystallization of leucite, the  $SiO_2$  content of

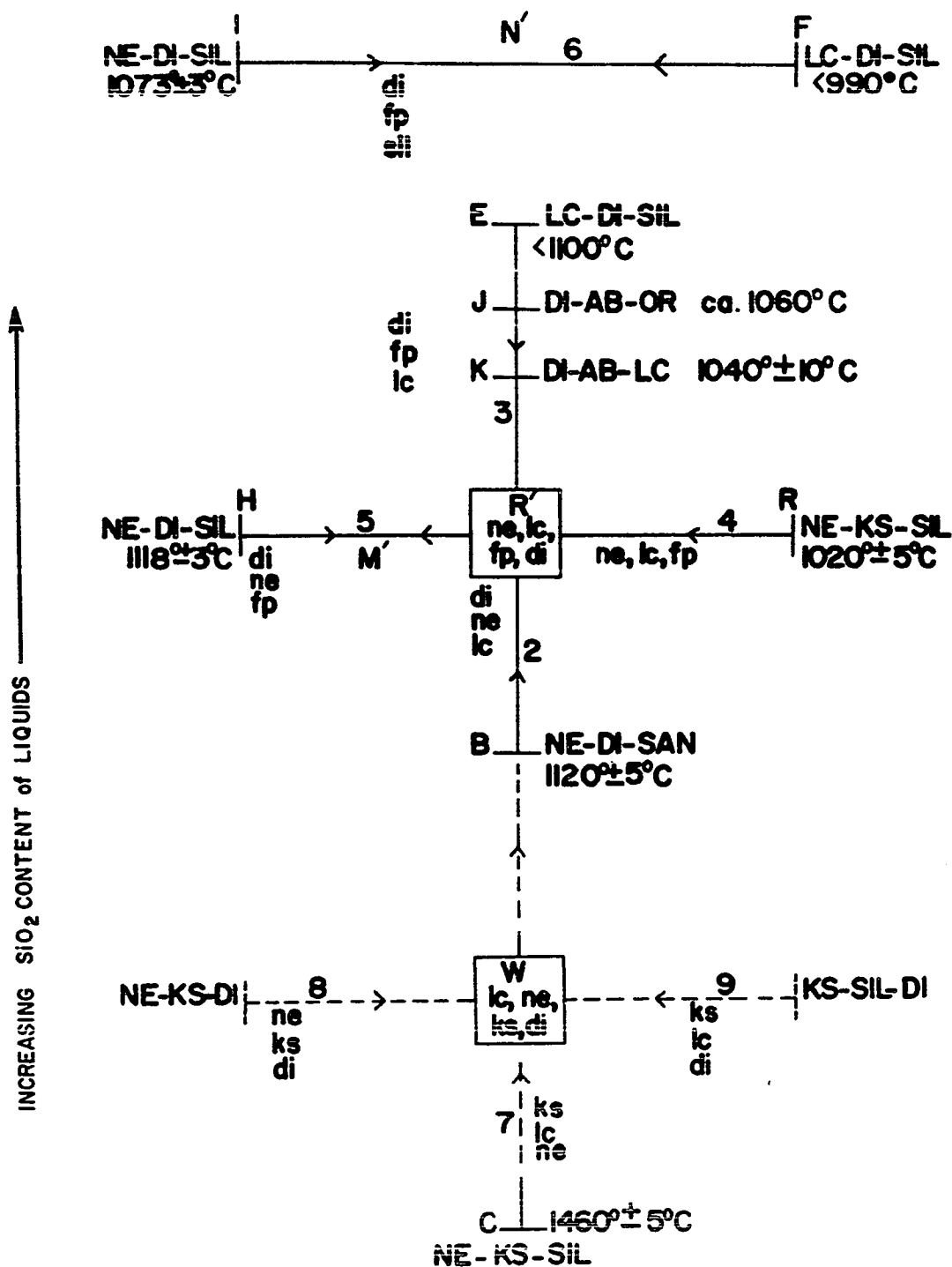


FIGURE 13. Flow diagram showing the univariant and invariant equilibria involving liquid lying within the system Nepheline-Kalsilite-Silica-Diopside.

Assemblages of dashed univariant lines are from theoretical considerations. Letters and numbers correspond with those in Tables 5 and 6.

Symbols: ne=nepheline, ks=kalsilite, lc=leucite, di=diopside, fp=Ca-poor ternary feldspar.

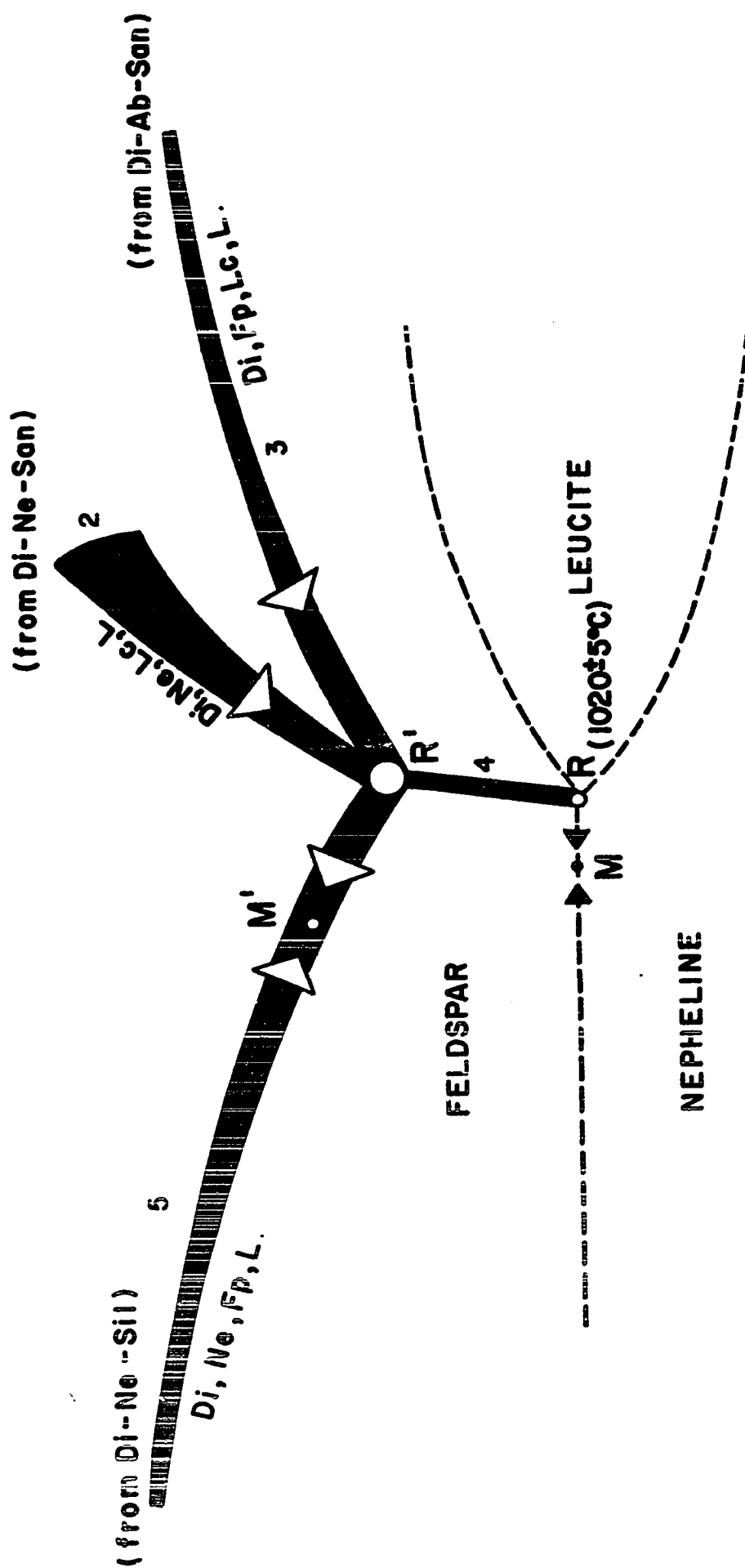


FIGURE 14. Schematic arrangement of univariant lines around the invariant point  $\text{ne} + \text{lc} + \text{fp} + \text{di} + \text{liq. (R')}$ .

Dashed lines represent phase relations in the system Nepheline-Kalsilite-Silica (see Figure 2).

residual liquids lying along this line must increase on approaching the Invariant Point  $R'$ . This invariant point must, therefore, lie at a more  $\text{SiO}_2$  rich composition than Point B (Table 5, Figure 7 and 13).

ii. The line  $di + fp + lc + liq.$  (Line 3, Table 6, Figures 13 and 14).

This line originates in the tetrahedron Nepheline-Kalsilite-Silica-Diopside at its intersection with the system Leucite-Diopside-Silica (Point E, Table 5, Figure 8 and 13). Further intersections of this line occur in the systems Diopside-Albite-Orthoclase (Point J, Table 5, Figures 10 and 13) and Diopside-Albite-Leucite (Point K, Table 5, Figures 11 and 13). In Figure 12 this line is represented as the dashed line, running from the system Leucite-Diopside-Silica into the volume of the tetrahedron. It is also shown schematically in Figures 13 and 14. Along this line, leucite undergoes a crystal-liquid reaction indicating that the invariant point  $ne + lc + fp + di + liq.$  (Point  $R'$ , Table 6, Figures 13 and 14), which it intersects, must also have a similar leucite-liquid reaction, i.e. this invariant point must be a reaction point. Evidence for the leucite-liquid reaction along the line  $di + fp + lc + liq.$  is obtained from the present study (Chapter 3, p. 46) and from the instability of leucite in the systems Leucite-Diopside-Silica (Schairer and Bowen, 1938) and Albite-Leucite-Diopside (Sood, 1969). Residual liquids along this line become impoverished in  $\text{SiO}_2$  towards the Invariant Point  $R'$ .

iii. The line ne + lc + fp + liq. (Line 4, Table 6, Figures 13 and 14).

This line, originating in the system Nepheline-Kalsilite-Silica at Point R (Table 5, Figures 2 and 13), is represented as the dashed line running from the base into the volume of the tetrahedron in Figure 12. It is also represented schematically in Figures 13 and 14. Point R is also an invariant point as the system Nepheline-Kalsilite-Silica is a true ternary system. At this point, the reaction:

$$\text{leucite} + \text{liquid} \rightarrow \text{alkali feldspar} + \text{nepheline}$$

occurs. A similar reaction must also occur along the length of this line, except that the feldspars produced by this reaction are probably ternary due to the presence of CaO in the liquids. Again, this line indicates the instability of leucite at the Invariant Point R' (Figures 13 and 14).

iv. The line di + fp + ne + liq. (Line 5, Table 6, Figures 13 and 14):

One intersection of this line occurs at Point H (Table 5, Figures 9 and 13) in the system Nepheline-Diopside-Silica. This line is shown schematically in Figures 13 and 14, and as the dashed line in Figure 12 running into the volume of the tetrahedron Nepheline-Kalsilite-Silica-Diopside from the system Nepheline-Diopside-Silica. As the temperature falls, liquids on this line migrate away from Point H (Figure 13) into the volume of the tetrahedron, and the feldspars change

in composition from plagioclase at Point H to ternary feldspar at the Invariant Point R'. As discussed in more detail later, there is believed to be a temperature minimum on this line which prevents residual liquids, moving from the Nepheline-Diopside-Silica system, from reaching the Invariant Point R'.

With the final disappearance of leucite at R', the residual liquid moves away from this invariant point along the line  $di + fp + ne + liq.$  (Line 5, Figures 13 and 14). The ultimate goal of this liquid is not known. However, by analogy with the system Nepheline-Kalsilite-Silica, in which the residual liquid migrates from the invariant point  $ne + lc + fp$  (Point R, Table 5, Figures 2 and 14) to a minimum on the nepheline-feldspar cotectic line (M, Figures 2 and 14), it is thought that the residual liquid in the more complex system Nepheline-Kalsilite-Silica-Diopside may move from the Invariant Point R' (Figures 13 and 14) towards a temperature minimum M' on the line  $ne + fp + di + liq.$  (Figures 13 and 14).

From the present study, it was impossible to determine either the composition or temperature of the Invariant Point R' or temperature minimum M' as no mixtures in the system Nepheline-Diopside-Sanidine have the compositions of either of these points. However, R' must lie on the silica-undersaturated side of the system Diopside-Albite-Orthoclase (see Figure 12) as nepheline occurs as one of the crystallizing phases at this point. It is probably quite close both in



temperature and composition to the invariant point in the system Nepheline-Kalsilite-Silica (Point R, Table 5, Figures 13 and 14).

In an attempt to obtain experimental data for R' (Figures 13 and 14) one glass was made with bulk composition  $\text{Ne}_{44.7}\text{Ks}_{19.5}\text{Sil}_{30.8}\text{Di}_5$ . This composition is approximately equivalent to that of the Invariant Point R in the system Nepheline-Kalsilite-Silica (ca.  $\text{Ne}_{47}\text{Ks}_{21}\text{Si}_{32}$ , Table 5) with 5 weight percent diopside added. The results of the quenching experiments on this glass are given in the Appendix. This glass crystallized completely at  $970^{\circ}\pm 20^{\circ}\text{C}$ . to a mixture of nepheline, feldspar and diopside suggesting that the temperature minimum M' (Figures 13 and 14) on the line di + fp + ne + liq. (Line 5, Figures 13 and 14) has approximately this temperature. The glass also gave a diopside liquidus at approximately  $1045\pm 10^{\circ}\text{C}$ . indicating that the temperature minimum M' and possibly the Invariant Point R' contain less than 5 weight percent of the diopside molecule.

Piercing points of two further lines are located in the known systems of the tetrahedron Nepheline-Kalsilite-Silica-Diopside. These lines are:

- i di + fp + sil + liq. (Line 6, Table 6, Figure 13)
- ii ks + lc + ne + liq. (Line 7, Table 6, Figure 13).

i. The line di + fp + sil + liq. (Line 6, Table 6, Figure 13) occurs in the silica-oversaturated part of the Nepheline-Kalsilite-Silica-Diopside tetrahedron as is apparent

from the crystallization of a silica mineral. Points on this line occur in the system Nepheline-Diopside-Silica (Point I, Table 5, Figures 9 and 13) and the system Leucite-Diopside-Silica (Point F, Table 5, Figures 8 and 13). By analogy with the temperature minimum on the silica-feldspar cotectic line in the system Nepheline-Kalsilite-Silica (Figure 2), it is assumed that a similar minimum N' (Figure 13) exists on the line  $di + fp + sil + liq.$  (Line 6, Figure 13), although no exact temperature or composition of this minimum was determined in the present study. Along the line  $di + fp + sil + liq.$ , feldspars vary in composition from plagioclases at sodic-rich compositions to potash feldspars at potash-rich compositions.

ii. The line  $ks + lc + ne + liq.$  (Line 7, Table 6, Figure 13) intersects the system Nepheline-Kalsilite-Silica at Point C (Table 5, Figures 2 and 13). As this system is ternary, Point C is an invariant point. Within the tetrahedron this line may intersect the primary volume of diopside resulting in an assemblage of  $lc + ne + ks + di + liq.$  This five phase assemblage delineates a further Invariant Point W in the volume of the tetrahedron (Table 6, Figure 13).

The four lines which would intersect at this invariant point are:

- i.  $ks + lc + ne + liq.$  (Line 7, Table 6, Figure 13)
- ii.  $ne + ks + di + liq.$  (Line 8, Table 6, Figure 13)
- iii.  $ks + lc + di + liq.$  (Line 9, Table 6, Figure 13)

iv.  $di + ne + lc + liq.$  (Line 2, Table 6, Figure 13)

These lines are shown schematically in Figure 13.

At the invariant point  $ks + lc + ne + liq.$  (Point C, Table 5, Figures 2 and 13), in the system Nepheline-Kalsilite-Silica, kalsilite may react with liquid forming nepheline and leucite. Likewise, along the line  $ks + lc + ne + liq.$  (Line 7, Figure 13) in the volume of the tetrahedron a similar reaction may take place. Therefore, at the proposed invariant point  $lc + ne + ks + di + liq.$  (Point W, Figure 13), kalsilite may eventually disappear by reaction, with the residual liquid migrating from this invariant point along the line  $di + ne + lc + liq.$  (Line 2, Figure 13). This line intersects the system Nepheline-Diopside-Sanidine at Point B (Table 5, Figures 7 and 13) and merges with three other lines at the Invariant Point R' (Figures 13 and 14). Thus the line  $di + ne + lc + liq.$  connects assemblages containing kalsilite and those containing feldspar. With falling temperature, residual liquids move from the Invariant Point W towards the Invariant Point R' (Figure 13).

The complete flow diagram (Figure 13) shows the relationship of the lines, invariant points and temperature minima lying in the volume of the Nepheline-Kalsilite-Silica-Diopside tetrahedron. This diagram is schematic and does not depict spatial relations of these lines and points. However, liquids lying on the lines generally tend to be more silica-rich towards the top of the diagram. The length of the lines are

arbitrary, with arrows representing directions of falling temperatures.

The second five phase assemblage (p.60) contains mel + ol + di + ne + liq. and corresponds to an equivalent invariant point (Table 6, Figure 15) lying outside the volume of the tetrahedron. Its exact composition is not known although its temperature is close to 1140°C. (Table 4). In the present study, only residual liquids from those mixtures whose bulk compositions contain 10 percent or less of the sanidine molecule reach this invariant point.

Four lines representing the following phases:

- i. ne + ol + di + liq. (Line 1, Table 6, Figure 15).
- ii. ne + ol + mel + liq. (Line 10, Table 6, Figure 15).
- iii. di + ol + mel + liq. (Line 11, Table 6, Figure 15).
- iv. ne + mel + di + liq. (Line 12, Table 6, Figure 15).

intersect at this invariant point, as shown schematically in Figure 15. Line 1 intersects the system Nepheline-Diopside-Sanidine at Point A (Table 5, Figures 7 and 15) and the system Nepheline-Diopside-Silica at Point G (Table 5, Figures 9 and 15). Along this line the reaction:

olivine + liquid  $\rightarrow$  pyroxene

takes place. A similar reaction also occurs along line 11.

After residual liquids reach the Invariant Point X mel + ol + di + ne + liq. (Figure 15), both melilite and olivine disappear by reaction with the liquid. Because of difficulties in identifying small amounts of olivine in charges containing



a high proportion of diopside, it was generally impossible to tell exactly whether melilite or olivine reacted out first at this invariant point, but both apparently disappear at temperatures close to one another.

Certain assumptions as to the possible reaction taking place at this Invariant Point X (Figure 15) can be made. Olivine-liquid reactions take place along the lines  $ne + ol + di + liq.$  (Line 1, Figure 15) and  $di + ol + mel + liq.$  (Line 11, Figure 15) which intersect at this invariant point where a similar olivine-liquid reaction must occur. Onuma and Yagi (1967) found an invariant point with a similar assemblage in the system Diopside-Akermanite-Nepheline at which olivine disappears by reaction with the liquid. This strengthens the hypothesis that olivine disappears by reaction at the invariant point  $mel + ol + di + ne + liq.$  in the present study.

With the final disappearance of olivine, the residual liquid migrates along the line  $ne + mel + di + liq.$  (Line 12, Figure 15) while melilite reacts with the liquid phase. The termination of this line is not known but if it is another invariant point, this must also show a melilite-liquid reaction.

Residual liquids which crystallize olivine but not melilite (see Table 4) at some stage of their cooling history reach the line  $ne + ol + di + liq.$  (Line 1, Table 6, Figure 15) which intersects the Invariant Point X (Figure 15). However, without the crystallization of melilite, residual

liquids will not reach this invariant point, so it is possible that such residual liquids, because of their greater than 10 weight percent sanidine content and subsequent melilite reaction, may trend towards some other invariant point whose composition is governed by the products of the melilite-feldspar reaction discussed in Section 3.5 of Chapter 3.

Possible solid phases, in addition to a liquid phase, which could coexist at this invariant point are any four of the following: olivine (from the nepheline-diopside reaction, see pp.32-34), nepheline, diopside, feldspar and wollastonite (from the melilite-feldspar reaction, Section 3.5, Chapter 3). However, as residual liquids move along the line  $ne + ol + di + liq.$  (Line 1, Figure 15), these three phases must coexist at this invariant point, thus reducing the possible assemblages to:

- i.  $ne + ol + di + fp + liq.$
- ii.  $ne + ol + di + wo + liq.$

In the systems Nepheline-Forsterite-Silica (Schairer and Yoder, 1961) and Leucite-Forsterite-Silica (Schairer, 1954) olivine coexists with albite but not with sanidine. The composition of alkali feldspar at which olivine becomes unstable in the system Albite-Sanidine-Forsterite is not known. However, it is possible that the invariant point  $ne + ol + di + fp + liq.$  can exist for a limited range of alkali feldspar compositions. The proximity of the albite-forsterite eutectic to pure albite (Schairer and Yoder, 1961) suggests that the

amount of olivine coexisting with feldspar at this invariant point is small.

Studies in the system Nepheline-Forsterite-Silica-Larnite (Schairer and Yoder, 1964), show that wollastonite and olivine cannot coexist and, therefore, it seems unlikely that the invariant point  $ne + ol + di + wo + liq.$  occurs.

The invariant point  $ne + ol + di + fp + liq.$  (Point Y, Table 6, Figure 15) is formed by the intersection of the lines:

- i.  $ne + ol + di + liq.$  (Line 1, Table 6, Figure 15).
- ii.  $ne + di + fp + liq.$  (Line 13, Table 6, Figure 15).
- iii.  $ol + di + fp + liq.$  (Line 14, Table 6, Figure 15).
- iv.  $ne + ol + fp + liq.$  (Line 15, Table 6, Figure 15).

Just as an olivine-liquid reaction occurs along the line  $ne + ol + di + liq.$  (Line 1, Figure 15) so must it occur at the Invariant Point Y (Figure 15). With the complete disappearance of olivine, residual liquids migrate from this invariant point along the line  $ne + di + fp + liq.$  (Line 13, Figure 15). As the liquids produced by the melilite-feldspar reaction (Section 3.5, Chapter 3) contain potential wollastonite, this line most probably intersects an invariant point  $ne + di + fp + wo + liq.$  (Point Z, Table 6, Figure 15). This invariant point forms at the intersection of the four lines:

- i.  $ne + di + fp + liq.$  (Line 13, Table 6, Figure 15).
- ii.  $ne + di + wo + liq.$  (Line 16, Table 6, Figure 15).
- iii.  $fp + wo + di + liq.$  (Line 17, Table 6, Figure 15).



iv. fp + wo + ne + liq. (Line 18, Table 6, Figure 15).

With the aid of the flow diagrams in Figures 13 and 15, residual liquid trends on equilibrium and fractional crystallization in the system Nepheline-Diopside-Sanidine can now be discussed.

The simplified rock types, with assemblages corresponding to those of the lines and invariant points, are given in Table 7. Certain of these will be referred to more extensively in the following chapters.

TABLE 7

Rock Types Corresponding to Assemblages of Univariant Lines,  
Invariant Points and Temperature Minima of Figures 13 and 15

<u>Assemblage</u>	<u>Position of the liquid phase</u>	<u>Rock Type</u>
<u>Figure 13.</u>		
di,ne,lc.	Line 2	leucitophyre
di,fp,lc.	Line 3	leucite trachyte
ne,lc,fp.	Line 4	leucite phonolite
di,ne,fp	Line 5	phonolite
di,ne,fp.	Temperature Minimum M'	phonolite
ne,lc,fp,di.	Invariant Point R'	leucite phonolite
di,fp,sil.	Line 6	rhyolite
di,fp,sil.	Temperature Minimum N'	rhyolite.
<u>Figure 15.</u>		
ne,ol,di.	Line 1	olivine nephelinite
ne,ol,mel	Line 10	olivine melilite nephelinite
di,ol,mel.	Line 11	olivine melilitite
ne,mel,di.	Line 12	melilite nephelinite
mel,ol,di,ne.	Invariant Point X	olivine melilite nephelinite
ne,ol,di,fp.	Invariant Point Y	olivine phonolite
ne,di,fp.	Line 13	phonolite
ne,di,wo.	Line 16	wollastonite nephelinite
ne,fp,di,wo.	Invariant Point Z	wollastonite phonolite

## CHAPTER 5

### CRYSTALLIZATION AND RESIDUAL LIQUID TRENDS IN THE SYSTEM NEPHELINE - DIOPSIDE - SANIDINE

#### 5.1 Introduction

In the previous chapter, four and five phase assemblages were treated as univariant lines and invariant points respectively. Similarly, in the present chapter, three phase assemblages are considered as indicative of divariant surfaces,<sup>1</sup> defined by liquids in equilibrium with two solid phases; and two phase assemblages as primary phase volumes, having a liquid phase in equilibrium with a single solid phase.

As the system Nepheline-Diopside-Sanidine is pseudo-ternary, residual liquids on crystallizing move away from the plane of the system along a series of curved paths through primary phase volumes, and on surfaces towards univariant lines. The ultimate goal of these liquids is either towards invariant points and/or temperature minima located on these lines.

Two types of crystallization occur in magmas. Under

---

1. Divariant surfaces will be referred to as surfaces for the remainder of this thesis.

perfect equilibrium conditions, crystals remain in contact with the liquid and cooling is sufficiently slow to maintain equilibrium between crystals and liquid. On cooling, the crystals continuously react with the magma changing their composition in response to changes in liquid compositions. The final product of this process is a single assemblage of minerals whose bulk composition corresponds to that of the initial magma. Quenching experiments correspond to equilibrium crystallization in nature, with the final assemblages occurring at the solidus being the simplified equivalents of the individual rock types produced from magmatic crystallization.

With perfect fractional crystallization, crystals are continuously removed from the magma and crystal-liquid equilibrium is not maintained resulting in varying assemblages of minerals corresponding to different rock types; but each with a different bulk composition from that of the initial magma. Fractional crystallization is one of the main factors controlling igneous rock differentiation whereby several rock types can be produced from a single magma. Other factors, such as gaseous transfer, liquid immiscibility, thermodiffusion and assimilation, may also be operative in the differentiation process. However, only the effects of fractional crystallization can be deduced from the present study.

As phase relations were determined at 1 atmosphere they are only applicable for magmas crystallizing at or near the

earth's surface. Under conditions of rapid cooling, it seems unlikely that a comagmatic suite of rocks could form from crystal-liquid fractionation except possibly in the extreme case of the formation of a differentiated lava flow caused by the slower cooling of the central portion with respect to its peripheral parts.

Fractional crystallization producing the rock types to be described in this chapter is assumed to have occurred at some depth in the earth's crust where the effects of pressure had little affect on the laboratory phase relations obtained at 1 atmosphere.

## 5.2 Equilibrium Crystallization.

In Table 4, the liquid phase of any two phase assemblage corresponds to a liquid crystallizing a single solid phase in a primary phase volume, whereas the liquid phase of a three phase assemblage lies on a surface and crystallizes two solid phases. Similarly, the liquid phase of a four phase assemblage lies on a line and crystallizes three solid phases, and that of a five phase assemblage lies at an invariant point and crystallizes four solid phases.

An example of the crystallization history of one of the mixtures studied is given in Table 8, and from it the trend of the residual liquid can be deduced. From this example residual liquid trends for the other mixtures studied can be deduced from the data in Table 4 and from Figures 13 and 15. The main features of these trends are now discussed.

TABLE 8

Equilibrium Crystallization History of Mixture Ne<sub>30</sub>Di<sub>10</sub>San<sub>60</sub>

<u>Temperature</u>	<u>Assemblage</u>	<u>Geometric position of the liquid phase</u>
1275°C	Glass	Above the liquidus, no crystallization.
1270°C	lc + gl.	Leucite primary phase volume
1135°C	di + lc + gl.	On the surface di + lc + liq.
1060°C	fp + di + lc + gl.	On the line di + fp + lc + liq. Line 3, Figure 13.
1030°C	ne + fp + di + lc + gl.	At the invariant point ne + lc + fp + di + liq. Point R', Figure 13.
980° ± 10°C	ne + fp + di + lc.*	Beginning of melting, i.e. Solidus.

\*Leucite decreased in amount compared to 1030°C and 1060°C.

Compare with Table 4, Chapter 3.

On perfect equilibrium crystallization, residual liquids trend towards the Invariant Point R' (Figure 13 and 14) and/or the temperature minimum M' (Figures 13 and 14) on the line  $di + ne + fp + liq.$  (Line 5, Figures 13 and 14). These points are equivalent in mineralogy to simplified leucite phonolites and phonolites respectively (Table 7). However, the last liquids may completely crystallize on a surface before reaching either of these points giving a mixture of two solid phases; or final crystallization may occur on a line producing an assemblage of three solid phases (Table 4). Such assemblages found in the present study include: leucite-diopside-nepheline equivalent to a simplified leucitophyre (Table 7), leucite-diopside-feldspar representing a simplified leucite trachyte (Table 7) and, nepheline-diopside which can be considered as a simplified nepheline (Table 7).

### 5.3 Fractional Crystallization.

With perfect fractional crystallization, residual liquid trends may differ from those of equilibrium crystallization. In the following section, these trends are discussed mainly for residual liquids lying on the following lines.

#### 5.31 Fractionation of Residual Liquids on the Line $di + ne + lc + liq.$ (Line 2, Figures 13 and 14)

The mixtures producing residual liquids which reach this line on crystallization can be obtained from Table 4. Fractional crystallization enables these residual liquids to

reach the Invariant Point R' (Figures 13 and 14) and, with further fractionation, to reach the temperature minimum M' (Figures 13 and 14) where the final assemblage is nepheline, feldspar and diopside. In most cases the volume of liquid reaching M' is probably small.

To reach the line  $di + ne + lc + liq.$  (Line 2, Figures 13 and 14) liquids migrate by one of the surfaces:

$ne + di + liq.$

$lc + di + liq.$

$lc + ne + liq.$

(see Table 4). If fractionation occurs while a residual liquid lies on any one of these surfaces, assemblages equivalent to simplified nephelinites (i.e. nepheline-pyroxene rocks, Table 7), leucitites (i.e. leucite-pyroxene rocks, Table 7) and leucitophyres (i.e. leucite-nepheline rocks, Table 7) are formed.

Fractionation on the line  $di + ne + lc + liq.$  produces an assemblage equivalent to a simplified leucitophyre (Table 7), whereas fractionation at the Invariant Point R';  $ne + lc + fp + di + liq.$  (Figures 13 and 14) gives an assemblage equivalent to a simplified leucite phonolite (Table 7). The assemblage formed at the temperature minimum M' (Figures 13 and 14) is equivalent to a simplified phonolite (Table 7).

A schematic rock diagram showing the rock types which could form by fractionation of residual liquids reaching the line  $di + ne + lc + liq.$  is given in Figure 16.



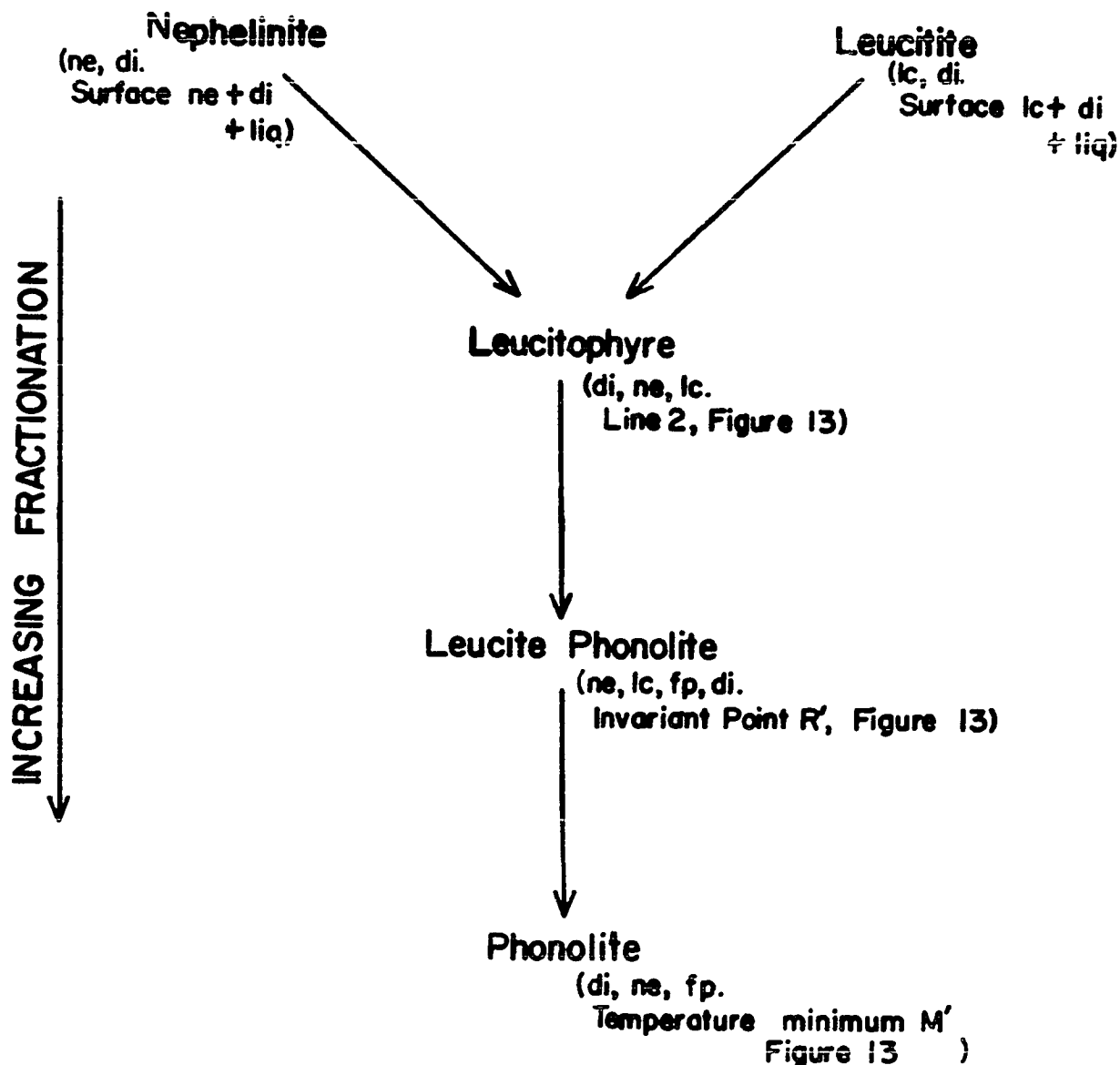


FIGURE 16. Simplified rock types produced by fractionation of residual liquids reaching the univariant line  $di + ne + lc + liq$ . (Line 2, Figure 13).

Solid phases and position of the corresponding residual liquid are given in brackets.

### 5.32 Fractionation of Residual Liquids on the Line di + fp + lc + liq. (Line 3, Figures 13 and 14).

Data for compositions producing residual liquids reaching this line are given in Table 4. This line is characterized by a leucite-liquid reaction and any change in residual liquid composition along it results from the continuous reaction of leucite. However, if the leucite is removed by fractionation, the leucite-liquid reaction prevents further crystallization of leucite and the residual liquids must migrate from the line. Consequently, fractional crystallization has a marked affect on residual liquids trending along this line.

This line extends from silica-oversaturated (Point E, Figure 13) to silica-undersaturated (Point K, Figure 13) compositions, the point of silica-saturation (Point J, Figure 13) occurring in the system Diopside-Albite-Orthoclase (Morse, 1968). On fractionation, residual liquids with silica-undersaturated compositions may migrate directly from the line di + fp + lc + liq. across the fp + di + liq. surface towards the temperature minimum M' (Figures 13 and 14) on the line di + ne + fp + liq. (Line 5, Figures 13 and 14) without passing through the Invariant Point R' (Figures 13 and 14).

Silica-oversaturated residual liquids, possibly produced from the crystallization of sanidine-rich compositions in the system Nepheline-Diopside-Sanidine, also leave this line on

fractionation; but, instead of migrating to the temperature minimum M', (Figures 13 and 14), they move across the  $fp + di + liq.$  surface towards the temperature minimum N' (Figure 13) on the line  $di + fp + sil + liq.$  (Line 6, Figure 13). The possible rock types produced by fractional crystallization of residual liquids after reaching the line  $di + fp + lc + liq.$  are given in Figure 17.

### 5.33 Fractionation of Residual Liquids on the Line $ne + ol + di + liq.$ (Line 1, Figure 15)

In the present study, residual liquids which reach this line (Table 4) do not crystallize melilite, probably due to the melilite-feldspar reaction outlined previously (Section 3.5, Chapter 3). On fractionation, these residual liquids must migrate from the line  $ne + ol + di + liq.$  because of the olivine-liquid reaction (see Chapter 4, p.78). The olivine nephelinite assemblages represented by this line should show some indication of an olivine reaction. Olivines from nepheline-basalts (olivine nephelinites) showing deep resorption embayments have been reported from Truk Islands, East Caroline Islands (Stark and Hay, 1963, p. 20) and this is possibly indicative of an olivine-liquid reaction occurring in nature similar to that postulated from the laboratory system.

Residual liquids migrating from the line  $ne + ol + di + liq.$  most probably trend to the line  $ne + di + fp + liq.$  (Line 13, Figure 15) across the surface  $ne + di + liq.$  As

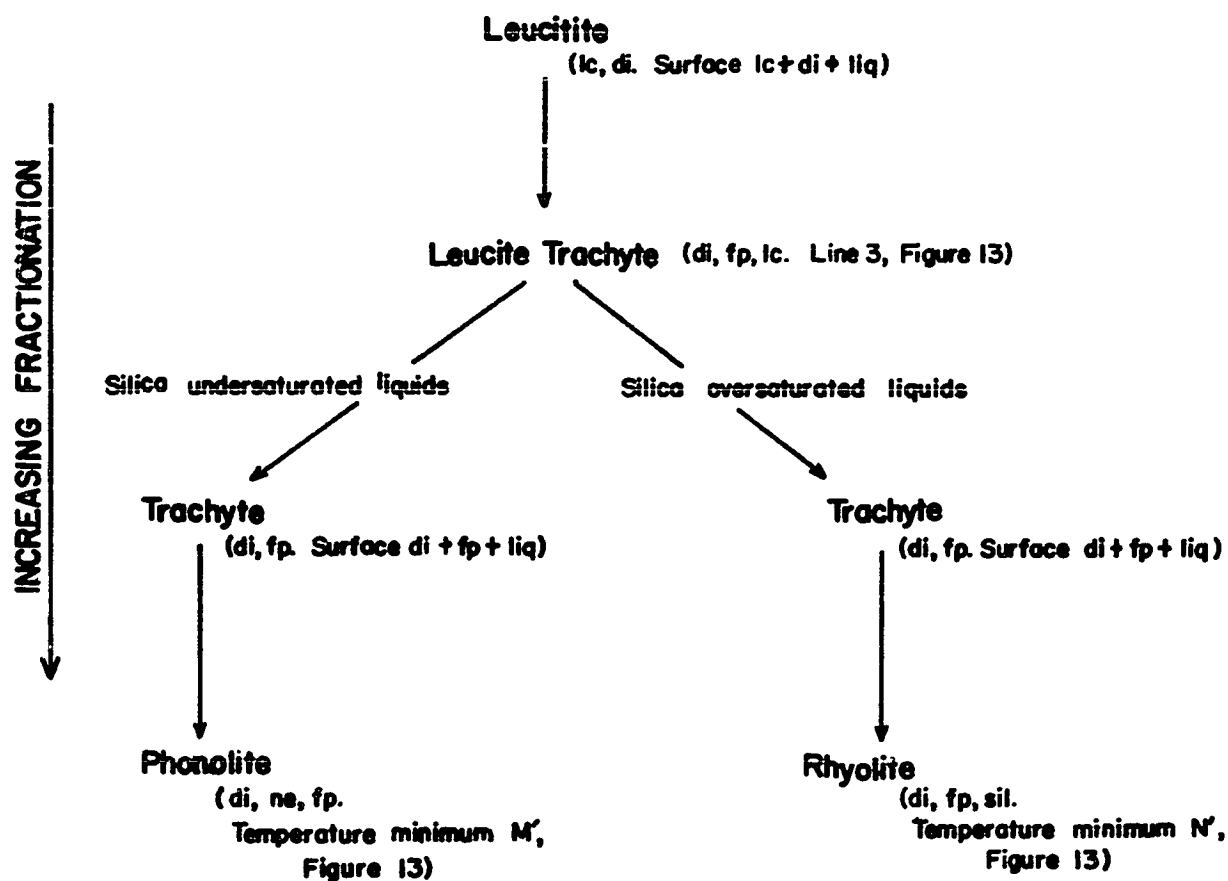


FIGURE 17. Simplified rock types produced by fractionation of residual liquids reaching the univariant line  $di + fp + lc + liq$ . (Line 3, Figure 13).

Solid phases and position of the corresponding residual liquid are given in brackets.

wollastonite is one of the products of the postulated melilite feldspar reaction, this phase could also crystallize. With fractionation, residual liquids on the line  $ne + di + fp + liq.$  (Line 13, Figure 15) could, therefore, trend to the Invariant Point Z (Figure 15). Possible rock types formed from these compositions by fractional crystallization are given in Figure 18. In nature the crystallization of wollastonite may be prevented due to its solid solution with pyroxene or by its combination with  $TiO_2$  to form sphene  $CaTiSiO_4(O,OH,F)$ .

#### 5.34 Fractionation of Residual Liquids on the Line $di + ol + mel + liq.$ (Line 11, Figure 15).

Mixtures producing residual liquids which reach this line can be deduced from the data in Table 4. Fractionation on this line causes residual liquids to move away from it as a consequence of the olivine-liquid reaction (Chapter 4, p.78). On migrating from this line, residual liquids move across a  $di + mel + liq.$  surface towards the line  $ne + mel + di + liq.$  (Line 12, Figure 15) where melilite begins to react with liquid. Because of the melilite-liquid reaction, fractionation on this line causes the residual liquid to migrate from it across the  $ne + di + liq.$  surface. Any melilite molecule remaining in the liquid probably reacts to produce potential wollastonite (Section 3.5, Chapter 3). With further fractionation on the  $ne + di + liq.$  surface, the liquid becomes enriched in feldspar and wollastonite and could, therefore, intersect

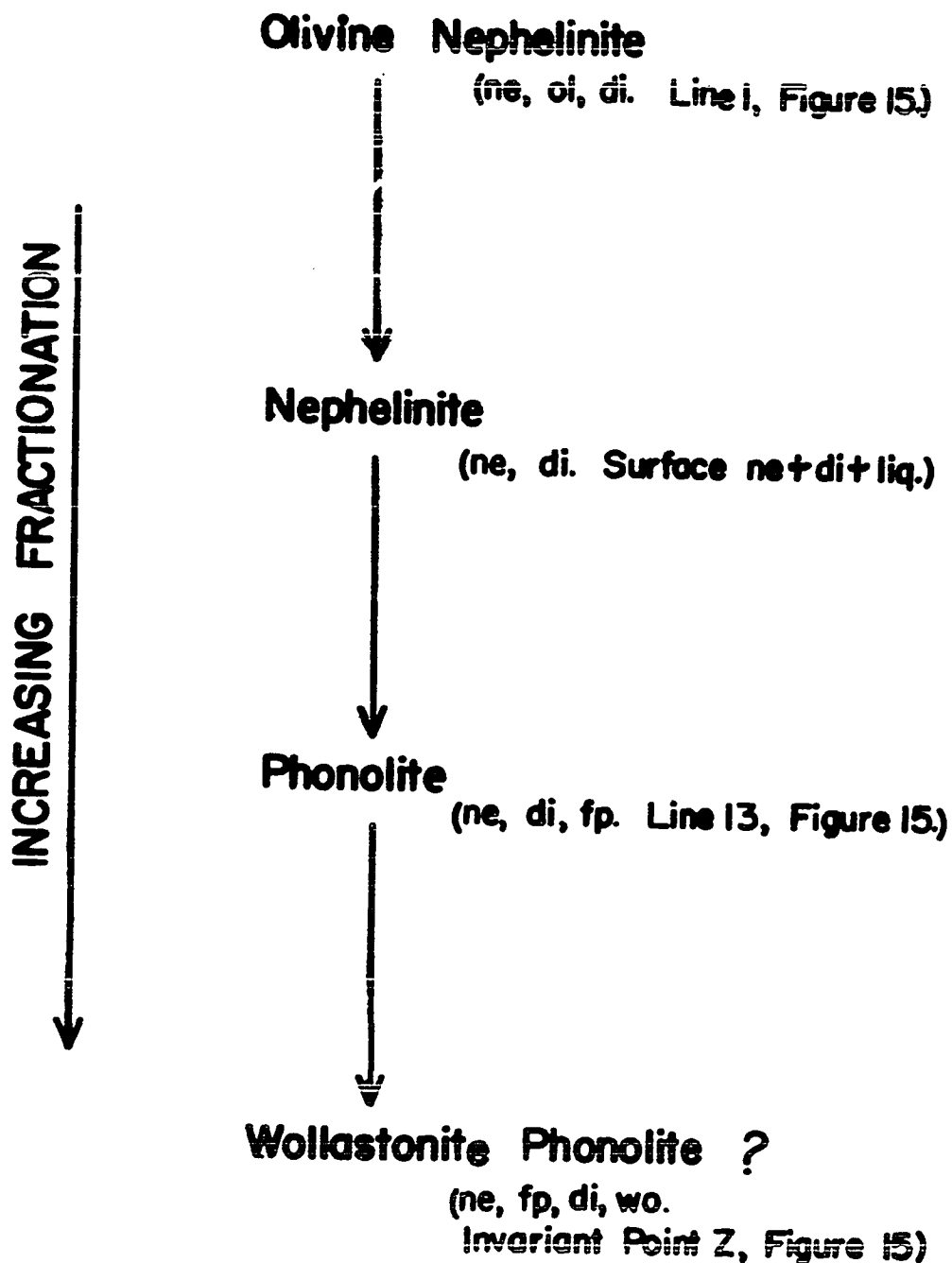


FIGURE 18. Simplified rock types produced by fractionation of residual liquids on the univariant line ne + ol + di + liq. (Line 1, Figure 15).

Solid phases and position of the corresponding residual liquid are given in brackets.

Wollastonite may not crystallize to form wollastonite phonolite.

either the line  $ne + di + fp + liq.$  (Line 13, Figure 15) or the line  $ne + di + wo + liq.$  (Line 16, Figure 15). Fractionation on either of these lines allows the residual liquids to migrate to the Invariant Point Z (Figure 15). Possible rock types forming from this fractionation sequence are given in Figure 19, although wollastonite may not crystallize for the reasons given on p.95.

#### 5.35 Fractionation of Residual Liquids on the Line $ne + ol + mel + liq.$ (Line 10, Figure 15).

Only one composition studied (i.e.  $Ne_{68}Di_{25}San_7$ , Table 4) reached this line. Residual liquids from fractionation on this line migrate to the Invariant Point X (Figure 5) and, with further fractionation, follow the same trends as described previously for residual liquids reaching the line  $di + ol + mel + liq.$  (Section 5.34). The rock types which can form from such crystallization are shown in Figure 20.

The relationship between all the possible rock types formed by fractional crystallization of synthetic compositions crystallizing melilite and/or olivine is given in Figure 21.

#### 5.36 Fractionation of Residual Liquids After the Disappearance of Melilite and Olivine.

In composition crystallizing melilite and/or olivine, these phases subsequently disappear with falling temperature (see Table 4). If fractionation occurs after their disappearance, residual liquids may follow two trends;

- i. Sanidine-poor compositions may produce residual liquids which trend across the  $ne + di + liq.$  surface to the

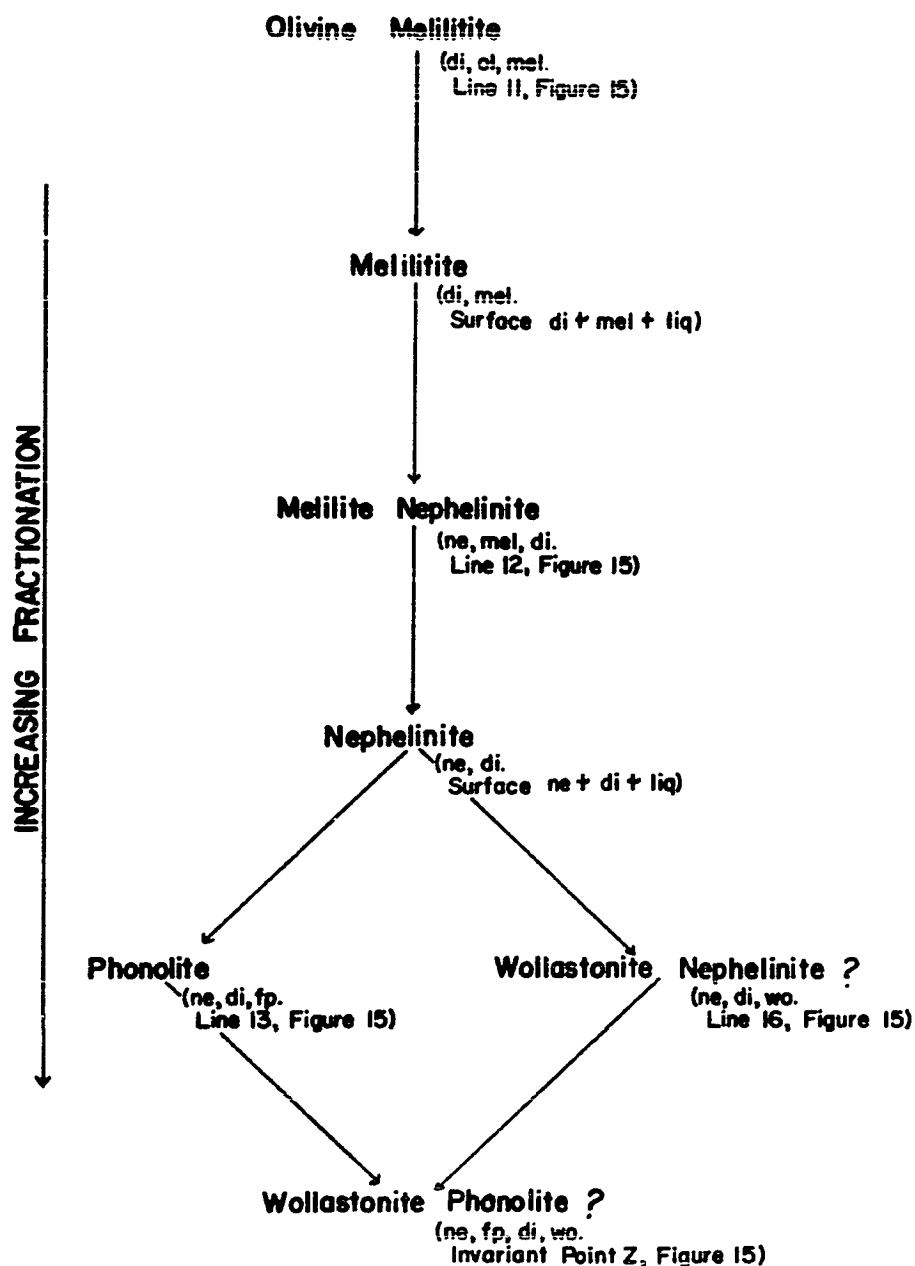


FIGURE 19. Simplified rock types produced by fractionation of residual liquids on the univariant line di + ol + mel + liq. (Line 11, Figure 15).

Solid phases and position of the corresponding residual liquid are given in brackets.

Wollastonite may not crystallize to form wollastonite nephelinite and wollastonite phonolite.



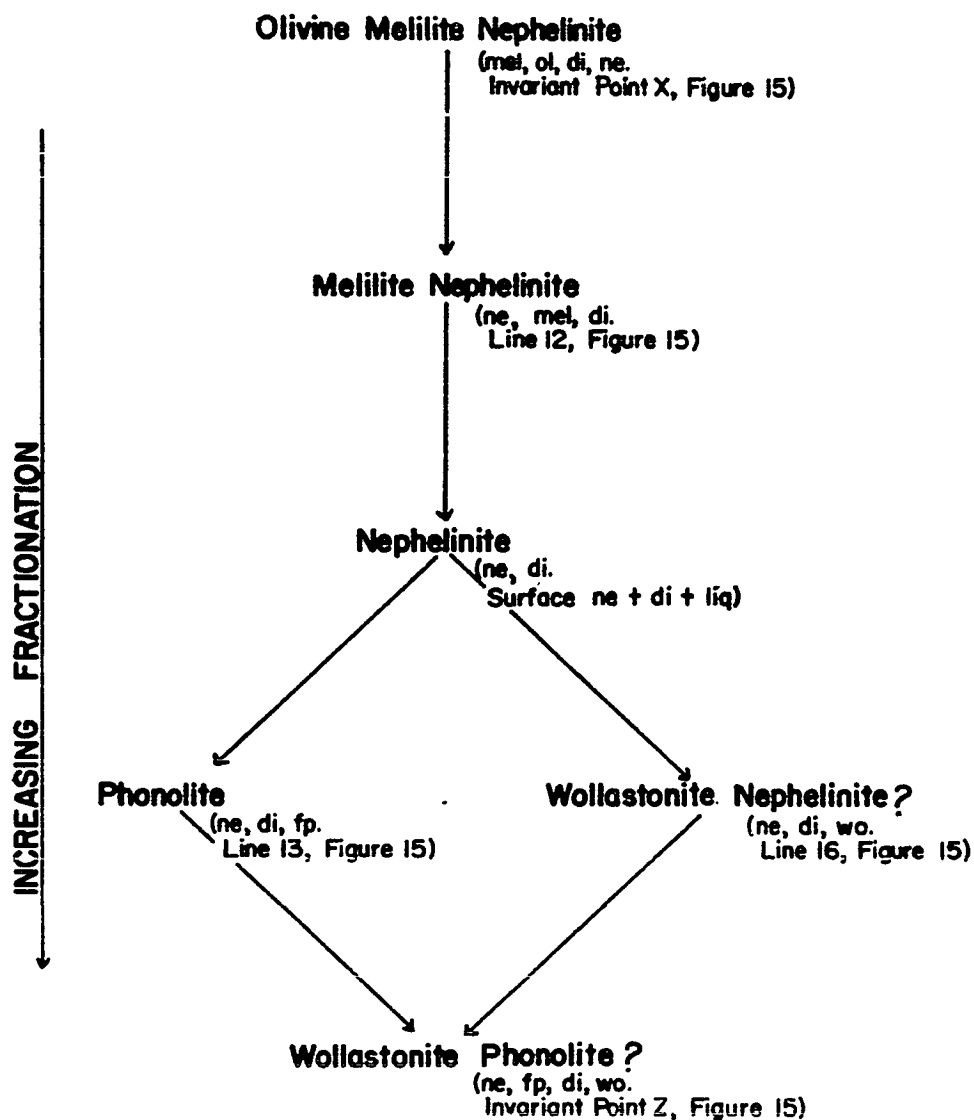


FIGURE 20. Simplified rock types produced by fractionation of residual liquids on the univariant line  $ne + ol + mel + liq$ . (Line 10, Figure 15).

Solid phases and position of the corresponding residual liquid are given in brackets.

Wollastonite may not crystallize to form wollastonite nephelinite and wollastonite phonolite.

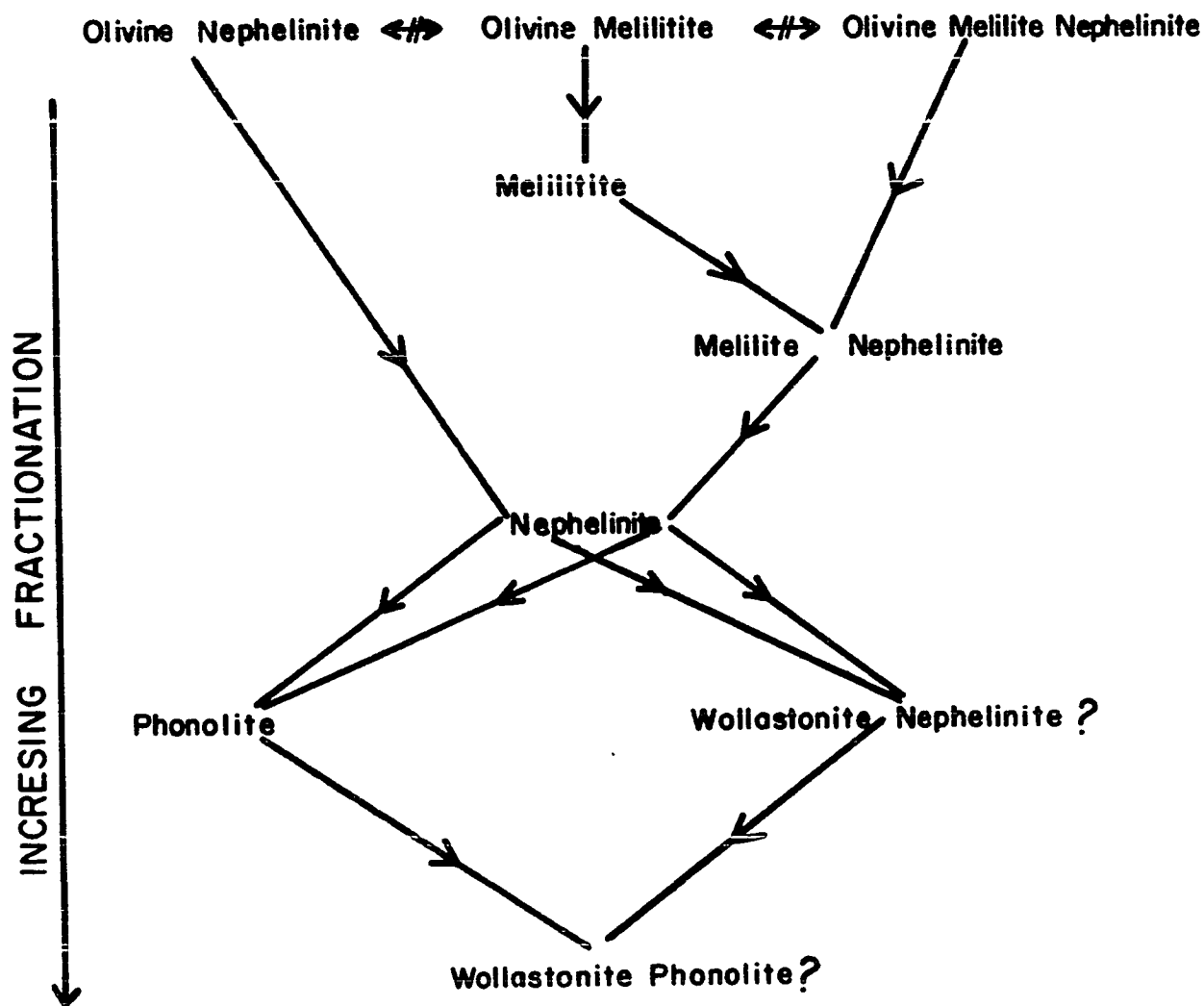


FIGURE 21. Relationship between all possible rock types formed by the fractional crystallization of synthetic compositions crystallizing melilitite and/or olivine.

Wollastonite may not crystallize to form wollastonite nephelinite and wollastonite phonolite.

line  $di + ne + fp + liq.$  (Line 5, Figure 13) and eventually to the temperature minimum  $M'$  on this line (Figure 13). The equivalent rock types produced trend from nephelinites to phonolites.

ii. Sanidine-Rich compositions (cf.  $Ne_{50}Di_{26}San_{24}$  Table 4) probably produce liquids which trend across the  $ne + di + liq.$  surface to the line  $di + ne + lc + liq.$  (Line 2, Figures 13 and 14). With further fractionation, such residual liquids reach the Invariant Point  $R'$  (Figures 13 and 14) and eventually the temperature minimum  $M'$  on the line  $di + ne + fp + liq.$  (Line 5, Figures 13 and 14). The equivalent rock types trending from nephelinites to leucitophyres and leucite phonolites to phonolites (cf. Figure 16).

## CHAPTER 6

### PETROLOGICAL IMPLICATIONS

Any comparison between assemblages formed in synthetic systems and those formed from more complex natural systems must be based on certain assumptions arising from the limitations inherent in experimental studies. The most basic assumption is that simplified synthetic systems can, in fact, duplicate to some extent the complex chemical and physical behavior present in nature. The frequent close similarities between the conditions of formation of many assemblages in the laboratory and those postulated for natural assemblages from field observations seems to justify the use of experimental techniques in explaining petrogenesis.

Although one of the main aims of experimental petrology is to help evaluate hypotheses proposed for the formation of rocks, it may also be of use in providing information about certain rocks which is not readily apparent from field studies. For example, in the present study none of the wholly crystalline assemblages contain either melilite or olivine, although these phases occur in certain compositions at liquidus and subliquidus temperatures (Table 4). For the majority of these compositions, the final assemblage consists of nepheline and diopside suggesting that certain nepheline-

pyroxene rocks (e.g. nephelinites) may in fact be the low temperature equivalents of melilite and/or olivine-bearing rocks such as olivine nephelinites, olivine melilite nephelinites, melilite nephelinites and olivine melilitites, whose simplified mineralogy is given in Table 7.

Experimental studies may also provide information about rocks which has possibly been overlooked by field workers. The reaction of olivine is well documented in olivine tholeiites and tholeiites but such reactions are thought to be absent from alkali basalts (Wilkinson, 1956). In the present study, an olivine-liquid reaction forming pyroxene (Chapter 4, p. 78) occurs in assemblages equivalent to olivine nephelinites (Line 1, Figure 15) and olivine melilitites (Line 11, Figure 15), both of which are akin to alkali basalts. These findings, which supplement those of Schairer and Yoder (1960), suggest that olivine reactions may, in fact, be more common in alkali basaltic rocks than once thought. Possible evidence for this is given in Chapter 5 (p. 93).

As an aid in the evaluation of hypotheses for the formation of certain rocks, the present study provides information on the close association of nephelinites and phonolites reported from many localities, particularly those along the East African rift system.

In Kenya, on the western side of this rift system, Wright (1963) has described a series of lavas ranging from melanephelinites, containing olivine and melilite, through

nephelinites to phonolites. For the rocks produced from probable fissure eruptives, the sequence of events was described as ( p. 168):

"Phonolites of Sotik, Mara, Naro, and probably Mau. Miocene in age, in part overlying the Kishaldoga melanephelinites.

Kishaldoga melanephelinites and olivine melanephelinites. Grading in part up to nephelinites."

For the central volcanoes of this area the sequence was described as ( p. 168) :

"Nephelinite and phonolitic plugs of Ruri. Miocene, post-dating the Kisingiri volcanic series.

Kisingiri Volcanic Series: melanephelinites, often olivine and melilite bearing, nephelinites and related pyroclastic deposits with minor intrusives."

Wright has suggested (p. 172) that these rocks were derived by the differentiation of a melanephelinitic parent magma. The present study tends to confirm this suggestion as compositions rich in nepheline and diopside with small amounts of sanidine (Table 4) differentiate to give similar trends (cf. Figures 18, 19 and 20).

Saggerson and Williams (1964) have shown that the rocks of the Northern Tanganyika alkaline district fall into two genetic series (Figure 22), one strongly alkaline, represented by the nepheline-bearing lavas (ankaratrites-melanephelinites-nephelinites-phonolites); and the other mildly alkaline, represented by the nepheline-free extrusives

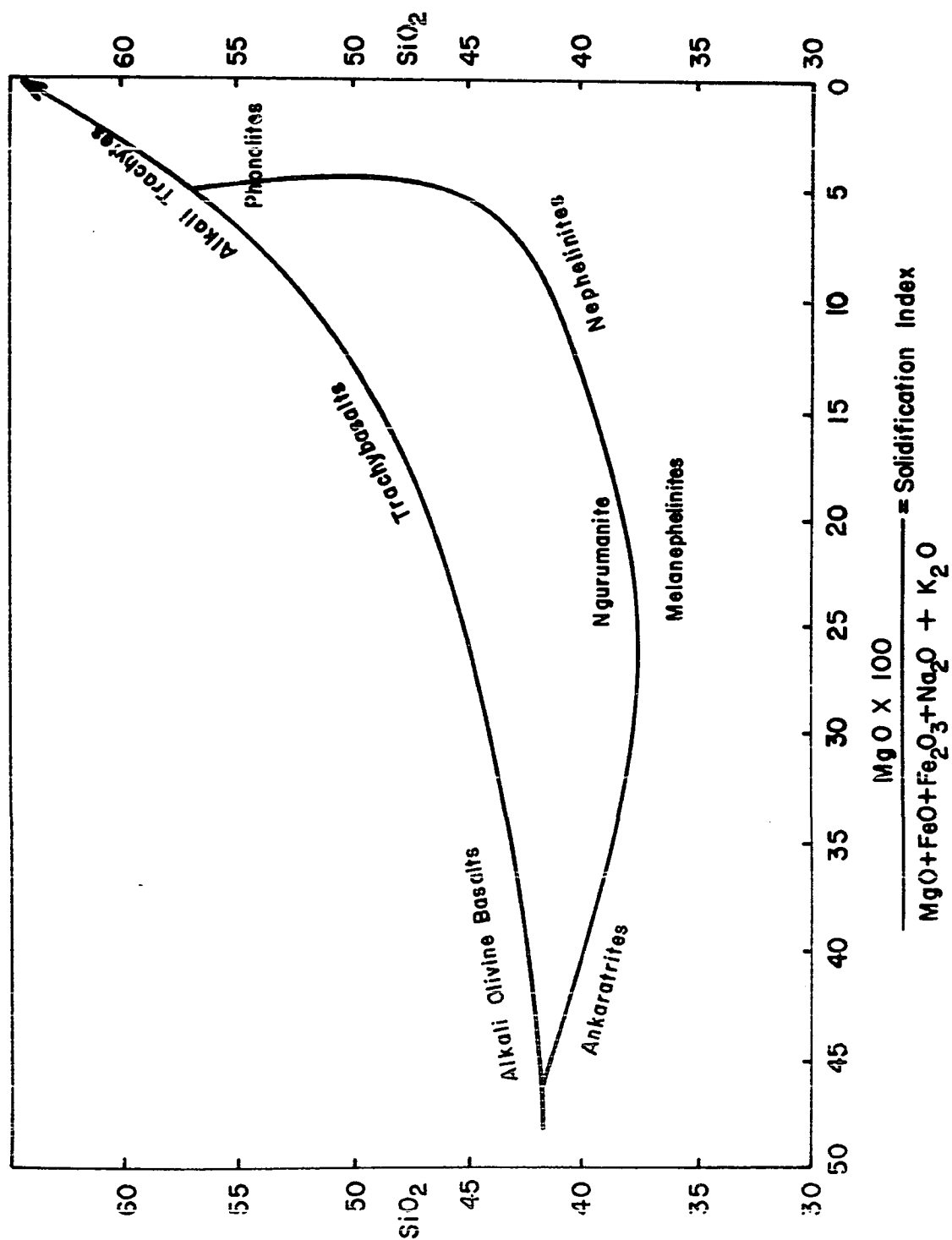


FIGURE 22. Differentiation trends of the mildly and strongly alkaline rocks of the northern Tanganyika alkaline district as indicated by a plot of SiO<sub>2</sub> against the Solidification Index (after Saggerson and Williams, 1964).

(alkali olivine basalt-trachybasalt-alkali trachytes). They consider these two series to have been derived independently from a common source in the mantle, possibly an alkali peridotite. Neither the derivation of these two trends from an alkali peridotite nor the derivation of the alkali olivine basalt-alkali trachyte series can be discussed in the light of the present work. However, if the melanephelinites in this area have been derived by fractionation, the results of the present study provide a mechanism for the fractionation trend suggested by Saggerson and Williams for the formation of the strongly alkaline, nepheline-bearing lavas.

King (1965) suggests that the nephelinites, phonolites and trachytes from volcanoes of Eastern Uganda (e.g. Elgon, Napak and Budeda) were derived by the early separation of forsterite, melilite and pyroxene from a magma of melanephelinitic composition. He infers that the early separation of these three minerals produces residual liquids in which the silica content, relative to alkalis and alumina, increases progressively from that of nepheline ( $\text{Na}_2\text{O}, \text{K}_2\text{O} : \text{Al}_2\text{O}_3 : 2\text{SiO}_2$ ) towards that of alkali feldspars ( $\text{Na}_2\text{O}, \text{K}_2\text{O} : \text{Al}_2\text{O}_3 : 6\text{SiO}_2$ ). This is basically the same trend as would be produced by fractionation of certain nepheline and diopside-rich compositions in the present study (cf. Figures 19 and 20) and consequently lends support to King's hypotheses. However, a notable difference between the natural and synthetic assemblages is the formation of trachytes in the



Ugandan rocks. Figure 21 shows that trachytic assemblages do not form from the differentiation of simplified melane-phelinitic liquids in the system Nepheline-Diopside-Sanidine, and thus the formation of trachytes cannot be explained from the present study.

Lavas from the Kisumu District of Kenya described by Saggerson (1952) have a differentiation trend from melilite nephelinite through phonolitic nephelinite to phonolite Wright, (1963). Comparison with fractional crystallization assemblages of certain compositions in the system Nepheline-Diopside-Sanidine (Figures 19 and 20), indicates that these rocks may have formed by the differentiation of a magma originally rich in nepheline and pyroxene molecules.

The present work has some bearing on the controversy of pseudoleucite formation in silica undersaturated alkaline rocks. Pseudoleucites are composed of a mixture of nepheline and potash feldspar and are thought to form as pseudomorphs after leucite. Two methods have been proposed for their formation; first, by the unmixing of Na-rich leucite with slow cooling originally proposed by Knight (1906) and later adhered to by Larsen and Buie (1938); second, by a leucite-liquid reaction first proposed by Bowen (1928). Both these hypotheses have gained support from experimental evidence. Fudali (1963) has shown that Na-rich leucite breaks down to nepheline and feldspar at subsolidus temperatures in the system Nepheline-Kalsilite-Silica at 1Kb.  $P_{H_2O}$ , while

Schairer and Bowen (1935), in their studies of the same system at atmospheric pressure, confirmed the existence of a leucite-liquid reaction to give nepheline and feldspar. This reaction takes place at Point R in Figures 2 and 13. In the present study, a leucite-liquid reaction producing nepheline-feldspar is believed to take place at R' (Figures 13 and 14) and, therefore, adds support to Bowen's hypothesis for the formation of pseudoleucites.

Experimental studies may be of some use in proposing hypotheses for the formation of a series of rocks where only empirical data on such rocks are available. Results from the system Nepheline-Diopside-Sanidine may be of use in explaining the origin of volcanic rocks from Monte Vico from the Ciminian District of the Roman Comagmatic Province, Italy. These rocks, described by Washington (1896), are composed mainly of leucite trachytes, forming as abundant flows and blocks in tuffs and containing phenocrysts of leucite, alkali feldspar and pale-green diopside, embedded in a groundmass of diopside, alkali feldspar, leucite, barkevikite and occasional plagioclase. Phonolites occur as blocks in the last tuffs ejected by Monte Vico and probably represent the last products of this volcano. These phonolites contain a small amount of haüyne, alkali feldspar and augite as phenocrysts in a groundmass of alkali feldspar, aegirine and nepheline. The fractional crystallization trends of certain compositions in the system Nepheline-Diopside-Sanidine display similar

trends to those of the Monte Vico lavas (Figure 17). Comparison of these trends suggests that the lavas from Monte Vico could have formed from a leucite trachytic magma by a process of fractional crystallization. Simplified trachyte (diopside-feldspar) assemblages are found in the synthetic fractionation scheme (Figure 17). Although no discrete trachytic rocks are found at Monte Vico, it is possible that the phenocrysts of augite and alkali feldspar in the phonolites may correspond to such trachytic assemblages.

Certain features of the experimental data, although not applied directly to specific examples of rocks, may be of some value to petrologists working in the field. The genesis of melilite-bearing rocks akin to nepheline basalts (e.g. melilite nephelinites, olivine melilite nepheline and olivine melilitites) has long been a source of controversy. Daly, in 1910, proposed that desilication of a basaltic magma by limestone assimilation accounted for the formation of these rocks, Bowen, in 1928, suggested that these rocks might form from an alkali magma, which is not particularly enriched in CaO, through the desilication of pyroxene (principally diopside) molecules by nepheline molecules. In the present study, melilite-bearing assemblages are formed from compositions which, although not particularly rich in CaO, are rich in nepheline and pyroxene molecules. For example, the composition  $\text{Ne}_{68}\text{Di}_{25}\text{San}_7$  crystallizing melilite and olivine contains 6.46 weight percent CaO, and the composition  $\text{Ne}_{45}\text{Di}_{50}\text{San}_5$

which also crystallizes these two minerals (Table 4) contains 12.92 weight percent CaO. The present work tends to confirm Bowen's hypothesis that melilite-bearing lavas need not necessarily form by limestone assimilation.

The present study has also indicated possible trends of fractionation for liquids which crystallize leucite (Figures 16 and 17) and it is possible that such trends might occur in natural comagmatic rocks.

From crystallization studies of one glass (Appendix), with a composition lying in the volume of the tetrahedron Nepheline-Kalsilite-Silica-Diopside close to the Invariant Point R in the system Nepheline-Kalsilite-Silica (Figures 2, 13 and 14), it is believed that the amount of diopside existing at the Invariant Point R' and temperature minimum M' in the tetrahedron (Figures 13 and 14) is less than 5 weight percent (see Chapter 4, p. 75). This temperature minimum is the goal towards which most residual liquids trend on fractionation. Its close proximity to the system Nepheline-Kalsilite-Silica tends to support Bowen's hypothesis (see Chapter 1) that a magma on fractionation becomes impoverished in the early-crystallizing minerals, in this case diopside, and enriched ultimately in alkali aluminosilicates.

The temperature of the minimum M' in the silica-under-saturated portion of the tetrahedron Nepheline-Kalsilite-Silica-Diopside, is  $970^{\circ} \pm 20^{\circ}\text{C}$ . (Appendix), a value at least  $30^{\circ}\text{C}$ . lower than the  $1020^{\circ}\text{C}$ . postulated by Morse (1968)

for the system Diopside-Albite-Orthoclase (Figure 10). A high temperature "saddle" must, therefore, exist in the system Diopside-Albite-Orthoclase within the tetrahedron (Figure 12). Consequently this system forms a thermal barrier between silica-saturated and silica-undersaturated liquids, at least as far as liquids in the silica-undersaturated portion of the tetrahedron are concerned. No data is yet available on the phase relations on the silica-saturated portion of this tetrahedron. This thermal barrier is only effective for silica-undersaturated compositions lying outside the primary phase volume of leucite, as compositions in this volume can cross the plane Diopside-Albite-Orthoclase to silica-saturated compositions by the incongruent melting of sanidine. This relationship between the high temperature "saddle" and low temperature minimum in the tetrahedron is analogous to the situation in the system Nepheline-Kalsilite-Silica (see Figure 2). The presence of the thermal barrier in the system Nepheline-Kalsilite-Silica-Diopside for compositions outside the leucite primary phase volume, prevents residual liquids of phonolitic composition (i.e. equivalent to the temperature minimum M', Figure 13) from fractionating to silica-oversaturated or rhyolitic compositions equivalent to the temperature minimum N' (Figure 13).

## CHAPTER 7

### CONCLUSIONS AND PROPOSALS FOR FUTURE WORK

#### 7.1 Conclusions

From crystallization studies at 1 atmosphere in the system Nepheline-Diopside-Sanidine, the following conclusions can be made.

On crystallization, residual liquids migrate from the plane of the system as a consequence of the complex solid solutions which crystallize. With equilibrium crystallization, residual liquids move towards an invariant point  $ne + lc + fp + di + liq$  (Point R', Figure 13) and a temperature minimum  $di + fp + ne$  (M', Figure 13) located in the volume of the tetrahedron Nepheline-Kalsilite-Silica-Diopside. Final assemblages correspond to simplified leucite trachytes, leucite phonolites, phonolites and nephelinites. Olivine and melilite, which crystallize at liquidus and subliquidus temperatures respectively, disappear by reaction before the solidus is reached; the final assemblages consisting of nepheline and pyroxene. This suggests that certain nepheline-pyroxene rocks (e.g. nephelinites) might be the low temperature equivalents of high temperature olivine-melilite rocks (i.e. olivine melilite nephelinites and melilite nephelinites).

With fractional crystallization, residual liquid trends are controlled by phase relations in the volume of the tetrahedron Nepheline-Kalsilite-Silica-Diopside and by phase relations lying outside this volume. At high temperatures fractionation of olivine and melilite, from compositions rich in nepheline and diopside molecules, leads to the formation of assemblages which, although simplified, range from basic, feldspar free, silica-undersaturated alkaline rocks akin to alkali olivine basalts (e.g. olivine nephelinites, melilite nephelinites, and olivine melilite nephelinites) to more felsic silica-undersaturated alkaline rocks characterized by the crystallization of Ca-poor ternary feldspars (e.g. phonolites). By this mechanism, the widespread association of melilite and olivine-bearing nephelinites with phonolites can be explained.

The formation of melilites in mixtures rich in nepheline and diopside molecules adds further support to Bowen's hypothesis (1928) for the formation of melilite-bearing lavas by the desilication of pyroxene molecules by nepheline.

The trends of residual liquids from mixtures crystallizing leucite are controlled by the phase relations in the tetrahedron Nepheline-Kalsilite-Silica-Diopside. The assemblages produced by fractional crystallization range from simple leucite-pyroxene rocks (leucitites) and leucitophyres to leucite phonolites and phonolites and from leucitites to

leucite trachytes to phonolites. As a consequence of the incongruent melting of sanidine, fractionation of compositions rich in this molecule may result in a final assemblage equivalent to a silica-oversaturated rhyolite. These fractionation assemblages containing leucite indicate the possible relationships of similar natural assemblages, if such rocks have formed by crystal-liquid fractionation.

The invariant point  $ne + lc + fp + di + liq$  (Point R', Figure 13) is a reaction point at which leucite reacts with liquid to form feldspar and nepheline. This reaction adds additional support to Bowen's hypothesis (1928) that pseudo-leucites can form by leucite-liquid reaction.

About five weight percent diopside is thought to be present in the compositions of the invariant point  $ne + lc + fp + di + liq$  (Point R', Figure 13) and the temperature minimum  $di + ne + fp$  (M', Figure 13). As the lowest melting residual liquids complete crystallization at this minimum, this confirms yet another of Bowen's hypotheses (1937) that through fractionation a magma becomes impoverished in early crystallizing minerals.

For silica-undersaturated compositions in the tetrahedron Nepheline-Kalsite-Silica-Diopside, lying outside the primary phase volume of leucite, the system Diopside-Albite-Orthoclase forms a thermal barrier. This prevents liquids with phonolitic compositions (i.e. silica-undersaturated)



from attaining either trachytic (i.e. silica-saturated) or rhyolitic compositions (silica-oversaturated) by simple fractional crystallization.

Therefore, from a study of the system Nepheline-Diopside-Sanidine, relationships between a wide variety of undersaturated alkaline rocks can be deduced. The information obtained from this work, together with that obtained by Morse (1968) and Sood (1969), on the effects of adding diopside to petrogeny's residua system Nepheline-Kalsilite-Silica, shows that the expanded system Nepheline-Kalsilite-Silica-Diopside provides a much better physico-chemical basis for explaining the genesis of a wider variety of undersaturated alkaline rocks than can be provided by 'petrogeny's residua system' alone.

## 7.2 Proposals for Future Work.

Additional work should be undertaken to delineate further the phase relations in the tetrahedron Nepheline-Kalsilite-Silica-Diopside, concentrating on three main points:

- i. The determination of changes in feldspar composition along the line  $di + ne + fp + liq$  (Line 5, Figure 13), as this line forms a possible connection between tephrites, where the feldspar is predominantly plagioclase, and phonolites, where the feldspar is predominantly alkali. Plagioclase crystallizes on this line at its intersection with the system Nepheline-Diopside-Silica (Schairer and Yoder, 1960)

while Ca-poor ternary feldspar crystallizes at the temperature minimum (M') in the volume of the tetrahedron.

ii. A study of the possible temperature minimum (N') on the line di + fp + sil + liq (Line 6, Figure 13) to ascertain if the high temperature saddle in the system Diopside-Albite-Orthoclase forms a thermal barrier for silica-oversaturated as well as silica-undersaturated liquids.

iii. Accurate temperature and compositional determinations of the invariant point ne + lc + fp + di + liq (Point R', Figure 13) and the temperature minimum (M') located on the univariant line di + ne + fp + liq (Line 5, Figure 13).

The addition of an acmitic pyroxene molecule ( $\text{NaFeSi}_2\text{O}_6$ ) to the tetrahedron Nepheline-Kalsilite-Silica-Diopside would be useful, as most pyroxenes in silica-undersaturated alkaline rocks are solid solutions of diopside and acmite. Special emphasis should be given to the change in pyroxene compositions from the high temperature assemblages (e.g. nephelinites) to the low temperature assemblages (e.g. phonolites).

Studies to ascertain the validity of certain of the theoretical considerations in the present study should also be made. These include:

i. The validity of the assemblage ne + ol + di + fp + liq (Point Y, Figure 15), which is equivalent to a simplified olivine phonolite. Such an assemblage possibly occurs in the system Nepheline-Diopside-Sanidine-Forsterite. This

system, except for the composition of the feldspar, is analogous to the system Nepheline-Diopside-Albite-Forsterite in which rocks of the alkali olivine basalt kindred can be represented (Yoder and Tilley, 1962). Combining the two systems by taking a series of feldspar compositions composed of mixtures of albite and sanidine would give more information as to the possible relationships between alkali olivine basaltic rocks and the felsic silica-undersaturated alkaline rocks akin to phonolites.

ii. In the present study, melilite molecules crystallize from compositions containing feldspar molecules (i.e. principally sanidine). This melilite becomes unstable and ultimately disappears, for which a theoretical melilite-feldspar reaction was proposed (Section 3.5, Chapter 3). A possible product of this reaction is wollastonite, the formation of which might have some bearing on the genesis of wollastonite phonolites and wollastonite nephelinites. For this reason, the stability of melilite and the possible products formed by a melilite reaction should be studied in the system Melilite (2 Akermanite-Soda Melilite)-Sanidine-Albite and ultimately in the system Melilite-Sanidine-Albite-Nepheline. The melilite composition of 2 parts akermanite to a single part soda melilite corresponds closely to natural melilites crystallizing from igneous rocks (Yoder, 1964).

---

## APPENDIX

---

Experimental Results! for the Mixture  $\text{Ne}_{44.7}\text{Ks}_{19.5}\text{Si}_{130.8}\text{Di}_5$

<u>T°C.</u>	<u>Time</u> ( <u>hours</u> )	<u>Phases</u>
1043*	96	tr. di + gl.
1015*	312	ne + di + gl.
1005*	120	fp + ne + di + gl.
995*	144	fp + ne + di + gl.
		B.M. $970^\circ \pm 20^\circ\text{C}.$

! Experimental results obtained from hydrothermally crystallized starting material.

\* All temperatures accurate to  $\pm 10^\circ\text{C}.$

For an explanation of the symbols, see Table 4, p.41.

## REFERENCES

- Bowen, N.L. (1912), The binary system:  $\text{Na}_2\text{Al}_2\text{Si}_2\text{O}_8$  (nephelite, carnegieite)- $\text{CaAl}_2\text{Si}_2\text{O}_8$  (anorthite). *Am. J. Sci.*, Vol. 33, pp. 551-573.
- \_\_\_\_\_ (1915), The crystallization of haplobasaltic, haplodioritic, and related magmas. *Am. J. Sci.*, Vol. 40, pp. 161-185.
- \_\_\_\_\_ (1922), Genetic features of alnöitic rocks from Isle Cadieux, Quebec. *Am. J. Sci.*, Vol. 3, pp. 1-34.
- \_\_\_\_\_ (1928), The Evolution of the Igneous Rocks. Princeton Univ. Press, 334 pp.
- \_\_\_\_\_ (1937), Recent high-temperature research on silicates and its significance in igneous geology. *Am. J. Sci.*, 5th. Series, Vol. XXXIII, pp. 1-21.
- \_\_\_\_\_ (1945), Phase equilibria bearing on the origin and differentiation of alkaline rocks. *Am. J. Sci.*, Vol. 243-A, pp. 75-89.
- \_\_\_\_\_ and Schairer, J.F. (1938), Crystallization equilibrium in nepheline-albite-silica mixtures with fayalite. *Jour. Geol.*, Vol. 46, pp. 397-411.
- Daly, R.A. (1910), Origin of the alkaline rocks. *Geol. Soc. Am. Bull.*, Vol. 87, pp. 87-118.
- Donnay, G., Schairer, J.F. and Donnay, J.D.H. (1959), Nepheline solid solutions. *Min. Mag.*, Vol. 32, pp. 93-109.
- Fudali, R.F. (1963), Experimental studies bearing on the origin of pseudoleucites and associated problems of alkalic rock systems. *Geol. Soc. Am. Bull.*, Vol. 74, pp. 1101-1126.
- Fyfe, W.S. (1960), Hydrothermal synthesis and determination of equilibrium in the minerals in the subliquidus region. *Jour. Geol.*, Vol. 68, pp. 553-566.
- Goldsmith, J.L. (1949), Some aspects of the system  $\text{NaAlSiO}_4$ - $\text{CaO} \cdot \text{Al}_2\text{O}_3$ . *Am. Min.*, Vol. 34, pp. 471-493.
- Goranson, R.W. (1931), The solubility of water in granite. *Am. J. Sci.*, Vol. 22, pp. 481-502.

- Gummer, W.K. (1943), The system  $\text{CaSiO}_3$ - $\text{CaAl}_2\text{Si}_2\text{O}_8$ - $\text{NaAlSiO}_4$ . Jour. Geol., Vol. 51, pp. 503-530.
- Hamilton, D.L. and MacKenzie, W.S. (1960), Nepheline solid solution in the system  $\text{NaAlSiO}_4$ - $\text{KAlSiO}_4$ - $\text{SiO}_2$ . J. Pet., Vol. 1, pp. 56-72.
- \_\_\_\_ (1965), Phase-equilibrium studies in the system  $\text{NaAlSiO}_4$  (nepheline)- $\text{KAlSiO}_4$  (kalsilite)- $\text{SiO}_2$ - $\text{H}_2\text{O}$ . Min. Mag., Vol. 34, pp. 214-231.
- Johannsen, A. (1938), A Descriptive Petrography of the Igneous Rocks. Vol. IV, Univ. of Chicago Press, Chicago, 523 pp.
- King, B.C. (1965), Petrogenesis of the alkaline igneous rock suites of the volcanic and intrusive centres of Eastern Uganda. J. Pet., Vol. 6, pp. 67-100.
- Knight, C.W. (1906), A new occurrence of pseudoleucite. Am. J. Sci., Vol. 21, pp. 286-295.
- Kracek, F.C. (1930), The system sodium oxide-silica. Jour. Phys. Chem., Vol. 34, pp. 1583-1598.
- \_\_\_\_ (1932), The ternary system  $\text{K}_2\text{SiO}_3$ - $\text{Na}_2\text{SiO}_3$ - $\text{SiO}_2$ . Jour. Phys. Chem., Vol. 36, pp. 2529-2542.
- \_\_\_\_ (1939), Phase equilibrium relations in the system,  $\text{Na}_2\text{SiO}_3$ - $\text{Li}_2\text{SiO}_3$ - $\text{SiO}_2$ . Am. Chem. Soc. Jour., Vol. 61, pp. 2863-2877.
- Kracek, F.C., Bowen, N.L. and Morey, G.W. (1929), The system potassium metasilicate-silica. Jour. Phys. Chem., Vol. 33, pp. 1857-1879.
- Larsen, E.S. and Buie, B.F. (1938), Potash analcime and pseudoleucite from the Highwood Mountains of Montana. Am. Min., Vol. 23, pp. 837-849.
- Morse, S.A. (1968), Diopside-albite-orthoclase at atmospheric pressure and at 5 Kb.  $\text{PH}_2\text{O}$ . Ann. Rept., Geophysical Lab., Carnegie Inst. Wash., Yearbook 67, pp. 119-120.
- Onuma, K. and Yagi, K. (1967), The system diopside-akermanite-nepheline. Am. Min., Vol. 52, pp. 227-243.
- Roedder, E.W. (1959), Silicate melt systems. In Physics and Chemistry of the Earth, Vol. 3, pp. 224-297. Editors: Ahrens, Press, Rankama and Runcorn, Pergamon Press, London, 464 pp.

- Saggerson, E.P. (1952), Geology of the Kisumu District, Kenya. Geol. Surv. Kenya., Rept. 21.
- Saggerson, E.P. and Williams, L.A.J. (1964), Ngurumanite from Southern Kenya and its bearing on the origin of rocks in the Northern Tanganyika alkaline district. J. Pet., Vol. 5, pp. 40-81.
- Schairer, J.F. (1942), The system  $\text{CaO-FeO-Al}_2\text{O}_3\text{-SiO}_2$ : 1, Results of quenching experiments on five joins. J. Am. Ceramic Soc., Vol. 25, pp. 241-274.
- \_\_\_\_\_ (1954), The system  $\text{K}_2\text{O-MgO-Al}_2\text{O}_3\text{-SiO}_2$ : 1, Results of quenching experiments on four joins in the tetrahedron cordierite-forsterite-leucite-silica and on the join cordierite-mullite-potash feldspar. J. Am. Ceramic Soc., Vol. 37, pp. 501-533.
- \_\_\_\_\_ (1957), Melting relations of the common rock-forming silicates. J. Am. Ceramic Soc., Vol. 40, pp. 215-235.
- \_\_\_\_\_ (1959), Phase equilibria with particular reference to silicate systems. In Physiochemical measurements at high temperature. pp. 117-134. Editors Bockris, White and Mackenzie, Butterworths Scientific Publications, London. 394 pp.
- Schairer, J.F. and Bowen, N.L. (1935), Preliminary report on equilibrium-relations between feldspathoids, alkali-feldspars, and silica. Am. Geophys. Un. Trans., 16th. Ann. Mtg., Pt. 1, pp. 325-328.
- \_\_\_\_\_ (1938), The system leucite-diopside-silica. Am. J. Sci., 5th Series, Vol. XXV-A, pp. 289-309.
- \_\_\_\_\_ (1947), The system anorthite-leucite-silica. Soc. Géol. Fin. Bull., Vol. XX, pp. 67-87.
- \_\_\_\_\_ (1955), The system  $\text{K}_2\text{O-Al}_2\text{O}_3\text{-SiO}_2$ . Am. J. Sci., Vol. 253, pp. 681-746.
- \_\_\_\_\_ (1956), The system  $\text{Na}_2\text{O-Al}_2\text{O}_3\text{-SiO}_2$ . Am. J. Sci., Vol. 254, pp. 129-195.
- Schairer, J.F., Yagi, K. and Yoder, H.S. (1962), The system nepheline-diopside. Ann. Rept., Geophysical Lab., Carnegie Inst. Wash., Yearbook 61, pp. 96-98.
- Schairer, J.F. and Yoder, H.S. (1960), The nature of residual liquids from crystallization, with data on the system nepheline-diopside-silica. Am. J. Sci., Vol. 258-A, pp. 273-283.



- Schairer, J.F. and Yoder, H.S. (1961), Crystallization in the system nepheline-forsterite-silica at one atmosphere pressure. Ann. Rept., Geophysical Lab., Carnegie Inst. Wash., Yearbook 60, pp. 141-144.
- \_\_\_\_ (1964), Crystal and liquid trends in simplified alkali basalts. Ann. Rept., Geophysical Lab., Carnegie Inst. Wash., Yearbook 63, pp. 65-74.
- Schairer, J.F., Yoder, H.S. and Tilley, C.E. (1965), Behaviour of melilites in the join gehlenite-soda melilite-akermanite at one-atmosphere pressure. Ann. Rept., Geophysical Lab., Carnegie Inst. Wash., Yearbook 64, pp. 95-100.
- Segnit, E.R. (1953), Some data on synthetic aluminous and other pyroxenes. Min. Mag., Vol. 30, pp. 218-226.
- Shepherd, E.S., Rankin, G.A. and Wright, E.F. (1909), The system of alumina with silica, lime and magnesia. Am. J. Sci., Vol. 28-A, pp. 293-333.
- Stark, J.T. and Hay, R.L. (1963), Geology and petrography of volcanic rocks of Truk Islands, East Caroline Islands. U.S.G.S. Prof. Paper 409, 41 pp.
- Sood, M.K. (1969), The join diopside-albite-leucite in the system diopside-nepheline-kalsilite-silica and its petrological implications. Unpublished Ph.D. thesis, Univ. Western Ontario.
- Turner, F.J. and Verhoogen, J. (1960), Igneous and Metamorphic Petrology. 2nd. edition, McGraw-Hill Book Company, Inc., New York, 694 pp.
- Tuttle, O.F. (1949), Two pressure vessels for silicate water studies. Geol. Soc. Am. Bull., Vol. 60, pp. 1727-1729.
- Tuttle, O.F. and Bowen, N.L. (1958), Origin of granite in the light of experimental studies in the system  $\text{NaAlSi}_3\text{O}_8$ - $\text{KAlSi}_3\text{O}_8$ - $\text{SiO}_2$ - $\text{H}_2\text{O}$ . Geol. Soc. Am., Mem. 74, 153 pp.
- Tyler, Ruth C. and King, B.C. (1967), The pyroxenes of the alkaline igneous complexes of Eastern Uganda. Min. Mag., Vol. 36, pp. 5-21.
- Washington, H.S. (1896), Italian petrological sketches. II. The Viterbo Region. Jour. Geol., Vol. 4, pp. 826-849.
- Wilkinson, J.F.G. (1956), Clinopyroxenes of alkali olivine-basalt magma. Am. Min., Vol. 41, pp. 724-743.

- Wright, J.B. (1963), A note on possible differentiation trends in Tertiary to Recent lavas of Kenya. Geol. Mag., Vol. 100, pp. 164-180.
- Yoder, H.S. (1964), Soda melilite. Ann. Rept., Geophysical Lab., Carnegie Inst. Wash., Yearbook 63, pp. 86-89.
- Yoder, H.S. and Tilley, C.E. (1962), Origin of basalt magmas: An experimental study of natural and synthetic rock systems. J. Pet., Vol. 3, pp. 342-532.